

## ABSTRACT

Title of Thesis: PASSIVE STAND-OFF LAYER DAMPING TREATMENT:  
THEORY AND EXPERIMENTS

Degree candidate: Atif H. Chaudry

Degree and year: Master of Science, 2006

Thesis directed by: Professor Amr Baz

Department of Mechanical Engineering

One of the techniques used to enhance the damping characteristics of constrained damping treatments utilizes a spacer layer, called a “stand-off” layer, which is sandwiched between the viscoelastic layer and the base structure. This “stand-off” layer acts as a strain magnifier that magnifies the shear strain in the viscoelastic layer by virtue of increasing the distance between the viscoelastic layer and the neutral axis of the base structure. The “stand-off” layer must have high shear stiffness and must not significantly affect the bending stiffness of the composite structure in order to achieve high damping characteristics. Slotted “stand-off” layers are used to achieve such high shear stiffness and low bending stiffness. In these slotted “stand-off” layer, the geometry of the slots play a very important role in determining the effectiveness of the damping treatment. It is therefore the purpose of this dissertation to model the dynamics and damping characteristics of Passive Stand-off damping treatments using distributed-parameter approach as well as the finite element method. The predictions of the developed models

are validated against the predictions of commercially available finite element software (ANSYS) and against experimental results. Close agreements are found between the predictions of the developed models, ANSYS models, and the experimental results.

The developed models present accordingly a valuable means for designing effective and optimal passive stand-off damping treatments for beams. The models can be easily extended to passive stand-off damping treatments for more complex structures such as plates and shells.

**PASSIVE STAND-OFF LAYER DAMPING TREATMENT: THEORY AND  
EXPERIMENTS**

by

Atif H. Chaudry

Thesis submitted to the Faculty of the Graduate School of the  
University of Maryland, College Park in partial fulfillment  
of the requirements for the degree of  
Master of Science  
2006

**Advisory Committee:**

Professor Amr Baz, Chair/Advisor  
Professor Balakumar Balachandran  
Assistant Professor Miao Yu

©Copyright by

Atif Hussain Chaudry

2006

## **Acknowledgements**

All praise is due to Allaah, I praise him, seek His help, and ask for his forgiveness. Peace and Blessings of Allah be upon His Slave and His Messenger, Prophet Mohammed. Thanks to Allaah, the most Merciful, the most Gracious, for all the uncountable bounties He has granted me and for helping me to successfully finish my research.

Special thanks are offered to Dr. Amr Baz for his encouragement, advice, and guidance throughout my graduate study as well as in completing this research.

I also would like to express my thanks to all my friends at Islamic Center of Maryland and Dar-us-Salaam for their support and encouragement.

I deeply appreciate the help of my friend and colleague Dr. Adel El-Sabbagh for his support whenever I most needed it and to all my friends at the University of Maryland.

Finally, this thesis is dedicated to my grandfather, now diagnosed with terminal cancer, for his love and unfailing support and patience, who perhaps has lost his ability to listen and communicate, who I hope recovers from his illness so I can give him the news that he waited for so long to hear. May Allaah give him recovery and grant him good of this world and hereafter.

# TABLE OF CONTENTS

|  |    |
|--|----|
| Acknowledgements .....   | ii |
| List Of Tables .....   | v  |
| List Of Figures .....  | vi |
| Nomenclature .....   | x  |
| 1. Introduction .....  | 1  |
| 1.1 Passive Damping .....  | 1  |
| 1.2 Literature Review .....  | 8  |
| 1.3 Thesis Outline .....   | 9  |
| 1.4 Summary .....  | 10 |
| 2. Derivation of Equations of Motion .....                                   | 11 |
| 2.1 Assumptions .....  | 11 |
| 2.2 Kinematic Equations .....  | 12 |
| 2.3 Constitutive Equations .....   | 14 |
| 2.4 Equilibrium Equations .....  | 16 |
| 2.5 Moment Equilibrium Equations .....                                       | 19 |
| 2.6 Boundary Conditions .....  | 27 |
| 2.7 Summary .....  | 28 |
| 3. Distributed Transfer Function Solution Method .....                       | 29 |
| 3.1 Solution By Distributed Parameter Systems Transfer Function Method ..... | 29 |
| 3.2 Equations In State Space Form .....                                      | 31 |
| 3.3 Boundary Conditions .....  | 33 |
| 3.4 Solution .....   | 34 |
| 3.5 Summary .....  | 35 |
| 4. Finite Element Model .....  | 36 |
| 4.1 Solution By Finite Element Method .....                                  | 36 |
| 4.2 Derivation Of Element Equations .....                                    | 37 |
| 4.3 Interpolation Functions .....  | 39 |
| 4.4 Assembly Of Matrices .....   | 45 |
| 4.5 Application of the Boundary Conditions .....                             | 47 |
| 4.6 Summary .....  | 49 |
| 5. Computer Implementation .....   | 50 |
| 5.1 Distributed Transfer Function Method .....                               | 50 |
| 5.2 Finite Element Method .....  | 56 |
| 5.3 Slotted Pso1 Finite Element Model Matlab Program .....                   | 63 |
| 5.4 Summary .....  | 64 |
| 6. ANSYS Modeling and Comparison .....                                       | 65 |
| 6.1 Overview .....   | 65 |
| 6.2 Damping In Ansys .....   | 65 |
| 6.3 Modeling In Ansys .....  | 67 |
| 6.4 Comparison .....   | 68 |
| 6.5 Summary .....  | 73 |

|   |     |
|---|-----|
| 7. Experimental Verification.....   | 74  |
| 7.1 Experimental Setup .....  | 74  |
| 7.2 Summary .....   | 92  |
| 8. Effect of PSOL Parameters on its Damping Characteristics.....                            | 93  |
| 8.1 Effect Of Thickness Of Vem And Sol Layers When Sol Layer Is Undamped....                | 95  |
| 8.2 Effect Of Thickness Of Vem And Sol Layers When Sol Layer Is Damped .....                | 96  |
| 8.3 Effect Of Young's Modulus Of Vem And Sol Layers When Sol Layer Is<br>Damped.....        | 97  |
| 8.4 Effect Of Thickness And Strength Of Constraining Layer .....                            | 99  |
| 8.5 Effect Of Elastic And Shear Moduli Of The Stand-Off Layer When Loss<br>Factor = 1 ..... | 100 |
| 8.6 Effect Of Thickness And Strength Of The Stand-Off Layer When Loss<br>Factor =0 .....    | 102 |
| 8.7 Summary .....   | 103 |
| 9. Conclusions and Recommendations.....   | 104 |
| Appendix .....  | 110 |
| Computer Program Codes .....  | 110 |
| References .....  | 128 |

## **List Of Tables**

|   |    |
|---|----|
| <b>Table (1)</b> - The main geometrical and physical parameters of the tested PSOL treatments   | 78 |
| <b>Table (2)</b> - Comparison between the theoretical and experimental modal characteristics of the 5mm thick plain beam                            | 80 |
| <b>Table (3)</b> - Comparison between the theoretical and experimental modal characteristics of the 3mm thick plain beam                            | 82 |
| <b>Table (4)</b> - Comparison between the theoretical and experimental modal characteristics of the 3.5mm thick beam with unslotted SOL             | 84 |
| <b>Table (5)</b> - Comparison between the theoretical and experimental modal characteristics of the 3.5mm thick beam with slotted SOL near free end | 86 |
| <b>Table (6)</b> - Comparison between the theoretical and experimental modal characteristics of a beam with slotted PSOL machined near free end     | 88 |
| <b>Table (7)</b> - Comparison between the theoretical and experimental modal characteristics of a beam with 27-slot PSOL                            | 90 |
| <b>Table (8)</b> - Comparison between the theoretical and experimental modal characteristics of a beam with 40-slot PSOL                            | 92 |



## List Of Figures

| Figure   | Page |
|--|------|
| <b>Figure (1)</b> - Unconstrained viscoelastic damping.                                      | 2    |
| <b>Figure (2)</b> - Stress profile of a beam cross-section subjected to axial load           | 3    |
| <b>Figure (3)</b> - Constrained Layer Damping  | 4    |
| <b>Figure (4)</b> - Shear in Viscoelastic Layer due to Constraining Layer                    | 4    |
| <b>Figure (5)</b> - PSOL Damping   | 5    |
| <b>Figure (6)</b> - Increased elastic strength due to high stiffness Stand-off layer         | 6    |
| <b>Figure (7)</b> - Reduced shear in viscoelastic layer due to low stiffness stand-off layer | 6    |
| <b>Figure (8)</b> - Slotted PSOL Damping   | 7    |
| <b>Figure (9)</b> - Axial Deflection of layers   | 12   |
| <b>Figure (10)</b> - Total Axial Deflection of layers  | 13   |
| <b>Figure (11)</b> - Base Beam and stand-off Layer Axial Forces                              | 17   |
| <b>Figure (12)</b> - Constraining Layer Axial Force  | 17   |
| <b>Figure (13)</b> - Base Beam and stand-off Layer Lateral Forces                            | 18   |
| <b>Figure (14)</b> - Viscoelastic Layer Lateral Forces                                       | 18   |
| <b>Figure (15)</b> - Constraining Layer Lateral Forces                                       | 19   |
| <b>Figure (16)</b> - Base beam& stand off layer equilibrium                                  | 19   |
| <b>Figure (17)</b> - Viscoelastic layer equilibrium  | 20   |
| <b>Figure (18)</b> - Constraining layer equilibrium  | 20   |
| <b>Figure (19)</b> - Damping in ANSYS  | 66   |



|   |    |
|---|----|
| <b>Figure (37)</b> - Comparison between the theoretical and experimental frequency response<br>of 5mm thick plain beam                  | 82 |
| <b>Figure (38)</b> - 3.5 mm thick beam with unslotted SOL (model 3)   | 83 |
| <b>Figure (39)</b> - Response for beam model 3 with unslotted stand-off layer treated in<br>middle                                      | 84 |
| <b>Figure (40)</b> - 3.5 mm thick beam with slotted PSOL (model 4)  | 85 |
| <b>Figure (41)</b> - Frequency response of a beam with slotted PSOL machined at the center  | 86 |
| <b>Figure (42)</b> - 3.5 mm thick beam with slotted PSOL machined at free end (model 5)   | 87 |
| <b>Figure (43)</b> - Frequency response of a beam with slotted PSOL machined at free end  | 88 |
| <b>Figure (44)</b> - 3.125 mm thick beam with a 40-slot PSOL (model 6)  | 89 |
| <b>Figure (45)</b> - Frequency response of a beam with a 27-slot PSOL   | 90 |
| <b>Figure (46)</b> - 3.125 mm thick beam with a 40-slot PSOL (model 7)  | 91 |
| <b>Figure (47)</b> - Frequency response of a beam with a 40-slot PSOL   | 92 |
| <b>Figure (48)</b> - A typical frequency response of a beam with PSOL defining the<br>performance index AUC                             | 94 |
| <b>Figure (49)</b> - Iso-contours of the AUC as a function of the thickness of the VEM and<br>SOL Layers when the SOL layer is undamped | 95 |
| <b>Figure (50)</b> - Iso-contours of the AUC as a function of the thickness of the VEM and SOL<br>Layers when the SOL layer is damped   | 97 |
| <b>Figure (51)</b> - Iso-contours of the AUC as a function of the strength of the VEM and SOL Layers<br>when the SOL layer is damped    | 98 |

|  |     |
|--|-----|
| <b>Figure (52)</b> - Iso-contours of the AUC as a function of the strength and thickness of the<br>constraining layer                  | 99  |
| <b>Figure (53)</b> - Iso-contours of the AUC as a function of the Elastic and Shear Moduli<br>of the SOL Layer when the loss factor =1 | 101 |
| <b>Figure (54)</b> - Iso-contours of the AUC as a function of the Elastic and Shear Moduli<br>of the SOL Layer when the loss factor =0 | 103 |
| <b>Figure (55)</b> - Passive constrained layer plate with stand-off layer patches  | 106 |
| <b>Figure (56)</b> - Cylindrical Shell with Slotted Stand-off layer  | 107 |
| <b>Figure (57)</b> - Variation of geometry of layers along the length of the   | 108 |
| <b>Figure (58)</b> - Passive stand-off layer treated beam with lateral strain in the layers  | 109 |

## Nomenclature

|        |  |
|--------|--|
| $A$    | cross sectional area                                     |
| $b$    | width of all layers                                      |
| $E$    | Modulus of Elasticity                                    |
| $f$    | Externally applied surface loads                         |
| $G$    | Complex shear Modulus                                    |
| $h_b$  | thickness of base beam                                   |
| $h_c$  | thickness of constraining layer                          |
| $h_v$  | thickness of viscoelastic layer                          |
| $h_s$  | thickness of stand-off layer                             |
| $I$    | Second moment of area                                    |
| $K$    | curvature of composite beam                              |
| $l$    | length of all layers                                     |
| $p$    | internal normal forces                                   |
| $q$    | Externally applied body loads                            |
| $T$    | Axial Tension  |
| $u_b'$ | axial deflection in base beam at neutral axis            |
| $u_b$  | normalized axial deflection in base beam at neutral axis |
| $u_c'$ | axial deflection in constraining layer                   |

|       |   |
|-------|---|
| $u_c$ | normalized axial deflection in constraining layer   |
| $V$   | Lateral Force                                       |
| $w'$  | lateral deflection of the composite beam            |
| $w$   | normalized lateral deflection of the composite beam |
| $y$   | Distance from N.A. in composite beam                |
| $y_b$ | $= \frac{h_b}{2}$                                   |

### ***Greek Symbols***

|                 |  |
|-----------------|--|
| $\varepsilon_0$ | Axial Strain at neutral axis of base beam            |
| $\varepsilon_x$ | Axial Strain across composite beam                   |
| $\gamma'$       | Angular deformation at viscoelastic layer            |
| $\gamma$        | Normalized angular deformation at viscoelastic layer |
| $\rho$          | mass per unit length                                 |
| $\psi'$         | Angular deformation at stand-off layer               |
| $\psi$          | Normalized angular deformation at stand-off layer    |
| $\tau$          | Shear Stress   |

### ***subscripts***

|            |   |
|------------|---|
| b, s, v, c | base beam, stand-off layer, viscoelastic material, and constraining layer respectively. |
|------------|---|

# CHAPTER 1

## Introduction

### 1.1 Passive Damping

Vibration damping is used to control and reduce undesirable vibration so that its harmful and unwanted effects are minimized. The energy dissipating mechanism of vibration control systems is known as damping. For passive damping treatments, viscoelastic materials are used as effective means for dissipating energy. Two types of methods are generally employed for the control of vibrations. These methods are namely: passive and active vibration control. In the **Passive damping** approach, damping layers are added to the structure in order to enhance its energy dissipation characteristics [1]. In the **Active damping** approach energy is dissipated from vibrating system through the use of external systems, such as control actuator, etc. Active vibration control systems are more expensive and less reliable than the passive damping systems.

Hence, the emphasis is placed in this dissertation on the intelligent use of viscoelastic damping treatments bonded to the base structure. Figure (1) shows the simplest approach of using viscoelastic treatments in their unconstrained form.



**Figure (1) - Unconstrained viscoelastic damping**

The viscoelastic material dissipates energy of the base structure when it is subject to acceleration, velocity or deflections. The viscoelastic material affects both the damping and stiffness of the system in a complex fashion as its properties vary with frequency and the operating temperature. The dissipation of energy is both due to direct strain and shear strain of the damping layer. In the case of plate and beam bending, the direct strain varies linearly as the distance from the neutral axis of the base beam/plate as shown in Figure (2). The greatest direct strain occurs at the farthest surfaces from the neutral surface. Therefore damping treatments are attached to those surfaces of the base structure that are as far as possible from the neutral axis. The bending stress and therefore the direct strain at the neutral axis of the viscoelastic treated beam are zero and are very small around the neutral axis [1].



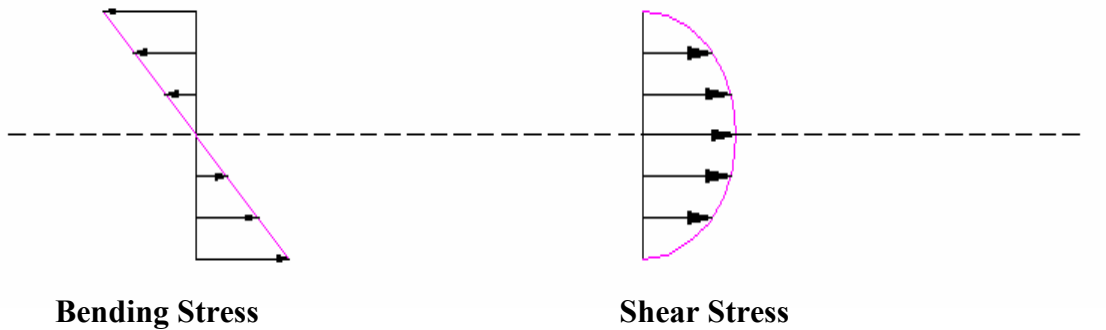


**Figure (2)** - Stress profile of a beam cross-section subjected to axial load

When the viscoelastic layer is attached alone to the outer surface of the beam, it is called **unconstrained layer damping**. Generally the properties of the viscoelastic materials are such that they tend to dissipate more energy when subjected to shear strain and direct strain. The transverse shear strain in a vibrating beam is greatest at the neutral axis and zero at the edges. Therefore, a viscoelastic layer bonded to the surface of the beam experiences negligible shear stress. Hence, the beam damping characteristics remain largely unchanged. To increase the shear strain in the viscoelastic material, the viscoelastic layer is sandwiched between two layers, the beam and the constraining layer plate. Thus both high direct and shear strains are thought to be produced in the viscoelastic layer, resulting in increased energy dissipation. This type of damping is called **constrained layer damping** as shown in Figures (3) and (4).

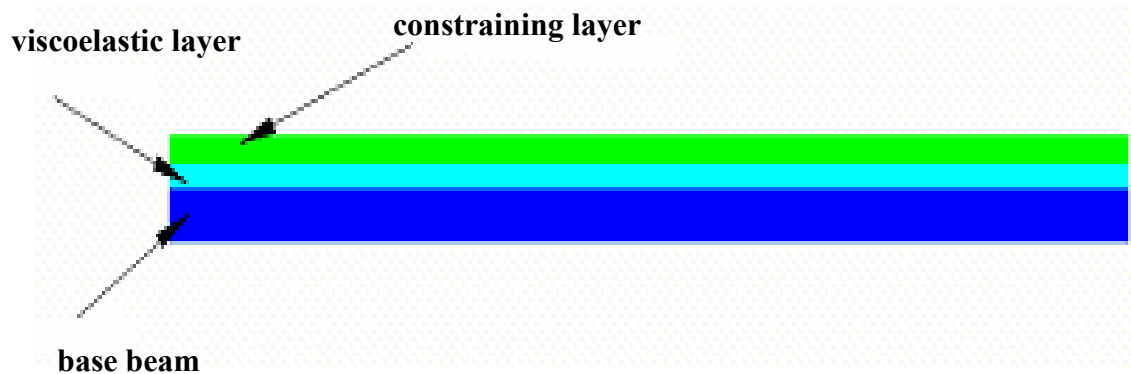


**Figure (3) - Constrained Layer Damping**

Both constrained and unconstrained layer damping treatments have advantages and disadvantages. Constrained layer damping treatment results in greater energy dissipation and can rely in its operation on low stiffness viscoelastic material.

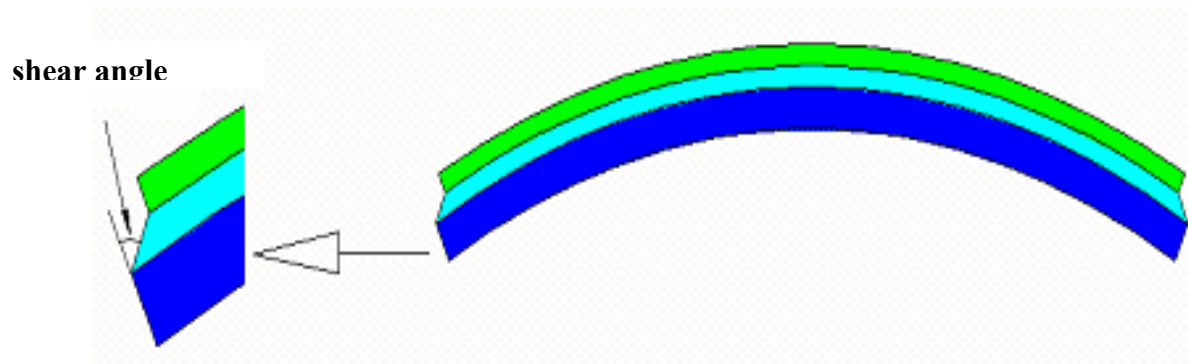
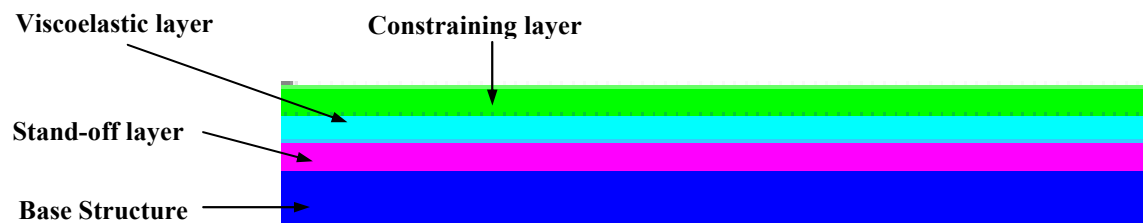


**Figure (4) - Shear in Viscoelastic Layer due to Constraining Layer**

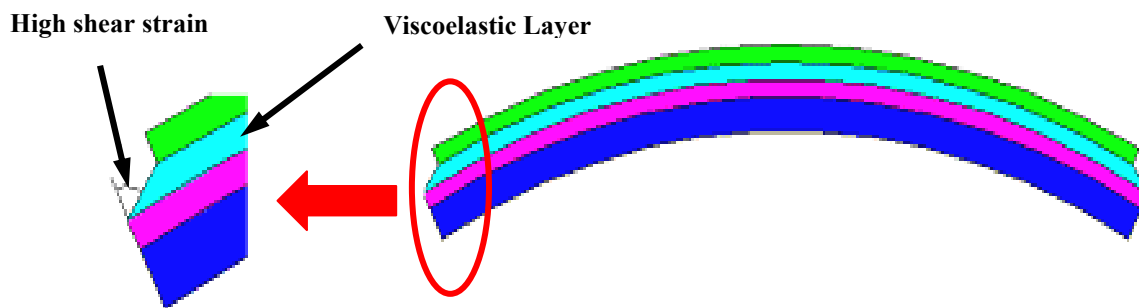
Unconstrained layer damping treatment produces less energy dissipation and requires high stiffness viscoelastic material but it can be used for extensional damping and can be easily

applied to the surface of the base structure. It can be added to the surface in the form of tiles or sheets or can even be sprayed on the surface for some applications.

One of the techniques used to increase the distance between the viscoelastic layer and the neutral axis of the base structure is the introduction of a spacer layer between the viscoelastic layer and the base structure as shown in Figure (5). Such an increase increases the strain and therefore the damping. This spacer layer is called "stand –off" layer and acts as a strain magnifier [2].



(a) – undeformed



(b) - deformed

**Figure (5) - PSOL Damping**

This arrangement is called the **Passive Stand-Off Layer (PSOL) Damping**. In the PSOL, the

spacer layer must have high shear stiffness and at the same time must not significantly affect the bending stiffness of the composite beam. If the stand-off layer has high bending stiffness it will have no other effect than increasing the flexural rigidity of the constrained layer beam and thus will negatively affect the damping performance of the constrained layer treatment as shown in Figure (6).

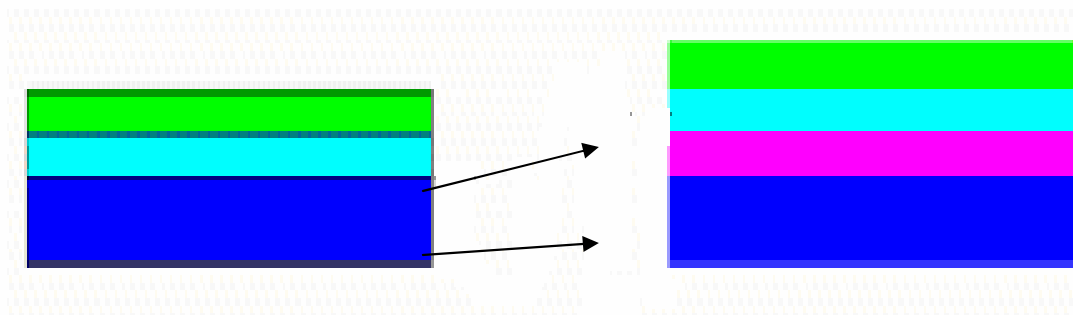


**Figure (6) - Increased elastic strength due to high stiffness Stand-off layer**

If the stiffness of the stand-off layer is weak then the strain will be absorbed in the weak layer and the viscoelastic layer will not experience enough strain to induce significant damping as illustrated in Figure (7).

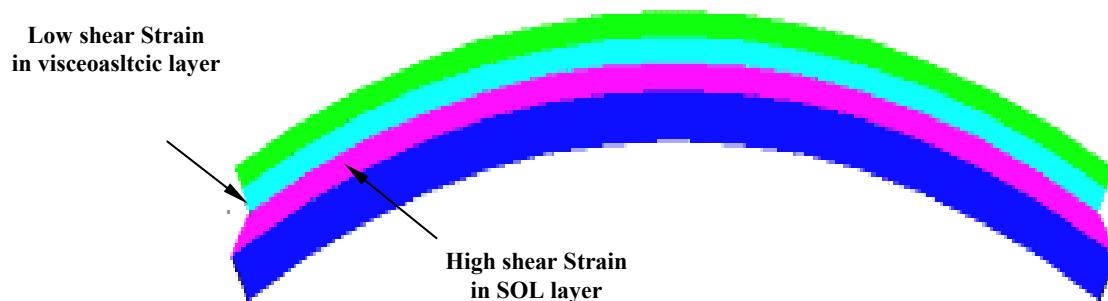


**Figure (7) - Reduced shear in viscoelastic layer due to low stiffness stand-off layer**

One method of avoiding this increase in flexural strength of the treated beam is to use **slotted stand-off layer** of very high shear strength compared to the viscoelastic material as shown in Figure (8).

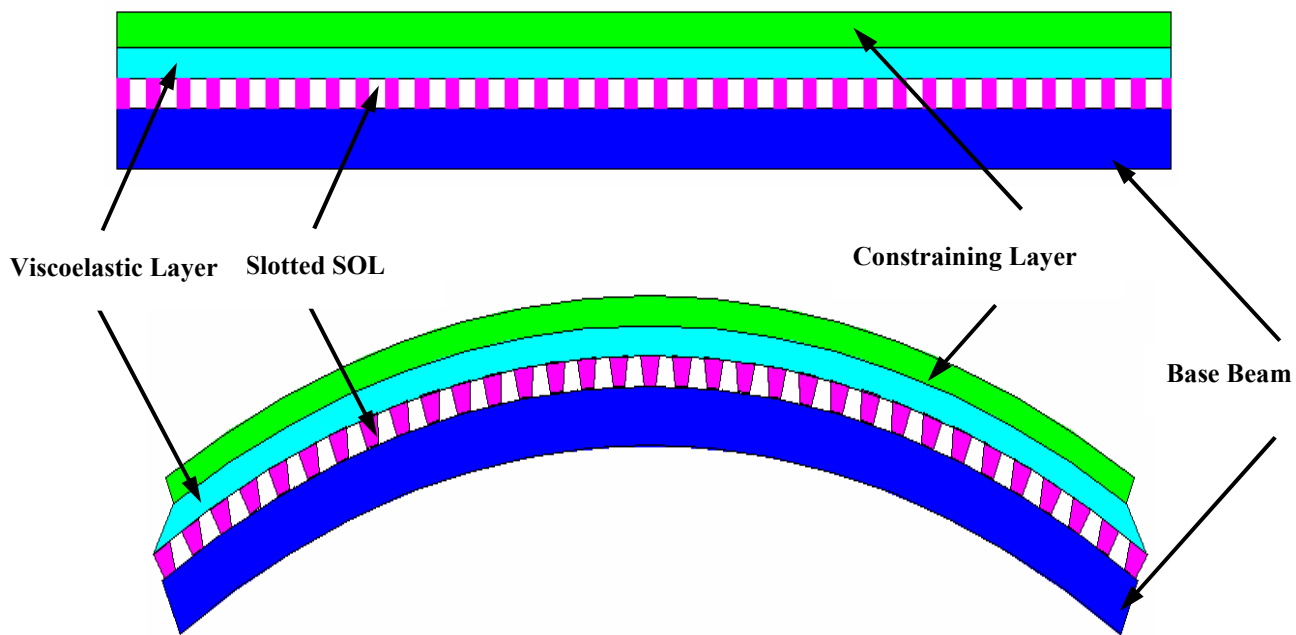


**Figure (8) - Slotted PSOL Damping**

In the slotted stand-off layer treatment, the geometry of the slots should be such that the stand-off layer does not significantly contribute to the flexural rigidity of the base structure but also has enough shear strength such that it does not absorb shear deformation that is desired to be passed on to the viscoelastic layer (i.e., it should pass on the shear stress to the viscoelastic layer).

## 1.2 Literature Review

The stand-off layer concept was first introduced by Whittier [2], who suggested that a spacer layer be introduced between the viscoelastic layer and the vibrating structure. The spacer layer moves the viscoelastic layer away from the neutral axis of the base structure. The shear strain is magnified by this displacement of the viscoelastic layer away from the neutral axis where the strain is a minimum. Most of the studies on passive stand-off layer damping assume ideal conditions of the stand-off layer, i.e. the stand-off layer is assumed to have infinite shear stiffness. Therefore, the SOL does not exhibit shear strain and permits the shear stress to be passed to the viscoelastic layer. Furthermore, the SOL is assumed to have zero bending stiffness and accordingly it does not contribute to the flexural rigidity of the beam. Some of these studies include theoretical and experimental work by Roger and Parin [3], Falugi [4], Falugi *et al.* [5], and Parin *et al.* [6] on slotted stand-off layer damping partially applied to airplane wings and plates. Garrison *et al.* [7] presented an analytical model of a beam treated passive stand-off layer damping. Tao *et al.* [8] confirmed with experimental and finite element analysis the effectiveness of slotted stand-off layer with the above mentioned assumptions

The first attempt to include shear strain of the stand-off layer was done by Mead [1] which considers shear stiffness and internal loss in the stand-off layer but his model did not include the affect of the stand-off layer on the bending characteristics and strength of the composite beam.

Yellin, *et al.* [9] developed an analytical model for the passive stand-off layer damping treatment

using the distributed transfer function method. They treated the base beam and stand-off layer as a composite beam and the stand-off layer is assumed to be modeled as a Euler-Bernoulli beam. However, their model can not handle slotted stand-off layers.

This thesis attempts to develop a finite element model in order to extend the applicability of the model developed by Yellin, *et al.* [9] to include the geometry of the slots. The developed finite element model accounts for finite bending stiffness and shear strength and allows for variability in the properties of stand-off layer across the length of layer.

### **1.3 Thesis Outline**

This thesis attempts to analytically model the dynamics and damping characteristics of passive stand-off layer treatment using the Distributed Transfer Function Method developed by Yang and Tan [10]. Furthermore, a finite element model of the stand-off layer constrained damping treatment will also be developed. The finite element model of the PSOL damping treatment is altered to include slots in the stand-off layer. The model enables investigation of the effect of the geometry of the slots, the thickness of the viscoelastic layer, stand-off layer and the constraining. The predictions of the finite element model are checked and compared by modeling of the passive stand-off layer damping treatment on the commercial finite element software ANSYS. Shape and geometry of the slotted stand-off layer for the optimal damping treatment are determined. Finally the prototypes of slotted stand-off layer treatment are manufactured and tested experimentally. The experimental results are compared with the theoretical predictions.

Therefore, the thesis is organized in eight chapters. In chapter 1, a brief introduction is presented. Chapter 2 presents the equations of motion of PSOL and in Chapter 3, the performance is obtained using the distributed transfer function method. In chapter 4, the finite element model (FEM) of the PSOL is developed and Chapter 5 presents the computer implementation of the FEM. Chapter 6 presents comparisons between the predictions of the FEM and the predictions obtained by commercial finite element software (ANSYS). Chapter 7 presents comparisons with experimental results and Chapter 8 presents the effect of the parameters of the SOL on its performance characteristics. Chapter 9 summarizes the conclusions and recommendations for future work.

## **1.4 Summary**

This chapter has presented briefly the concept of passive stand-off layer (PSOL) damping treatments as a simple and effective means for enhancing the damping characteristics of constrained layer damping. The outline of the thesis dissertation is presented and a brief review of the literature is summarized in an attempt to justify the need and emphasize the importance of the present study.



## CHAPTER 2

# Derivation of Equations of Motion

### 2.1 Assumptions

The following is brief summary of the basic assumptions considered in the analysis of passive stand-off layers.

- Small displacement amplitudes
- Lateral deflection for all layers remains the same.
- No shear deformation in the base beam and the constraining layer.
- The viscoelastic layer is assumed to have no bending stiffness and therefore deforms only in pure shear.
- System has steady state response to the external harmonic excitation. Therefore Complex modulus can be used for viscoelastic and standoff layers
- Standoff layer is continuous and solid in the initial model.
- Stand Off layer and base beam layer are modeled as asymmetric composites so that planes remain planes under combined bending and axial loads.
- Stand off layer has finite shear stiffness, hence Shear deformation occurs in stand off layer when shear loads are present.
- Bending and shear stiffness of stand Off layer is less than that of the base beam and

constraining layer.

This assumption is made to simplify the model by assuming that all shear deformations occur in two core layers.

## 2.2 Kinematic Equations

### SHEAR ANGLE FOR STAND OFF LAYER & VISCOELASTIC LAYER.

The shear deformation in the two layers is due to the

- Difference in axial deformation of the base beam and the constraining layer
- Lateral deflection of the beam

The deformation for the two cases are calculated separately and then add to determine the total deflection.

### Deformation due to deformation of the base beam and the constraining layer in axial direction.

As shown in Figure(9), it is given by

$$u_c' - u_b' \quad (1)$$

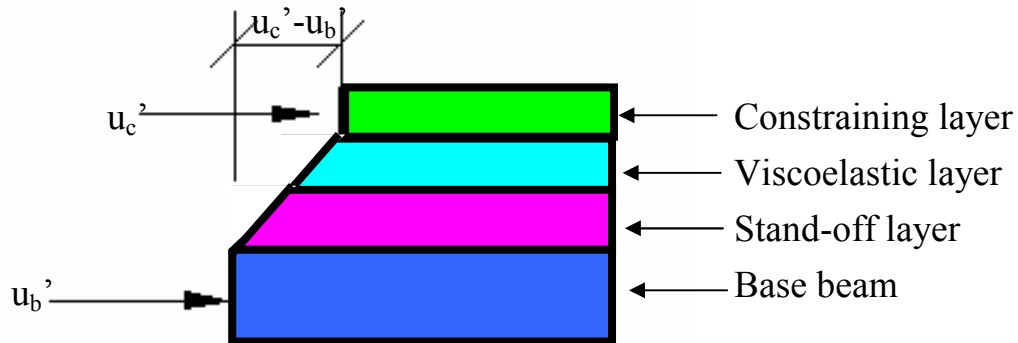


**Figure (9) - Axial Deflection of layers**

where  $u_b'$  and  $u_c'$  are the axial deflections of the beam and the constraining layers respectively.

Axial Deformation due to lateral deflection of the base beam and constraining layer,

$$\frac{\partial w'}{\partial x'} \left( \frac{h_b}{2} + h_s + h_v + \frac{h_c}{2} \right) \quad (2)$$

Hence, the total deformation  $\delta$ , shown in Figure (10), is given by

$$\delta = (u_c' - u_b') + \frac{\partial w'}{\partial x'} \left( \frac{h_c}{2} + h_s + h_v + y_b \right) \quad (3)$$

which is the sum of the deformations due to axial and lateral deformations.

Note that  $w'$  and  $x'$  denote the transverse deflection of the composite beam and the axial coordinate along the beam. Furthermore,  $h_i$  denotes the thickness of the  $i^{th}$  layer where the subscript  $i=c$ =constraining layer,  $i=v$ =viscoelastic layer,  $i=s$ =stand-off layer, and  $i=b$ =beam. Note that the primes denote non-normalized variables.

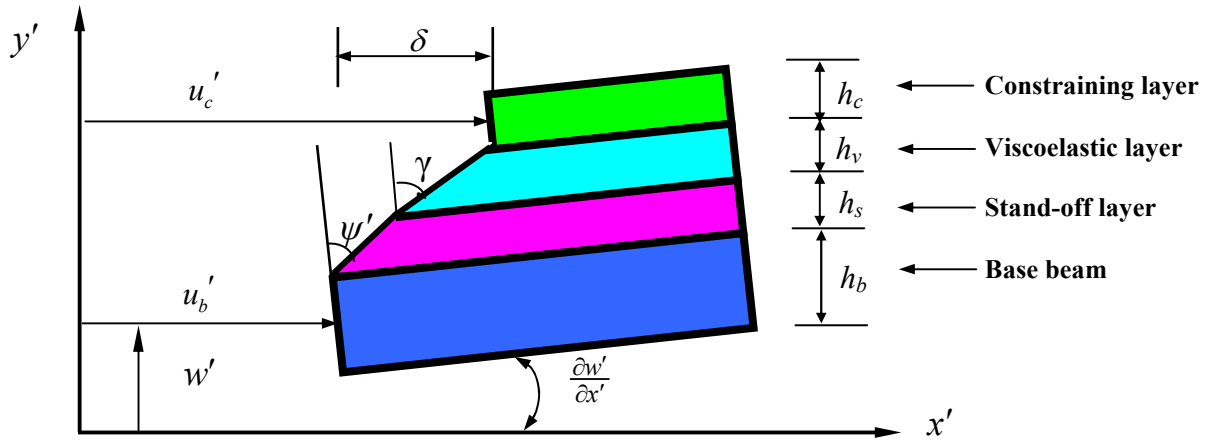


**Figure (10) - Total Axial Deflection of layers**

For small displacement magnitudes the deformation can be expressed in terms of angular

displacement as

$$h_s \psi' + h_v \gamma' \quad (4)$$

where  $\gamma'$  and  $\psi'$  denote the shear strains in the viscoelastic and stand-off layers.

Comparing the above two equations

$$h_s \psi' + h_v \gamma' = (h_s + h_v + \frac{h_c}{2} + y_b) \frac{\partial w'}{\partial x'} + (u_c' - u_b') \quad (5)$$

Rearranging in terms of  $\psi'$  gives

$$\psi' = \frac{u_c' - u_b'}{h_s} + (1 + \frac{h_c + 2h_v + 2y_b}{2h_s}) \frac{\partial w'}{\partial x'} \quad (6)$$

## 2.3 Constitutive Equations

### For Base Beam and Stand-off layer

Using the composite beam theory for base beam and SOL, then the axial strain  $\varepsilon_o$  at the neutral axis of the base beam is given by

$$\varepsilon_o = \frac{\partial u_b'}{\partial x'} \quad (7)$$

and the curvature  $\kappa$  of composite beam

$$\kappa = \frac{\partial^2 w'}{\partial x'^2} \quad (8)$$

Therefore, the axial strain  $\varepsilon_x$  across the composite beam (i.e., the base beam and SOL) is given by:

$$\varepsilon_x = \varepsilon_o - y\kappa \quad (9)$$

Hence, the stress  $\sigma_x$  in the axial direction for base beam becomes:

$$\sigma_x = E_b(\varepsilon_o - y\kappa) \quad (10)$$

and for the SOL

$$\sigma_x = E_s(\varepsilon_o - y\kappa) \quad (11)$$

The total axial force  $T_{bs}$  across the base beam and SOL can be determined by integrating across the cross-section to give:

$$T_{bs} = \int_{b,s} \sigma_x A = (EA)_{bs} \varepsilon_o - (EQ)_{bs} \kappa \quad (12)$$

where  $(EA)_{bs}$  is axial rigidity of the composite base beam/stand-off layer

$$(EA)_{bs} = E_b A_b + E_s A_s \quad (13)$$

and  $(EQ)_{bs}$  is product of first moment of area of each layer and its Elastic Modulus.

$$(EQ)_{bs} = E_b Q_b + E_s Q_s \quad (14)$$

Similarly, the total moment  $M_{bs}$  acting across the composite of base beam/stand-off layers can be determined from

$$M_{bs} = - \int_{b,s} \sigma_x y dA = -(EQ)_{bs} \varepsilon_o + (EI)_{bs} \kappa \quad (15)$$

where flexural rigidity  $(EI)_{bs}$  is defined as

$$(EI)_{bs} = E_b I_b + E_s I_s \quad (16)$$

The moments the base beam and stand-off layer  $M_{b,s}$  are taken from the neutral axis of the base beam.

#### For Constraining Layer

The internal axial tension  $T_c$  in the constraining layer can be found by the equation

$$T_c = E_c h_c b \frac{\partial u_c'}{\partial x'} \quad (17)$$

The bending moment  $M_c$  of the constraining layer is give by the equation

$$M_c = \frac{E_c b h_c^3}{12} \frac{\partial^2 w'}{\partial x'^2} \quad (18)$$

#### For Viscoelastic and stand-off Layer

The constitutive equations for the viscoelastic layer and the stand-off layer in the Laplace transform domain are given as

$$\tau_v = G_v \gamma' \text{ and } \tau_s = G_s \psi' \quad (19)$$

where  $G_v$  and  $G_s$  denote the shear moduli of the viscoelastic layer and the SOL.

## **2.4 Equilibrium Equations**

### Axial Direction

*a. base beam and stand-off layer composite*

From Figure (11), Newton's second law gives

$$\frac{dT_{bs}}{dx'} + \tau_s b + f_{bs} = (\rho_b + \rho_s) \ddot{u}'_b \quad (20)$$

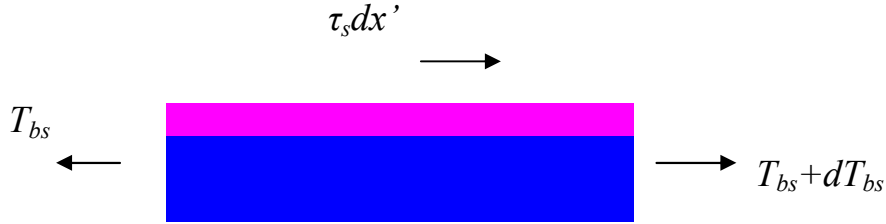


**Figure (11)** - Base Beam and stand-off Layer Axial Forces

*b. constraining layer in axial direction*

From Figure (12), Newton's second law gives

$$\frac{dT_c}{dx'} + \tau_v b + f_c = \rho_c \ddot{u}'_c \quad (21)$$

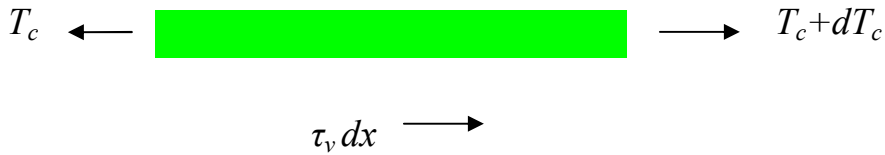


**Figure (12)** - Constraining Layer Axial Force

### Lateral Direction

The following equations are results of the application of Newton's second law applied in the lateral direction

*a. Base beam and stand-off layer:*

From Figure (13),

$$\frac{dV_{bs}}{dx'} - p_s + q_{bs} = (\rho_b + \rho_s)\ddot{w}' \quad (22)$$

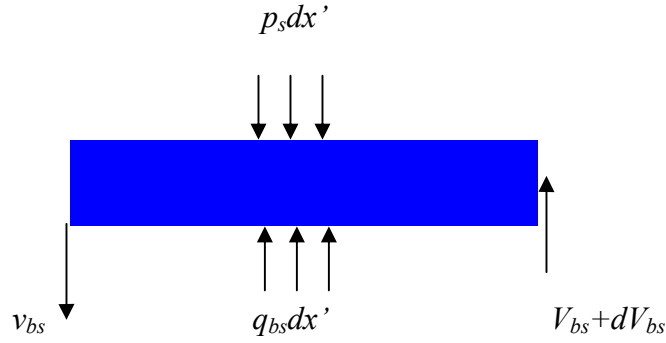


**Figure (13)** - Base Beam and stand-off Layer Lateral Forces

*b. Viscoelastic Layer:*

From Figure (14),

$$\frac{dV_v}{dx'} - p_c + p_s + q_v = \rho_v \ddot{w}' \quad (23)$$

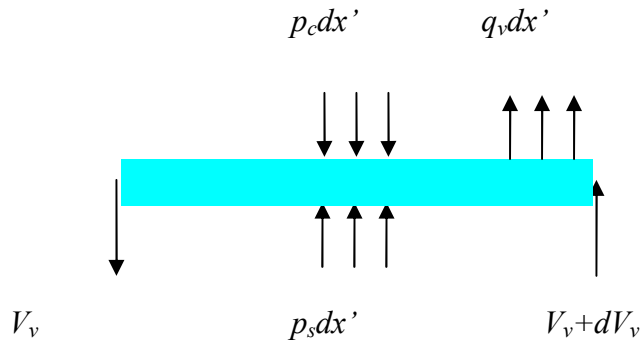


**Figure (14)** - Viscoelastic Layer Lateral Forces



*c. Constraining layer*

From Figure (15),

$$\frac{dV_c}{dx'} + p_c + q_c = \rho_c \ddot{w}' \quad (24)$$

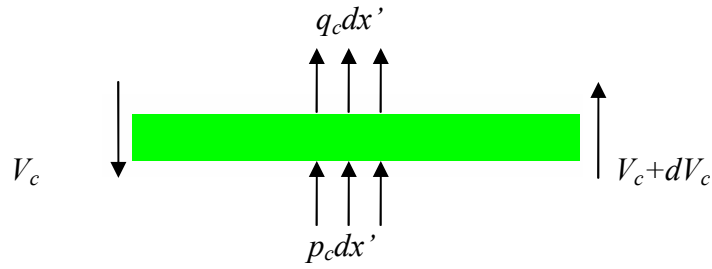


**Figure (15) - Constraining Layer Lateral Forces**

## 2.5 Moment Equilibrium Equations

*a. Base Beam and stand-off layer*

From Figure (16),

$$\frac{dM_{bs}}{dx'} + V_{bs} - \tau_s b(h_s + y_b) = 0 \quad (25)$$

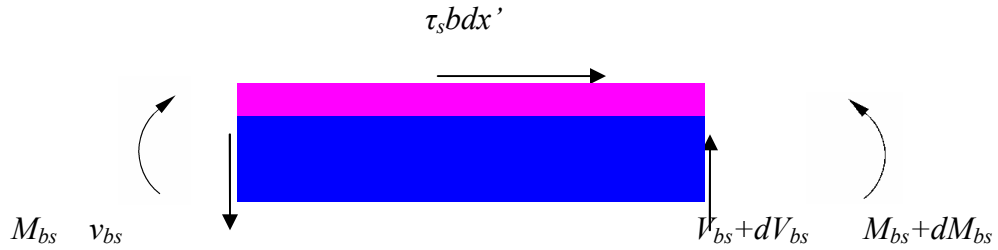


**Figure (16) - Base beam & stand off layer equilibrium**

*b. Viscoelastic Layers*

From Figure (17),

$$V_v = \tau_v b h_v \quad (26)$$

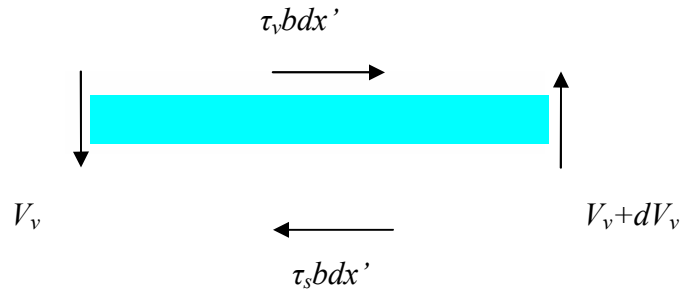


**Figure (17)** - Viscoelastic layer equilibrium

*c. Constraining layer*

$$\frac{dM_c}{dx'} + V_c + \tau_v b \frac{h_c}{2} = 0 \quad (27)$$

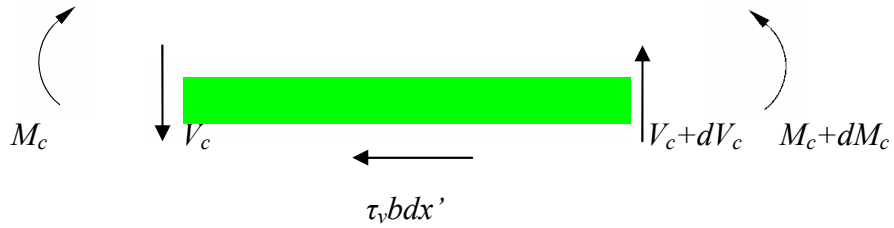


**Figure (18)** - Constraining layer equilibrium

In equations (20) through (27),  $b$  denotes the beam width,  $\tau_i$  is the shear stress,  $p_i$  defines the internal normal forces per unit length,  $q_i$  is the externally applied body forces per unit length,  $V_i$  and  $M_i$  denote the shear force and moment acting on  $i^{th}$  layer, also  $\rho_i$  denotes the density of the  $i^{th}$  layer with ( $i=c,v,s, b$ ).

For axial equilibrium of the viscoelastic layer

$$\tau_v = \tau_s \quad (28)$$

From Equations (19) and (28)

$$\psi' = \frac{G_v}{G_s} \gamma' \quad (29)$$

From Equations (6) and (29)

$$\psi' = \left( \frac{G_v}{h_s G_v + h_v G_s} \right) (u_c' - u_b') + \left( \frac{G_v}{h_s G_v + h_v G_s} \right) \left( \frac{2h_s + h_c + 2h_v + 2y_b}{2} \right) \frac{\partial w'}{\partial x'} \quad (30)$$

From Equations (19) and (28)

$$\tau_v = \left( \frac{G_s G_v}{h_s G_v + h_v G_s} \right) (u_c' - u_b') + \left( \frac{G_s G_v}{h_s G_v + h_v G_s} \right) \left( \frac{2h_s + h_c + 2h_v + 2y_b}{2} \right) \frac{\partial w'}{\partial x'} \quad (31)$$

From Equations (26) and (31)

$$V_v = \left( \frac{b h_v G_s G_v}{h_s G_v + h_v G_s} \right) + \frac{1}{2} \left( \frac{b h_v G_s G_v}{h_s G_v + h_v G_s} \right) (2h_s + 2h_v + h_c + 2y_b) \frac{\partial w'}{\partial x'} \quad (32)$$

From Equations (2).and (32)

$$\left(\frac{bh_v G_s G_v}{h_c G_v + h_v G_s}\right)\left(\frac{\partial u_c'}{\partial x'} - \frac{\partial u_b'}{\partial x'}\right) + \left(\frac{bh_v G_s G_v}{h_s G_v + h_v G_s}\right)\left(\frac{2h_c + 2h_v + h_c + 2y_b}{2}\right)\frac{\partial^2 w'}{\partial x'^2} + p_s + p_c + q_v = \rho_v \ddot{w}' \quad (33)$$

From Equation (25)

$$-(EQ)_{bs} \frac{\partial^2 u_b}{\partial x'^2} + (EZ)_{bs} \frac{\partial^3 w'}{\partial x'^3} + V_{bs} - G_s b(h_s + y_b) \left(\frac{G_v}{h_s G_v + h_v G_s}\right)(u_c' - u_b') - \frac{G_s b(h_s + y_b) G_v}{2} \left(\frac{2h_s + 2h_v + h_c + 2y_b}{h_s + G_v + h_v G_s}\right) \frac{\partial w'}{\partial x'} = 0 \quad (34)$$

From Equations (22) and (34)

$$(EQ)_{bs} \frac{\partial^3 u_b'}{\partial x'^3} - (EI)_{bs} \frac{\partial^4 w'}{\partial x'^4} + \frac{G_s b(h_s + y_b) G_v}{h_s G_v + h_s G_s} \left(\frac{\partial u_c'}{\partial x'} - \frac{\partial u_b'}{\partial x'}\right) + \frac{G_s b(h_s + y_b) G_v}{2} \left(\frac{2h_s + 2h_v + h_c + 2y_b}{h_s G_v + h_v G_s}\right) \frac{\partial^2 w'}{\partial x'^2} - p_s + q_{bs} = (\rho_b + \rho_s) \ddot{w}' \quad (35)$$

From Equation (27)

$$\frac{E_c b h_c^3}{12} \frac{\partial^3 w'}{\partial x'^3} + V_c - \frac{h_c G_s G_v b}{2(h_c G_v + h_v G_s)}(u_c' - u_b') - \left(\frac{2h_c b G_v G_s}{h_c G_v + h_v G_s}\right) \left(\frac{2h_c + 2h_v + h_c + 2y_b}{4}\right) \frac{\partial w'}{\partial x'} = 0 \quad (36)$$

From Equations (24) and (36)

$$\begin{aligned}
& -\frac{E_c b h^3}{12} \frac{\partial^4 w'}{\partial x'^4} + \frac{h_c G_s G_v b}{2(h_c G_v + h_v G_s)} \left( \frac{\partial u_c'}{\partial x'} - \frac{\partial u_b'}{\partial x'} \right) \\
& + \left( \frac{h_c b G_v G_s}{h_s G_v + h_v G_s} \right) \left( \frac{2h_c + 2h_v + h_c + 2y_b}{4} \right) \frac{\partial^2 w'}{\partial x'^2} + p_c + q_c = \rho_c \ddot{w}'
\end{aligned} \tag{37}$$

Adding Equations (33), (35) and (37)

$$\begin{aligned}
& \left( \frac{G_s G_v b}{h_s G_v + h_v G_s} \right) \left( \frac{h_v + h_s + 2h_v + h_c}{2} \right) \left( h_c + h_s + y_b + \frac{h_c}{2} \right) \left( \frac{\delta^2 w'}{\delta x'} - \frac{\delta u_b'}{\delta x'} \right) \\
& + \left( \frac{G_s G_v b}{h_s G + h_v G_s} \right) \left( \frac{2h_s + 2h_v + 2y_b + h_c}{2} \right) \left( h_c + h_s + y_b + \frac{h_c}{2} \right) \frac{\delta^2 w'}{\delta x'^2} = (\rho_b + \rho_s + \rho_v + \rho_c) \ddot{w}'
\end{aligned} \tag{38}$$

Let

$$\alpha \equiv y_b + h_s + h_v + \frac{h_c}{2} \quad \rho = \rho_b + \rho_s + \rho_v + \rho_c$$

$$q = q_{bs} + q_v + q_c$$

Then, equation (38) reduces to

$$\begin{aligned}
& \frac{G_s G_v b}{(h_s G_s + G_s h_v)} \alpha \left( \frac{\partial u_c'}{\partial x'} - \frac{\partial u_b'}{\partial x'} \right) + \frac{G_s G_v b}{(h_s G_s + h_v G_s)} \alpha^2 \frac{\partial^2 w'}{\partial x'^2} + \\
& (EQ)_{bs} \frac{\partial^3 u_b'}{\partial x'^3} - (EI)_{bs} \frac{\partial^4 w'}{\partial x'^4} - (EI)_c \frac{\partial^4 w'}{\partial x'^4} + (q_{bs} + q_c + q_c) = \rho \ddot{w}'
\end{aligned} \tag{39}$$

Substituting in above

$$D_t = (EI)_{bs} + (EI)_c$$

We get the following equation

$$\begin{aligned} & \left( -\frac{G_s G_v b \alpha}{h_s G_s + G_s h_v} \frac{\delta}{\delta x'} + (EQ)_{bs} \frac{\delta^3}{\delta x'^3} \right) u'_b + \left( \frac{G_s G_v b \alpha}{h_s G_v + h_v G_s} \frac{\delta}{\delta x'} \right) u'_c \\ & + \left( \frac{G_s G_v b \alpha^2}{h_s G_v + h_v G_s} \frac{\delta^2}{\delta x'^2} - D_t \frac{\delta^4}{\delta x'^4} \right) w' - \rho \ddot{w} = -q \end{aligned} \quad (40)$$

$$\begin{aligned} & \left( D_t \frac{\delta^4}{\delta x'^4} - \frac{G_s G_v b \alpha^2}{h_s G_v + h_v G_s} \frac{\delta^2}{\delta x'^2} \right) w' - \left( \frac{b \alpha G_s G_v}{h_s G_v + G_s h_v} \frac{\delta}{\delta x'} \right) u'_c \\ & + \left( - (EQ)_{bs} \frac{\delta^3}{\delta x'^3} + \frac{G_s G_v b \alpha}{G_s h_v + G_v h_s} \frac{\delta}{\delta x'} \right) u'_b + \rho \ddot{w}' = q \end{aligned} \quad (41)$$

From Equation (20)

$$\begin{aligned} & - (EQ)_{bs} \frac{\partial w'^3}{\partial x'^3} w' + (EA)_{bs} \frac{\partial^2}{\partial x'^2} u'_b + \left( \frac{b G_s G_v}{h_s G_v + h_v G_s} \right) (u'_c - u'_b) + \\ & f_{bs} + \left( \frac{b G_s G_v}{h_s G_v + h_v G_s} \right) \alpha \frac{\partial w'}{\partial x'} = (\rho_b + \rho_s) \ddot{u}'_b \end{aligned} \quad (42)$$

$$\begin{aligned} & \left( (EQ)_{bs} \frac{\partial^3}{\partial x'^3} - \frac{b \alpha G_s G_v}{(h_s G_v + h_v G_s)} \frac{\partial}{\partial x'} \right) w' + \left( - (EA)_{bs} \frac{\partial^2}{\partial x'^2} + \frac{b G_s G_v}{h_s G_v + h_v G_s} \right) u'_b \\ & - \left( \frac{b G_s G_v}{h_s G_v + h_v G_s} \right) u'_c + (\rho_b + \rho_s) \ddot{u}'_b = f_{bs} \end{aligned} \quad (43)$$

From Equation (21)

$$E_c h_c b \frac{\partial^2 u'_c}{\partial x'^2} - \frac{b G_s G_v}{h_s G_v + h_v G_s} (u'_c - u'_b) - \left( \frac{b G_s G_v}{h_s G_v + h_v G_s} \right) \alpha \frac{\partial w'}{\partial x'} - \rho_c \ddot{u}'_c = f_c \quad (44)$$

$$\begin{aligned}
& \left( \frac{G_v G_s b}{h_s G_v + h_v G_s} \alpha \frac{\partial}{\partial x'} \right) w' - \left( \frac{b G_s G_v}{h_s G_v + h_s G_v} \right) u_b' + \\
& \left( -E_c h_c b \frac{\partial^2}{\partial x'^2} + \frac{b G_s G_v}{h_s G_v + h_v G_s} \right) u_c' + \rho_c \ddot{u}_c' = f_c
\end{aligned} \tag{45}$$

Equations (41), (43) and (45) are combined in the following matrix form

$$\begin{aligned}
& \left[ \begin{array}{ccc}
D_t \frac{\partial^4}{\partial x'^4} - \frac{b \alpha^2 G_v G_s}{G_v h_s + G_s h_v} \frac{\partial^2}{\partial x'^2} & - \frac{b \alpha G_v G_s}{G_v h_s + G_s h_v} \frac{\partial}{\partial x'} & - (EQ)_{bs} \frac{\partial^3}{\partial x'^3} + \frac{b \alpha G_v G_s}{G_v h_s + G_s h_v} \frac{\partial}{\partial x'} \\
\frac{b \alpha G_v G_s}{G_v h_s + G_s h_v} \frac{\partial}{\partial x'} & - E_c A_c \frac{\partial^2}{\partial x'^2} + \frac{b G_v G_s}{G_v h_s + G_s h_v} & - \frac{b G_v G_s}{G_v h_s + G_s h_v} \\
(EQ)_{bs} \frac{\partial^3}{\partial x'^3} - \frac{b \alpha G_v G_s}{G_v h_s + G_s h_v} \frac{\partial}{\partial x'} & - \frac{b G_v G_s}{G_v h_s + G_s h_v} & - (EA)_{bs} \frac{\partial^2}{\partial x'^2} + \frac{b G_v G_s}{G_v h_s + G_s h_v}
\end{array} \right] \\
& + s'^2 \begin{bmatrix} \rho & 0 & 0 \\ 0 & \rho_c & 0 \\ 0 & 0 & \rho_b + \rho_s \end{bmatrix}
\end{aligned} \tag{46}$$

$$\begin{pmatrix} \bar{w}'(x', s') \\ \bar{u}_c'(x', s') \\ \bar{u}_b'(x', s') \end{pmatrix} = - \begin{pmatrix} q' \\ f'_c \\ f'_{bs} \end{pmatrix}$$

The equations of motion can now be normalized by using the following substitutions:

$$w(x, s) \equiv \frac{\bar{w}'(x', s')}{h_b}, u_c(x, s) \equiv \frac{\bar{u}'_c(x', s')}{h_b}, u_b(x, s) \equiv \frac{\bar{u}'_b(x', s')}{h_b}$$

$$x = \frac{x'}{l}, s \equiv \sqrt{\frac{\rho l^4}{D_t}} s' \quad (47)$$

$$q \equiv \frac{q' l^4}{D_t h_b}, f_c \equiv \frac{f'_c l^4}{D_t h_b}, f_{bs} \equiv \frac{f'_{bs} l^4}{D_t h_b} \quad (48)$$

The following dimensionless parameters and constants are used to simplify equations of motion

$$\varepsilon(s) \equiv \frac{b \alpha^2 G_v G_s l^2}{D_t (G_v h_s + G_s h_v)}$$

$$c_1^2 \equiv \frac{\rho_c}{\rho} \quad c_2^2 \equiv \frac{\rho_b + \rho_s}{\rho}$$

$$\beta \equiv \frac{l}{\alpha} \quad a_1 \equiv \frac{(E Q_{bs} l)}{D_t}$$

$$a_2 \equiv \frac{E_c A_c l^2}{D_t} \quad a_3 \equiv \frac{(EA)_{bs} l^2}{D_t} \quad (49)$$

The normalized equations of motion take the following form



$$\begin{aligned}
& \left\{ \begin{aligned} & D_t \frac{\partial^4}{\partial x'^4} - \frac{b\alpha^2 G_v G_s}{G_v h_s + G_s h_v} \frac{\partial^2}{\partial x'^2} & - \frac{b\alpha G_v G_s}{G_v h_s + G_s h_v} \frac{\partial}{\partial x'} & - (EQ)_{bs} \frac{\partial^3}{\partial x'^3} + \frac{b\alpha G_v G_s}{G_v h_s + G_s h_v} \frac{\partial}{\partial x'} \\ & \frac{b\alpha G_v G_s}{G_v h_s + G_s h_v} \frac{\partial}{\partial x'} & - E_c A_c \frac{\partial^2}{\partial x'^2} + \frac{bG_v G_s}{G_v h_s + G_s h_v} & - \frac{bG_v G_s}{G_v h_s + G_s h_v} \\ (EQ)_{bs} \frac{\partial^3}{\partial x'^3} - \frac{b\alpha G_v G_s}{G_v h_s + G_s h_v} \frac{\partial}{\partial x'} & - \frac{bG_v G_s}{G_v h_s + G_s h_v} & - (EA)_{bs} \frac{\partial^2}{\partial x'^2} + \frac{bG_v G_s}{G_v h_s + G_s h_v} \end{aligned} \right\} + \\
& + s'^2 \begin{bmatrix} \rho & 0 & 0 \\ 0 & \rho_c & 0 \\ 0 & 0 & \rho_b + \rho_s \end{bmatrix} \\
& \begin{pmatrix} \bar{w}'(x', s') \\ \bar{u}_c'(x', s') \\ \bar{u}_b'(x', s') \end{pmatrix} = - \begin{pmatrix} q' \\ f'_c \\ f'_{bs} \end{pmatrix}
\end{aligned} \tag{50}$$

## 2.6 Boundary Conditions

The normalized boundary conditions for a cantilever beam excited at its base are as follows:

For the fixed end ( $x=0$ ) are:

$$w(0, s) = P(s) \tag{51}$$

$$\frac{dw(0, s)}{dx} = u_b(0, s) = \frac{du_c(0, s)}{dx} = 0 \tag{52}$$

For the free end ( $x=1$ ) :

$$\frac{d^2 w(1, s)}{dx^2} = 0 \tag{53}$$

$$\frac{du_c(1, s)}{dx} = \frac{du_b(1, s)}{dx} = 0, \tag{54}$$

$$-\frac{d^3 w(1,s)}{dx^3} + a_1 \frac{d^2 u_b(1,s)}{dx^2} + \varepsilon(s) \left\{ \frac{dw(1,s)}{dx} + \beta u_c(1,s) - \beta u_b(1,s) \right\} = 0 \quad (55)$$

The above equations and boundary conditions are now solved using Distributed Transfer Function Method and Finite Element Method and the two solutions are compared.

## 2.7 Summary

This chapter formulates the equations of motion of the passive stand off layer treated cantilever beam subjected to dynamic loading at the fixed end with the assumptions given in the beginning of the chapter. The equations of motion constitute one variable (lateral deflection of beam) with 4<sup>th</sup> order differential equation and two variables (axial deflections of base beam and constraining layer) with 2<sup>nd</sup> order differential equation of motion.

## CHAPTER 3

# Distributed Transfer Function Solution

## Method

### 3.1 Solution By Distributed Parameter Systems Transfer Function Method

The PSOL beam is solved analytically by the distributed transfer function method developed by Yang and Tan [10].

Equation (50) gives the simplified equations of motion in the Laplace Domain and Equations (51) to (55) give the boundary conditions.

Since the first equation in the Equation (51) has the term  $\frac{\partial^3 u_b}{\partial x^3}$ , therefore this equation has to be modified in order to be solved by the distributed transfer function method.

Partially differentiating the third equation in (50) with respect to  $x$ , gives

$$\begin{aligned} & \left( a_1 \frac{\partial^4}{\partial x^4} - \beta \frac{\partial^2}{\partial x^2} \varepsilon(s) \right) w + \left( -\beta \frac{\partial^2}{\partial x^2} \varepsilon(s) \right) w + \left( -\beta^2 \varepsilon(s) \frac{\partial}{\partial x} \right) u_c + \\ & \left( -a_3 \frac{\partial^3}{\partial x^3} + c_2^2 s^2 \frac{\partial}{\partial x} + \beta^2 \varepsilon(s) \frac{\partial}{\partial x} \right) u_b = -\frac{\partial}{\partial x} f_{bs} \end{aligned} \quad (56)$$

Multiply the above equation by  $-\alpha_1/\alpha_3$  yields

$$\begin{aligned} & \left( -\frac{a_1^2}{a_3} \frac{\partial^4}{\partial x^4} + \beta \frac{a_1}{a_3} \varepsilon(s) \frac{\partial^2}{\partial x^2} \right) w + \left( \frac{a_1 \beta^2}{a_3} \varepsilon(s) \frac{\partial}{\partial x} \right) u_c + \\ & \left( a_1 \frac{\partial^3}{\partial x^3} - \frac{a_1}{a_3} c_2^2 s^2 \frac{\partial}{\partial x} - \frac{a_1 \beta^2}{a_3} \varepsilon(s) \frac{\partial}{\partial x} \right) u_b = + \frac{a_1}{a_3} \frac{\partial f_{bs}}{\partial x} \end{aligned} \quad (57)$$

Adding this equation to the first equation in Equation (50) gives

$$\begin{aligned} & \left( \left( 1 + \frac{a_1^2}{a_3} \right) \frac{\partial^4}{\partial x^4} + s^2 + \beta \frac{a_1}{a_3} \varepsilon(s) \frac{\partial^2}{\partial x^2} - \varepsilon(s) \frac{\partial^2}{\partial x^2} \right) w + \left( \left( \frac{a_1}{a_3} \beta^2 - \beta \right) \varepsilon \frac{\partial}{\partial x} \right) u_c \\ & + \left( -\frac{a_1}{a_3} c_2^2 s^2 \frac{\partial}{\partial x} + \varepsilon \left( \beta - \frac{a_1}{a_3} \beta^2 \right) \frac{\partial}{\partial x} \right) u_b = -q + \frac{a_1}{a_3} \frac{\partial f_{bs}}{\partial x} \end{aligned} \quad (58)$$

As all external forces are zero and the beam is excited dynamically at its fixed end, then the modified equations of motion are given by:

$$\left\{ \begin{bmatrix} \left( 1 - \frac{a_1^2}{a_3} \right) \frac{\partial^4}{\partial x^4} + s^2 & 0 & -\frac{a_1}{a_3} c_2^2 s^2 \frac{\partial}{\partial x} \\ 0 & -a_2 \frac{\partial^2}{\partial x^2} + c_1^2 s^2 & 0 \\ a_1 \frac{\partial^3}{\partial x^3} & 0 & -a_3 \frac{\partial^2}{\partial x^2} + c_2^2 s^2 \end{bmatrix} + \right.$$

$$\varepsilon(s)x \begin{bmatrix} \left( \beta \frac{a_1}{a_3} - 1 \right) \frac{\partial^2}{\partial x^2} & \left( \frac{\beta^2 a_1}{a_3} - \beta \right) \frac{\partial}{\partial x} & \left( \beta - \frac{\beta^2 a_1}{a_3} \right) \frac{\partial}{\partial x} \\ \beta \frac{\partial}{\partial x} & \beta^2 & -\beta^2 \\ -\beta \frac{\partial}{\partial x} & -\beta^2 & \beta^2 \end{bmatrix} \begin{cases} w(x,s) \\ u_c(x,s) \\ u_b(x,s) \end{cases} = \begin{pmatrix} -q + \frac{\partial f_{bs}}{\partial x} \\ -f_c \\ -f_{bs} \end{pmatrix} \quad (59)$$

For the sake of simplicity, all the initial conditions are assumed to be zero.

### 3.2 Equations In State Space Form

The equations of motion can be written in the state space form as follows

$$\frac{\partial}{\partial x} y(x,s) = F(s)y(x,s) + q(x,s), \dots \dots \dots x \in (0,1) \quad (60)$$

where  $y(x,s)$ ,  $q(s)$ , and  $F(s)$  are given by

$$y(x,s) = \left\{ w \quad \frac{\partial w}{\partial x} \quad \frac{\partial^2 w}{\partial x^2} \quad \frac{\partial^3 w}{\partial x^3} \quad u_c \quad \frac{\partial}{\partial x} u_c \quad u_b \quad \frac{\partial}{\partial x} u_b \right\}^T, \quad (61)$$

$$q(x,s) = \{0 \quad 0 \quad 0 \quad 0 \quad 0 \quad 0 \quad 0 \quad 0\}^T, \quad (62)$$

and

$$F(s) = \begin{bmatrix} 0 & 1 & 0 & 0 & 0 & 0 & 0 & 0 \\ 0 & 0 & 1 & 0 & 0 & 0 & 0 & 0 \\ 0 & 0 & 0 & 1 & 0 & 0 & 0 & 0 \\ -s^2 \left( \frac{a_3}{a_3 - a_1^2} \right) & 0 & \frac{a_3}{(a_3 - a_1^2)} \left[ \varepsilon - \frac{\beta \varepsilon a_1}{a_3} \right] & 0 & 0 & \frac{a_3}{(a_3 - a_1^2)} \left[ \varepsilon \beta - \frac{\varepsilon \beta^2 a_1}{a_3} \right] & 0 & \frac{a_3}{(a_3 - a_1^2)} \left[ \frac{c_2^2 s^2 a_1}{a_3} + \frac{\beta^2 \varepsilon a_1}{a_3} - \beta \varepsilon \right] \\ 0 & 0 & 0 & 0 & 0 & 1 & 0 & 0 \\ 0 & \frac{+\varepsilon \beta}{a_2} & 0 & 0 & \frac{c_1^2 s^2 + \varepsilon \beta^2}{a_2} & 0 & \frac{-\varepsilon \beta^2}{a_2} & 0 \\ 0 & 0 & 0 & 0 & 0 & 0 & 0 & 1 \\ 0 & \frac{-\beta \varepsilon}{a_3} & 0 & \frac{a_1}{a_3} & \frac{-\varepsilon \beta^2}{a_3} & 0 & \frac{c_2^2 s^2 + \varepsilon \beta^2}{a_3} & 0 \end{bmatrix}$$

### 3.3 Boundary Conditions

The boundary condition indicating the shear force equilibrium at the free end of cantilever beam has to be modified to enable it to be incorporated into the State Space model

Equation (55) which is given by

$$-\frac{d^3w(1,s)}{dx^3} + a_1 \frac{d^2u_b(1,s)}{dx^2} + \varepsilon(s) \left\{ \frac{dw(1,s)}{dx} + \beta u_c(1,s) - \beta u_b(1,s) \right\} = 0 \quad (63)$$

is converted to the following form in order to eliminate  $\partial^2 u_b / \partial x^2$

$$\left( \frac{a_1^2}{a_3} - 1 \right) \frac{d^3w}{dx^3} + \varepsilon \left( 1 - \beta \frac{a_1}{a_3} \right) \frac{dw}{dx} + \left( 1 - \beta \frac{a_1}{a_3} \right) \varepsilon \beta u_c + \left( \beta \frac{a_1}{a_3} - 1 \right) \varepsilon \beta u_b = 0 \quad (64)$$

Hence, the boundary conditions can be formulated as

$$M(s)y(0,s) + N(s)y(1,s) = \gamma(s) \quad (65)$$

where

$$M(s) = \begin{bmatrix} 1 & 0 & 0 & 0 & 0 & 0 & 0 & 0 \\ 0 & 1 & 0 & 0 & 0 & 0 & 0 & 0 \\ 0 & 0 & 0 & 0 & 0 & 1 & 0 & 0 \\ 0 & 0 & 0 & 0 & 0 & 0 & 1 & 0 \\ 0 & 0 & 0 & 0 & 0 & 0 & 0 & 0 \\ 0 & 0 & 0 & 0 & 0 & 0 & 0 & 0 \\ 0 & 0 & 0 & 0 & 0 & 0 & 0 & 0 \\ 0 & 0 & 0 & 0 & 0 & 0 & 0 & 0 \end{bmatrix},$$

$$N(s) = \begin{bmatrix} 0 & 0 & 0 & 0 & 0 & 0 & 0 & 0 \\ 0 & 0 & 0 & 0 & 0 & 0 & 0 & 0 \\ 0 & 0 & 0 & 0 & 0 & 0 & 0 & 0 \\ 0 & 0 & 0 & 0 & 0 & 0 & 0 & 0 \\ 0 & 0 & 1 & 0 & 0 & 0 & 0 & 0 \\ 0 & 0 & 0 & 0 & 1 & 0 & 0 & 0 \\ 0 & 0 & 0 & 0 & 0 & 0 & 0 & 1 \\ 0 & \varepsilon \left( 1 - \frac{\beta a_1}{a_3} \right) & 0 & -\frac{1}{K} & \varepsilon \left( \beta - \frac{\beta^2 a_1}{a_3} \right) & 0 & \varepsilon \left( \frac{\beta^2 a_1}{a_3} - \beta \right) & 0 \end{bmatrix},$$

and

$$\gamma(s) = \{P(s) \ 0 \ 0 \ 0 \ 0 \ 0 \ 0 \ 0\}^T$$

### 3.4 Solution

The solution to the above system of equations is given as follows

$$y(x, s) = \int_0^1 G(x, \varepsilon, s) q(\varepsilon, s) d\varepsilon + H(x, s) \gamma(s), x \in (0, 1) \quad (66)$$

where

$$G(x, \varepsilon, s) = \begin{cases} e^{F(s)x} \left( M(s) + N(s) e^{F(s)} \right)^{-1} M(s) e^{-F(s)\varepsilon}, & \varepsilon < x \\ -e^{F(s)x} \left( M(s) + N(s) e^{F(s)} \right)^{-1} N(s) e^{F(s)(1-\varepsilon)}, & \varepsilon > x \end{cases} \quad (67)$$



$$H(x,s) = e^{F(s)x} \left( M(s) + N(s)e^{F(s)} \right)^{-1} \quad (68)$$

As all the external forces are zeros, the solution reduces to

$$y(x,s) = H(x,s)\gamma(s), x \in (0,1) \quad (69)$$

or

$$\bar{w}(x,s) = \sum_{j=1}^n h_{1j}(x,s) \bar{y}_j(s) \quad (70)$$

The matrix  $e^{F(s)x}$  is called the fundamental matrix of  $F(s)$ . The fundamental matrix can be evaluated by the following **MATLAB** command *expm(F)*

### 3.5 Summary

A transfer function model of the PSOL treated beam treatment has been developed. The equations of motion have been modified to facilitate the formulation. The transfer function method will then be used to validate the predictions of the finite element method. The transfer function model is modeled only for uniform stand-off layer which is bonded along the length of the beam.

## CHAPTER 4

### Finite Element Model

#### 4.1 Solution By Finite Element Method

The development of the finite element solution of the system of equations and boundary conditions given by Equations (50) to (55), requires that the equations are transformed to the form given by the equation (59)

$$\left\{ \begin{bmatrix} \left(1 - \frac{a_1^2}{a_3}\right) \frac{\partial^4}{\partial x^4} + s^2 & 0 & -\frac{a_1}{a_3} c_2^2 s^2 \frac{\partial}{\partial x} \\ 0 & -a_2 \frac{\partial^2}{\partial x^2} + c_1^2 s^2 & 0 \\ a_1 \frac{\partial^3}{\partial x^3} & 0 & -a_3 \frac{\partial^2}{\partial x^2} + c_2^2 s^2 \end{bmatrix} + \right.$$

$$\left. \varepsilon(s) x \begin{bmatrix} \left(\beta \frac{a_1}{a_3} - 1\right) \frac{\partial^2}{\partial x^2} & \left(\frac{\beta^2 a_1}{a_3} - \beta\right) \frac{\partial}{\partial x} & \left(\beta - \frac{\beta^2 a_1}{a_3}\right) \frac{\partial}{\partial x} \\ \beta \frac{\partial}{\partial x} & \beta^2 & -\beta^2 \\ -\beta \frac{\partial}{\partial x} & -\beta^2 & \beta^2 \end{bmatrix} \right\} \begin{pmatrix} w(x, s) \\ u_c(x, s) \\ u_b(x, s) \end{pmatrix} = \begin{pmatrix} -q + \frac{\partial f_{bs}}{\partial x} \\ -f_c \\ -f_{bs} \end{pmatrix}$$

## 4.2 Derivation Of Element Equations

In this step, a typical element is considered and a weak form of the equations of motion is constructed over the element. The weak form of the above equations over an element is derived after defining the following terms:

$$K_1 = 1 - \frac{a_1^2}{a_3}$$

$$K_2 = \frac{a_1}{a_3} \beta \varepsilon - \varepsilon$$

$$K_3 = \beta^2 \varepsilon \frac{a_1}{a_3} - \beta \varepsilon$$

$$K_4 = \beta \varepsilon - c_2^2 s^2 \frac{a_1}{a_3} - \beta^2 \varepsilon \frac{a_1}{a_3},$$

$$K_5 = c_1^2 s^2 + \beta^2 \varepsilon,$$

$$K_6 = -\beta^2 \varepsilon,$$

$$K_7 = c_2^2 s^2 + \beta^2 \varepsilon, \text{ and}$$

$$K_8 = -\beta \varepsilon$$

Substituting these terms in the equations of motion, gives

$$\left[ \begin{array}{ccc} K_1 \frac{\partial^4}{\partial x^4} + K_2 \frac{\partial^2}{\partial x^2} + s^2 & K_3 \frac{\partial}{\partial x} & K_4 \frac{\partial}{\partial x} \\ -K_8 \frac{\partial}{\partial x} & -a_2 \frac{\partial^2}{\partial x^2} + K_5 & K_6 \\ a_1 \frac{\partial^3}{\partial x^3} + K_8 \frac{\partial}{\partial x} & K_6 & -a_3 \frac{\partial^2}{\partial x^2} + K_7 \end{array} \right] \begin{pmatrix} w(x,s) \\ u_c(x,s) \\ u_b(x,s) \end{pmatrix} = \begin{pmatrix} 0 \\ 0 \\ 0 \end{pmatrix}$$

The following Hermite Interpolation functions are used for the normalized lateral deflection and Lagrange interpolation functions are employed for the axial deflections.

$$w = u_1^e v_1 + u_2^e v_2 + u_3^e v_3 + u_4^e v_4$$

$$u_1 = w(x_e), \dots, u_2 = -\frac{dw}{dx} \Big|_{x_e}, \dots, u_3 = w(x_{e+1}), \dots, u_4 = -\frac{dw}{dx} \Big|_{x_{e+1}},$$

$$u_c^e = u_5^e \theta_1 + u_6^e \theta_2, \text{ and}$$

$$u_b^e = u_7^e \Phi_1 + u_8^e \Phi_2.$$

where  $v_i$ ,  $\theta_i$  and  $\Phi_i$  are interpolation functions to be defined in Section 4.3.

Hence, the weak form of the first equation is given by

$$\int \left( \left( K_1 \frac{\partial^4}{\partial x^4} + K_2 \frac{\partial^2}{\partial x^2} + s^2 \right) w + \left( K_3 \frac{\partial}{\partial x} \right) u_c + \left( K_4 \frac{\partial}{\partial x} \right) u_b \right) v dx = 0$$

or

$$\begin{aligned}
& \int \left( -K_1 \frac{d^3 w}{dx^3} \frac{dv}{dx} + \left( K_2 \frac{d^2 w}{dx^2} + s^2 w + K_3 \frac{du_c}{dx} + K_4 \frac{du_b}{dx} \right) v \right) dx + \left[ v K_1 \frac{d^3 w}{dx^3} \right]_{xc}^{xc+1} = 0 \\
& \int \left( K_1 \frac{d^2 w}{dx^2} \frac{d^2 v}{dx^2} + \left( K_2 \frac{d^2 w}{dx^2} + s^2 w + K_3 \frac{du_c}{dx} + K_4 \frac{du_b}{dx} \right) v \right) dx + \\
& \quad \left[ v K_1 \frac{d^3 w}{dx^3} - K_1 \frac{dv}{dx} \frac{d^2 w}{dx^2} \right]_{xc}^{xc+1} = 0 \\
& \int \left( \left( K_1 \frac{d^2 w}{dx^2} \frac{d^2 v}{dx^2} - K_2 \frac{dw}{dx} \frac{dv}{dx} \right) + v \left( s^2 w + K_3 \frac{du_c}{dx} + K_4 \frac{du_b}{dx} \right) \right) dx + \\
& \quad \left[ v K_1 \frac{d^3 w}{dx^3} - K_1 \frac{dv}{dx} \frac{d^2 w}{dx^2} + v K_2 \frac{dw}{dx} \right]_{xc}^{xc+1} = 0
\end{aligned}$$

Similarly, the weak form of the second equation becomes

$$\int \left( -K_8 \frac{dw}{dx} - a_2 \frac{d^2 u_c}{dx^2} + K_5 u_c + K_6 u_b \right) \theta dx = 0$$

$$\text{or} \quad \int \left( -K_8 \frac{dw}{dx} \theta + a_2 \frac{du_c}{dx} \frac{d\theta}{dx} + K_5 u_c \theta + K_6 u_b \theta \right) dx - \left[ a_2 \frac{du_c}{dx} \theta \right] = 0$$

And the weak form of the third equation reduces to

$$\int \left( a_1 \frac{d^3 w}{dx^3} + K_8 \frac{dw}{dx} + K_6 u_c - a_3 \frac{d^2 u_b}{dx^2} + K_7 u_b \right) \Phi dx = 0$$

or

$$\int \left( a_1 \frac{d^3 w}{dx^3} \Phi + K_8 \frac{dw}{dx} \Phi + K_6 u_c \Phi + a_3 \frac{du_b}{dx} \frac{d\Phi}{dx} + K_7 u_b \Phi \right) dx + \left[ a_2 \frac{du_c}{dx} \Phi \right] = 0$$

### 4.3 Interpolation Functions

The interpolation functions and their derivatives are given as

$$\theta_1 = \Phi_1 = 1 - \frac{x}{h}$$

$$\theta_2 = \Phi_2 = \frac{x}{h}$$

$$\frac{d\theta_1}{dx} = \frac{d\Phi_1}{dx} = -1$$

$$\frac{d\theta_2}{dx} = \frac{d\Phi_2}{dx} = 1$$

$$v_1 = 1 - 3\left(\frac{x}{h}\right)^2 + 2\left(\frac{x}{h}\right)^3$$

$$\frac{dv_1}{dx} = -\frac{6}{h^2}x\left(1 - \frac{x}{h}\right)$$

$$\frac{d^2v_1}{dx^2} = -\frac{6}{h^2}\left(1 - 2\frac{x}{h}\right)$$

$$\frac{d^3v_1}{dx^3} = \frac{12}{h^3}$$

$$v_2 = -x\left(1 - \frac{x}{h}\right)^2$$

$$\frac{dv_2}{dx} = -1\left[1 + \frac{3x^2}{h^2} - 4\frac{x}{h}\right]$$

$$\frac{d^2v_2}{dx^2} = -\frac{2}{h}\left(\frac{3x}{h} - 2\right)$$

$$\frac{d^3 v_2}{dx^3} = -\frac{6}{h^2}$$

$$v_3 = 3\frac{x^2}{h^2} - 2\frac{x^3}{h^3}$$

$$\frac{dv_3}{dx} = \frac{6}{h^2} x \left(1 - \frac{x}{h}\right)$$

$$\frac{d^2 v_3}{dx^2} = +\frac{6}{h^2} \left(1 - \frac{2x}{h}\right)$$

$$\frac{d^3 v_3}{dx^3} = -\frac{12}{h^3}$$

$$v_4 = -x \left( \frac{x^2}{h^2} - \frac{x}{h} \right)$$

$$\frac{dv_4}{dx} = -\frac{x}{h} \left( 3\frac{x}{h} - 2 \right)$$

$$\frac{d^2 v_4}{dx^2} = -\frac{2}{h} \left( 3\frac{x}{h} - 2 \right)$$

$$\frac{d^3 v_4}{dx^3} = -\frac{6}{h^2}$$

Hence, the finite element model of the equations can be written in the form

$$[K]\{U\} = \{F\} + \{Q\}$$

where  $[K]$  = Stiffness matrix  $[K]$  is given by  $[K] = [K1 \ K2 \ K3 \ K4 \ K5 \ K6 \ K7 \ K8]$ . The elements  $Ki$  are defined below. Also,  $\{F\} = 0$ , and  $\{Q\} = 0$  except at the boundaries where it will

incorporate boundary conditions

The elements  $K_i$  are given by:

$$KI = \begin{bmatrix} K_1 \frac{d^2 v_1}{dx^2} \frac{d^2 v_1}{dx^2} + K_2 \frac{dv_2}{dx} \frac{dv_1}{dx} + s^2 v_1 v_1 \\ K_1 \frac{d^2 v_1}{dx^2} \frac{d^2 v_2}{dx^2} + K_2 \frac{dv_2}{dx} \frac{dv_2}{dx} + s^2 v_1 v_2 \\ -K_8 \frac{dv_1}{dx} \theta_1 \\ a_1 \frac{d^3 v_1}{dx^3} \phi_1 + K_8 \frac{dv_1}{dx} \phi_1 \\ K_1 \frac{d^2 v_1}{dx^2} \frac{d^2 v_3}{dx^2} + K_2 \frac{dv_2}{dx} \frac{dv_3}{dx} + s^2 v_1 v_3 \\ K_1 \frac{d^2 v_1}{dx^2} \frac{d^2 v_4}{dx^2} + K_2 \frac{dv_2}{dx} \frac{dv_4}{dx} + s^2 v_1 v_4 \\ -K_8 \frac{dv_1}{dx} \theta_2 \\ a_1 \frac{d^3 v_1}{dx^3} \phi_2 + K_8 \frac{dv_1}{dx} \phi_2 \end{bmatrix},$$



$$\mathbf{K2} = \begin{bmatrix} K_1 \frac{d^2 v_2}{dx^2} \frac{d^2 v_1}{dx^2} + K_2 \frac{dv_2}{dx} \frac{dv_1}{dx} + s^2 v_2 v_1 \\ K_1 \frac{d^2 v_2}{dx^2} \frac{d^2 v_2}{dx^2} + K_2 \frac{dv_2}{dx} \frac{dv_2}{dx} + s^2 v_2 v_2 \\ -K_8 \frac{dv_2}{dx} \theta_1 \\ a_1 \frac{d^3 v_2}{dx^3} \phi_1 + K_8 \frac{dv_2}{dx} \phi_1 \\ K_1 \frac{d^2 v_2}{dx^2} \frac{d^2 v_3}{dx^2} + K_2 \frac{dv_2}{dx} \frac{dv_3}{dx} + s^2 v_2 v_3 \\ K_1 \frac{d^2 v_2}{dx^2} \frac{d^2 v_4}{dx^2} + K_2 \frac{dv_2}{dx} \frac{dv_4}{dx} + s^2 v_2 v_4 \\ -K_8 \frac{dv_2}{dx} \theta_2 \\ a_1 \frac{d^3 v_2}{dx^3} \phi_2 + K_8 \frac{dv_2}{dx} \phi_2 \end{bmatrix},$$

$$\mathbf{K3} = \begin{bmatrix} K_3 \frac{d\theta_1}{dx} v_1 \\ K_3 \frac{d\theta_1}{dx} v_2 \\ a_2 \frac{d\theta_1}{dx} \frac{d\theta_1}{dx} + K_5 \theta_1 \theta_1 \\ K_6 \theta_1 \phi_1 \\ K_3 \frac{d\theta_1}{dx} v_3 \\ K_3 \frac{d\theta_1}{dx} v_4 \\ a_2 \frac{d\theta_1}{dx} \frac{d\theta_2}{dx} + K_5 \theta_1 \theta_2 \\ K_6 \theta_1 \phi_2 \end{bmatrix}, \mathbf{K4} = \begin{bmatrix} K_4 \frac{d\phi_1}{dx} v_1 \\ K_4 \frac{d\phi_1}{dx} v_2 \\ K_6 \phi_1 \theta_1 \\ a_3 \frac{d\phi_1}{dx} \frac{d\phi_1}{dx} + K_7 \phi_1 \phi_1 \\ K_4 \frac{d\phi_1}{dx} v_3 \\ K_4 \frac{d\phi_1}{dx} v_4 \\ K_6 \phi_1 \theta_2 \\ a_3 \frac{d\phi_1}{dx} \frac{d\phi_2}{dx} + K_7 \phi_2 \phi_1 \end{bmatrix},$$

$$\begin{aligned}
\mathbf{K5} &= \begin{bmatrix} K_1 \frac{d^2 v_3}{dx^2} \frac{d^2 v_1}{dx^2} + K_2 \frac{dv_4}{dx} \frac{dv_1}{dx} + s^2 v_3 v_1 \\ K_1 \frac{d^2 v_3}{dx^2} \frac{d^2 v_2}{dx^2} + K_2 \frac{dv_4}{dx} \frac{dv_2}{dx} + s^2 v_3 v_2 \\ -K_8 \frac{dv_3}{dx} \theta_1 \\ a_1^3 \frac{d^3 v_3}{dx^3} \phi_1 + K_8 \frac{dv_3}{dx} \phi_1 \\ K_1 \frac{d^2 v_3}{dx^2} \frac{d^2 v_3}{dx^2} + K_2 \frac{dv_4}{dx} \frac{dv_3}{dx} + s^2 v_3 v_3 \\ K_1 \frac{d^2 v_3}{dx^2} \frac{d^2 v_4}{dx^2} + K_2 \frac{dv_4}{dx} \frac{dv_4}{dx} + s^2 v_3 v_4 \\ -K_8 \frac{dv_3}{dx} \theta_2 \\ a_1^3 \frac{d^3 v_3}{dx^3} \phi_2 + K_8 \frac{dv_3}{dx} \phi_2 \end{bmatrix}, \mathbf{K6} = \begin{bmatrix} K_1 \frac{d^2 v_4}{dx^2} \frac{d^2 v_1}{dx^2} + K_2 \frac{dv_4}{dx} \frac{dv_1}{dx} + s^2 v_4 v_1 \\ K_1 \frac{d^2 v_4}{dx^2} \frac{d^2 v_2}{dx^2} + K_2 \frac{dv_4}{dx} \frac{dv_2}{dx} + s^2 v_4 v_2 \\ -K_8 \frac{dv_4}{dx} \theta_1 \\ a_1^3 \frac{d^3 v_4}{dx^3} \phi_1 + K_8 \frac{dv_4}{dx} \phi_1 \\ K_1 \frac{d^2 v_4}{dx^2} \frac{d^2 v_3}{dx^2} + K_2 \frac{dv_4}{dx} \frac{dv_3}{dx} + s^2 v_4 v_3 \\ K_1 \frac{d^2 v_4}{dx^2} \frac{d^2 v_4}{dx^2} + K_2 \frac{dv_4}{dx} \frac{dv_4}{dx} + s^2 v_4 v_4 \\ -K_8 \frac{dv_4}{dx} \theta_2 \\ a_1^3 \frac{d^3 v_4}{dx^3} \phi_2 + K_8 \frac{dv_4}{dx} \phi_2 \end{bmatrix}, \\
\mathbf{K7} &= \begin{bmatrix} K_3 \frac{d\theta_2}{dx} v_1 \\ K_3 \frac{d\theta_2}{dx} v_2 \\ a_2 \frac{d\theta_2}{dx} \frac{d\theta_1}{dx} + K_5 \theta_2 \theta_1 \\ K_6 \theta_2 \phi_1 \\ K_3 \frac{d\theta_2}{dx} v_3 \\ K_3 \frac{d\theta_2}{dx} v_4 \\ a_2 \frac{d\theta_2}{dx} \frac{d\theta_2}{dx} + K_5 \theta_2 \theta_2 \\ K_6 \theta_2 \phi_2 \end{bmatrix}, \text{ and } \mathbf{K8} = \begin{bmatrix} K_4 \frac{d\phi_2}{dx} v_1 \\ K_4 \frac{d\phi_2}{dx} v_2 \\ K_6 \phi_2 \theta_1 \\ a_3 \frac{d\phi_2}{dx} \frac{d\phi_1}{dx} + K_7 \phi_2 \phi_1 \\ K_4 \frac{d\phi_2}{dx} v_3 \\ K_4 \frac{d\phi_2}{dx} v_4 \\ K_6 \phi_2 \theta_2 \\ a_3 \frac{d\phi_2}{dx} \frac{d\phi_2}{dx} + K_7 \phi_2 \phi_2 \end{bmatrix}
\end{aligned}$$

Hence, the finite element model takes the following form

$$\begin{bmatrix} K_{11}^e & K_{12}^e & K_{13}^e & K_{14}^e & K_{15}^e & K_{16}^e & K_{17}^e & K_{18}^e \\ K_{21}^e & K_{22}^e & K_{23}^e & K_{24}^e & K_{25}^e & K_{26}^e & K_{27}^e & K_{28}^e \\ K_{31}^e & K_{32}^e & K_{33}^e & K_{34}^e & K_{35}^e & K_{36}^e & K_{37}^e & K_{38}^e \\ K_{41}^e & K_{42}^e & K_{43}^e & K_{44}^e & K_{45}^e & K_{46}^e & K_{47}^e & K_{48}^e \\ K_{51}^e & K_{52}^e & K_{53}^e & K_{54}^e & K_{55}^e & K_{56}^e & K_{57}^e & K_{58}^e \\ K_{61}^e & K_{62}^e & K_{63}^e & K_{64}^e & K_{65}^e & K_{66}^e & K_{67}^e & K_{68}^e \\ K_{71}^e & K_{72}^e & K_{73}^e & K_{74}^e & K_{75}^e & K_{76}^e & K_{77}^e & K_{78}^e \\ K_{81}^e & K_{82}^e & K_{83}^e & K_{84}^e & K_{85}^e & K_{86}^e & K_{87}^e & K_{88}^e \end{bmatrix} \begin{Bmatrix} u_1^e \\ u_2^e \\ u_3^e \\ u_4^e \\ u_5^e \\ u_6^e \\ u_7^e \\ u_8^e \end{Bmatrix} = \begin{Bmatrix} f_1^e \\ f_2^e \\ f_3^e \\ f_4^e \\ f_5^e \\ f_6^e \\ f_7^e \\ f_8^e \end{Bmatrix} + \begin{Bmatrix} Q_1^e \\ Q_2^e \\ Q_3^e \\ Q_4^e \\ Q_5^e \\ Q_6^e \\ Q_7^e \\ Q_8^e \end{Bmatrix}$$

or, in a compact matrix form:

$$[K] \{U\} = \{F\} + \{Q\}$$

#### 4.4 Assembly Of Matrices

For illustration purposes, the assembly of the matrices of two elements will take the form

$$[K] \{U\} = \{F\} + \{Q\}$$

where  $\{F\} = 0$ .

$$Q = \begin{Bmatrix} Q_1^1 \\ Q_2^1 \\ Q_3^1 \\ Q_4^1 \\ Q_5^1 + Q_2^1 \\ Q_6^1 + Q_2^2 \\ Q_7^1 + Q_b^2 \\ Q_8^1 + Q_u^2 \\ Q_5^2 \\ Q_6^2 \\ Q_7^2 \\ Q_8^2 \end{Bmatrix},$$

and  $[K]$  for two elements is given by:

$$[K] = \begin{bmatrix} K_{11}^1 & K_{12}^1 & K_{13}^1 & K_{14}^1 & K_{15}^1 & K_{16}^1 & K_{17}^1 & K_{18}^1 & 0 & 0 & 0 & 0 \\ K_{21}^1 & K_{22}^1 & K_{23}^1 & K_{24}^1 & K_{25}^1 & K_{26}^1 & K_{27}^1 & K_{28}^1 & 0 & 0 & 0 & 0 \\ K_{31}^1 & K_{32}^1 & K_{33}^1 & K_{34}^1 & K_{35}^1 & K_{36}^1 & K_{37}^1 & K_{38}^1 & 0 & 0 & 0 & 0 \\ K_{41}^1 & K_{42}^1 & K_{43}^1 & K_{44}^1 & K_{45}^1 & K_{46}^1 & K_{47}^1 & K_{48}^1 & 0 & 0 & 0 & 0 \\ K_{51}^1 & K_{52}^1 & K_{53}^1 & K_{54}^1 & K_{55}^1 + K_{11}^2 & K_{56}^1 + K_{12}^2 & K_{57}^1 + K_{13}^2 & K_{58}^1 + K_{14}^2 & K_{15}^2 & K_{16}^2 & K_{17}^2 & K_{18}^2 \\ K_{61}^1 & K_{62}^1 & K_{63}^1 & K_{64}^1 & K_{65}^1 + K_{21}^2 & K_{66}^1 + K_{22}^2 & K_{67}^1 + K_{23}^2 & K_{68}^1 + K_{24}^2 & K_{25}^2 & K_{26}^2 & K_{27}^2 & K_{28}^2 \\ K_{71}^1 & K_{72}^1 & K_{73}^1 & K_{74}^1 & K_{75}^1 + K_{31}^2 & K_{76}^1 + K_{32}^2 & K_{77}^1 + K_{33}^2 & K_{78}^1 + K_{34}^2 & K_{35}^2 & K_{36}^2 & K_{37}^2 & K_{38}^2 \\ K_{81}^1 & K_{82}^1 & K_{83}^1 & K_{84}^1 & K_{85}^1 + K_{41}^2 & K_{86}^1 + K_{42}^2 & K_{87}^1 + K_{43}^2 & K_{88}^1 + K_{44}^2 & K_{45}^2 & K_{46}^2 & K_{47}^2 & K_{48}^2 \\ 0 & 0 & 0 & 0 & K_{51}^2 & K_{52}^2 & K_{53}^2 & K_{54}^2 & K_{55}^2 & K_{56}^2 & K_{57}^2 & K_{58}^2 \\ 0 & 0 & 0 & 0 & K_{61}^2 & K_{62}^2 & K_{63}^2 & K_{64}^2 & K_{65}^2 & K_{66}^2 & K_{67}^2 & K_{68}^2 \\ 0 & 0 & 0 & 0 & K_{71}^2 & K_{72}^2 & K_{73}^2 & K_{74}^2 & K_{75}^2 & K_{76}^2 & K_{77}^2 & K_{78}^2 \\ 0 & 0 & 0 & 0 & K_{81}^2 & K_{82}^2 & K_{83}^2 & K_{84}^2 & K_{85}^2 & K_{86}^2 & K_{87}^2 & K_{88}^2 \end{bmatrix}$$

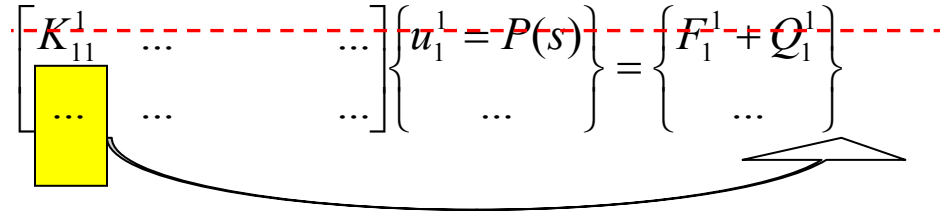
## 4.5 Application of the Boundary Conditions

At  $x=0$ , i.e., at the first node of the first element, there are four boundary conditions

$$w(0, s) = P(s)$$

$$\frac{dw(0, s)}{dx} = u_b(0, s) = \frac{du_c(0, s)}{dx} = 0$$

Substituting the value of  $w(0) = u_1^1$  and deleting the first row and moving all entries of the first column to the right hand side gives:

$$\begin{bmatrix} K_{11}^1 & \dots & \dots \\ \dots & \dots & \dots \end{bmatrix} \begin{Bmatrix} u_1^1 = P(s) \\ \dots \end{Bmatrix} = \begin{Bmatrix} F_1^1 + Q_1^1 \\ \dots \end{Bmatrix}$$


$$\begin{bmatrix} K_{22}^1 & \dots & \dots \\ \dots & \dots & \dots \end{bmatrix} \begin{Bmatrix} u_2^1 \\ \dots \end{Bmatrix} = \begin{Bmatrix} F_2^1 + Q_2^1 - K_{21}^1 P(s) \\ \dots \end{Bmatrix}$$

Similarly for  $\frac{dw(0, s)}{dx} = 0$ , and  $u_b(0, s) = 0$ , the rows and columns for  $u_2^1$  and  $u_4^1$  are deleted

For  $\frac{du_c(0, s)}{dx} = 0$ , substitute this value in

$$Q_3^1 = \left[ a_2 \frac{du_c}{dx} \theta \right]_{x=0}$$

to get  $Q_3^1 = 0$ .

At  $x=l$ , we have the following boundary conditions

$$\frac{du_c(1,s)}{dx} = \frac{du_b(1,s)}{dx} = 0$$

The terms for the last element in the overall matrix equation are

$$\begin{bmatrix} & & \dots \\ & \dots & \dots \\ \dots & \dots & K_{88}^n \end{bmatrix} \begin{Bmatrix} \dots \\ \dots \\ u_8^n \end{Bmatrix} = \begin{Bmatrix} \dots \\ \dots \\ F_8^n \end{Bmatrix} + \begin{Bmatrix} \dots \\ Q_7^n \\ Q_8^n \end{Bmatrix}$$

where

$$Q_7^n = \left[ a_2 \frac{du_c}{dx} \theta \right]_{x=1} \text{ to get } Q_7^n = 0,$$

$$Q_8^n = \left[ a_2 \frac{du_b}{dx} \theta \right]_{x=1} \text{ to get } Q_8^n = 0,$$

$$\frac{d^2 w(1,s)}{dx^2} = 0, \text{ and}$$

$$-\frac{d^3 w(1,s)}{dx^3} + a_1 \frac{d^2 u_b(1,s)}{dx^2} + \varepsilon(s) \left\{ \frac{dw(1,s)}{dx} + \beta u_c(1,s) - \beta u_b(1,s) \right\} = 0$$

Imposing these boundary conditions, the overall equation is simplified to

$$-K_1 \frac{d^3 w}{dx^3} - K_2 \frac{dw}{dx} - K_3 u_c - K_4 u_b = 0$$

$$Q_6^n = Q_5^n = \left[ vK_1 \frac{d^3 w}{dx^3} - K_1 \frac{dv}{dx} \frac{d^2 w}{dx^2} + vK_2 \frac{dw}{dx} \right]_{x=1}$$

or

$$Q_6^n = Q_5^n = \left[ K_1 \frac{d^3 w}{dx^3} + K_2 \frac{dw}{dx} \right]_{x=1}$$

or

$$Q_6^n = Q_5^n = -K_3 u_c - K_4 u_b$$

Finally,  $\{F\} = \{0\}$  as there are no external forces acting on the system except for dynamic displacement excitation applied at the fixed end.

## 4.6 Summary

A finite element model of the PSOL treated beam has been developed. Hermite interpolation functions have been used for the 4<sup>th</sup> order variable (lateral deflection) and Lagrangian interpolation functions have been used for the 2<sup>nd</sup> order variables (axial deflections of the base beam and stand-off layer).

# CHAPTER 5

## Computer Implementation

In this chapter, MATLAB codes are developed to determine the response of beams treated with PSOL using both the distributed transfer function method and the developed finite element model. A step-by-step development of the codes is presented for beams that have been analyzed by Yellin et al. [9] in order to validate the predictions of the developed models.

### 5.1 Distributed Transfer Function Method

The following table gives the properties of the materials that are used to illustrate the computer implementation of several test numerical examples.

|  |          |
|--|----------|
| <b>Beam material</b>                         | Al6061   |
| <b>SOL material</b>                          | DYAD 606 |
| <b>VEM material</b>                          | ISD 112  |
| <b>Constraining layer material</b>           | Al       |
| <b>Beam thickness (<math>h_b</math>)</b>     | 2.29 mm  |
| <b>SOL thickness (<math>h_s</math>)</b>      | 2.64 mm  |
| <b>VEM thickness (<math>h_v</math>)</b>      | .127 mm  |
| <b>Constraining layer (<math>h_c</math>)</b> | .203 mm  |
| <b>Width (<math>b</math>)</b>                | 11.75 mm |
| <b>Length (<math>l</math>)</b>               | 150 mm   |

The complex moduli  $G_v$  and  $G_s$  for the viscoelastic and PSOL layer are assumed to be  $1e^5(1+i)$ .



Also, these parameters are assumed to be constant through the frequency range.

## **Defining the constants (used in the code listed in Appendix A.1)**

### ***Excitation Function***

$P=1;$

$z=0 ;$

### ***Length***

$l=.15;$

### ***Width***

$b=.01175;$

### ***Stand off layer Height***

$h_s=.264*1e-3;$

### ***Constraining Layer***

$h_c=.203*1e-3;$

### ***Viscoelastic layer***

$h_v=.127*1e-3;$

### ***Base beam***

$h_b=2.29*1e-3;$

### ***Viscoelastic layer***

$G_v=1e5*(1+i);$

### ***Stand off layer Height***

$G_s=1e5*(1+i);$

### ***Mass/unit length of base beam***

$$p_b = 2850 \cdot b \cdot h_b;$$

### ***Constraining Layer***

$$p_c = 2850 \cdot b \cdot h_c;$$

### ***Viscoelastic layer***

$$p_v = 1100 \cdot b \cdot h_v;$$

### ***Stand off layer Height***

$$p_s = 1100 \cdot b \cdot h_s;$$

$$E_b = 72e9;$$

$$E_c = 72e9;$$

$$E_s = G_s \cdot 2.9;$$

$$E_v = G_v \cdot 2.9;$$

$$(EA)_{bs} = E_b A_b + E_s A_s$$

$$EA_{bs} = E_b \cdot (h_b \cdot b) + E_s \cdot (h_s \cdot b);$$

$$(EI)_{bs} = E_b I_b + E_s I_s$$

$$EI_{bs} = E_b \cdot (b \cdot h_b^3 / 12) + E_s \cdot (b \cdot h_s^3 / 12 + b \cdot h_s \cdot (h_s / 2 + h_b / 2)^2);$$

$$(EQ)_{bs} = E_b Q_b + E_s Q_s$$

$$EQ_{bs} = E_b \cdot (0) \cdot h_b / 4 + E_s \cdot (h_s \cdot b) \cdot (h_b / 2 + h_s / 2);$$

$$EA_c = E_c \cdot b \cdot h_c;$$

$$EI_c = E_c \cdot (b \cdot h_c^3 / 12);$$

$$\rho = \rho_b + \rho_s + \rho_v + \rho_c$$

$$p = p_s + p_c + p_v + p_b;$$

$$D_t = (EI)_{bs} + (EI)_c$$

$$D_t = EI_{bs} + EI_c;$$

$$\alpha \equiv y_b + h_s + h_v + \frac{h_c}{2}$$

$$\alpha = h_v + h_s + (h_b + h_c)/2;$$

$$\varepsilon(s) \equiv \frac{b \alpha^2 G_v G_s l^2}{D_t (G_v h_s + G_s h_v)}$$

$$E = b * \alpha^2 * G_v * G_s * l^2 / (D_t * (G_v * h_s + G_s * h_v));$$

$$c^2_1 \equiv \frac{\rho_c}{\rho}$$

$$c_1 = p_c/p;$$

$$c^2_1 \equiv \frac{\rho_c}{\rho}$$

$$c_2 = (p_b + p_s)/p;$$

$$\beta \equiv \frac{l}{\alpha}$$

$$B = l/\alpha;$$

$$a_1 \equiv \frac{(EQ_{bs}l)}{D_t}$$

$$a_1 = EQ_{bs} * l / D_t;$$

$$a_2 \equiv \frac{E_c A_c l^2}{D_t}$$

$$a_2 = E A c * l^2 / D_t;$$

$$a_3 \equiv \frac{(EA)_{bs} l^2}{D_t}$$

$$a_3 = E A b s * l^2 / D_t;$$

### Implementation of the program with for loop

for sr = 1:5:5000

$$s \equiv \sqrt{\frac{\rho l^4}{D_t}} s'$$

$$s = sr * i * (p * l^4 / Dt)^{.5} * \pi * 2;$$

$$F(s) =$$

$$\begin{bmatrix} 0 & 1 & 0 & 0 & 0 & 0 & 0 & 0 \\ 0 & 0 & 1 & 0 & 0 & 0 & 0 & 0 \\ 0 & 0 & 0 & 1 & 0 & 0 & 0 & 0 \\ -s^2 \left( \frac{a_3}{a_3 - a_1^2} \right) & 0 & \frac{a_3}{(a_3 - a_1^2)} \left[ \varepsilon - \frac{\beta a_1}{a_3} \right] & 0 & 0 & \frac{a_3}{(a_3 - a_1^2)} \left[ \varepsilon \beta - \frac{\varepsilon \beta^2 a_1}{a_3} \right] & 0 & \frac{a_3}{(a_3 - a_1^2)} \left[ \frac{c^2 2s^2 a_1}{a_3} + \frac{\beta^2 a_1}{a_3} - \beta \varepsilon \right] \\ 0 & 0 & 0 & 0 & 0 & 1 & 0 & 0 \\ 0 & \frac{+\varepsilon \beta}{a_2} & 0 & 0 & \frac{c^2 1s^2 + \varepsilon \beta^2}{a_2} & 0 & \frac{-\varepsilon \beta^2}{a_2} & 0 \\ 0 & 0 & 0 & 0 & 0 & 0 & 0 & 1 \\ 0 & \frac{-\beta \varepsilon}{a_3} & 0 & \frac{a_1}{a_3} & \frac{-\varepsilon \beta^2}{a_3} & 0 & \frac{c^2 2s^2 + \varepsilon \beta^2}{a_3} & 0 \end{bmatrix}$$

$$F = \begin{bmatrix} 0, 1, 0, 0, 0, 0, 0, 0; \\ 0, 0, 1, 0, 0, 0, 0, 0; \\ 0, 0, 0, 1, 0, 0, 0, 0; \\ -s^2 * k, 0, (E - B * E * a_1 / a_3) * k, 0, 0, (E * B - E * B^2 * a_1 / a_3) * k, 0, (c^2 * s^2 * a_1 / a_3 \dots \\ + B^2 * E * a_1 / a_3 - B * E) * k; \\ 0, 0, 0, 0, 0, 1, 0, 0; \\ 0, E * B / a_2, 0, 0, (c^2 * s^2 + E * B^2) / a_2, 0, -E * B^2 / a_2, 0; \\ 0, 0, 0, 0, 0, 0, 0, 1; \\ 0, -B * E / a_3, 0, a_1 / a_3, -E * B^2 / a_3, 0, (c^2 * s^2 + E * B^2) / a_3, 0 \end{bmatrix};$$

$$M(s) = \begin{bmatrix} 1 & 0 & 0 & 0 & 0 & 0 & 0 & 0 \\ 0 & 1 & 0 & 0 & 0 & 0 & 0 & 0 \\ 0 & 0 & 0 & 0 & 0 & 1 & 0 & 0 \\ 0 & 0 & 0 & 0 & 0 & 0 & 1 & 0 \\ 0 & 0 & 0 & 0 & 0 & 0 & 0 & 0 \\ 0 & 0 & 0 & 0 & 0 & 0 & 0 & 0 \\ 0 & 0 & 0 & 0 & 0 & 0 & 0 & 0 \\ 0 & 0 & 0 & 0 & 0 & 0 & 0 & 0 \end{bmatrix}$$

M=[ 1,0,0,0,0,0,0,0;  
0,1,0,0,0,0,0,0;  
0,0,0,0,0,1,0,0;  
0,0,0,0,0,0,0,1;  
0,0,0,0,0,0,0,0;  
0,0,0,0,0,0,0,0;  
0,0,0,0,0,0,0,0;  
0,0,0,0,0,0,0,0;  
0,0,0,0,0,0,0,0];

$$N(s) = \begin{bmatrix} 0 & 0 & 0 & 0 & 0 & 0 & 0 & 0 \\ 0 & 0 & 0 & 0 & 0 & 0 & 0 & 0 \\ 0 & 0 & 0 & 0 & 0 & 0 & 0 & 0 \\ 0 & 0 & 0 & 0 & 0 & 0 & 0 & 0 \\ 0 & 0 & 1 & 0 & 0 & 0 & 0 & 0 \\ 0 & 0 & 0 & 0 & 1 & 0 & 0 & 0 \\ 0 & 0 & 0 & 0 & 0 & 0 & 0 & 1 \\ 0 & \varepsilon \left( 1 - \frac{\beta a_1}{a_3} \right) & 0 & -\frac{1}{K} & \varepsilon \left( \beta - \frac{\beta^2 a_1}{a_3} \right) & 0 & \varepsilon \left( \frac{\beta^2 a_1}{a_3} - \beta \right) & 0 \end{bmatrix}$$

N=[ 0,0,0,0,0,0,0,0;  
0,0,0,0,0,0,0,0;  
0,0,0,0,0,0,0,0;  
0,0,0,0,0,0,0,0;  
0,0,1,0,0,0,0,0;  
0,0,0,0,0,1,0,0;  
0,0,0,0,0,0,1;  
0,E\*(1-B\*a1/a3),0,-1/k,E\*(B-B^2\*a1/a3),0,-E\*(B-B^2\*a1/a3),0];

$$\gamma(s) = \{P(s) \quad 0 \quad 0 \quad 0 \quad 0 \quad 0 \quad 0 \quad 0\}^t$$

Gamma=[ P 0 0 0 0 0 0 0 ]';

efs=expm(F);

$$H(x,s) = e^{F(s)x} (M(s) + N(s)e^{F(s)})^{-1}$$

H=efs\*(M+N\*efs)^-1;

```

H0=eye(8)/(M+N*efs)^-1;

 $y(x,s) = H(x,s)\gamma(s), x \in (0,1)$ 

eta=H*Gamma;

eta0=H0*Gamma;

z=z+1;

splot(z)=sr;

w(z)=abs(real(eta(1))/real(eta0(1)));

end

```

### ***Plotting***

```
semilogy(splot,w)
```

A complete listing of the MATLAB code is given in Section A.1 of the appendix.

## **5.2 Finite Element Method**

### ***Provide number of elements***

```
nem=11;
```

### ***Define constants (used in the code listed in Appendix A.2)***

#### ***Excitation Function***

```
P=1;
```

```
z=0 ;
```

#### ***Length***

```
l=.15;
```

***Width***

$$b=.01175;$$

***Stand off layer Height***

$$hs=.264*1e-3;$$

***Constraining Layer***

$$hc=.203*1e-3;$$

***Viscoelastic layer***

$$hv=.127*1e-3;$$

***Base beam***

$$hb=2.29*1e-3;$$

***Viscoelastic layer***

$$Gv=1e5*(1+i);$$

***Stand off layer Height***

$$Gs=1e5*(1+i);$$

***Mass/unit length of base beam***

$$pb=2850*b*hb;$$

***Constraining Layer***

$$pc=2850*b*hc;$$

***Viscoelastic layer***

$$pv=1100*b*hv;$$

***Stand off layer Height***

$$ps=1100*b*hs;$$

$$Eb=72e9;$$

$$E_c = 72e9;$$

$$E_s = G_s * 2.9;$$

$$E_v = G_v * 2.9;$$

$$(EA)_{bs} = E_b A_b + E_s A_s$$

$$E A_{bs} = E_b * (h_b * b) + E_s * (h_s * b);$$

$$(EI)_{bs} = E_b I_b + E_s I_s$$

$$E I_{bs} = E_b * (b * h_b^3 / 12) + E_s * (b * h_s^3 / 12 + b * h_s * (h_s / 2 + h_b / 2)^2);$$

$$(EQ)_{bs} = E_b Q_b + E_s Q_s$$

$$E Q_{bs} = E_b * (0) * h_b / 4 + E_s * (h_s * b) * (h_b / 2 + h_s / 2);$$

$$E A_c = E_c * b * h_c;$$

$$E I_c = E_c * (b * h_c^3 / 12);$$

$$\rho = \rho_b + \rho_s + \rho_v + \rho_c$$

$$p = p_s + p_c + p_v + p_b;$$

$$D_t = (EI)_{bs} + (EI)_c$$

$$D_t = E I_{bs} + E I_c;$$

$$\alpha \equiv y_b + h_s + h_v + \frac{h_c}{2}$$

$$\alpha = h_v + h_s + (h_b + h_c) / 2;$$

$$\varepsilon(s) \equiv \frac{b \alpha^2 G_v G_s l^2}{D_t (G_v h_s + G_s h_v)}$$

$$E = b * \alpha^2 * G_v * G_s * l^2 / (D_t * (G_v * h_s + G_s * h_v));$$

$$c^2_1 \equiv \frac{\rho_c}{\rho}$$



$$c1=pc/p;$$

$$c^2_1 \equiv \frac{\rho_c}{\rho}$$

$$c2=(pb+ps)/p;$$

$$\beta \equiv \frac{l}{\alpha}$$

$$B=l/\alpha;$$

$$a_1 \equiv \frac{(EQ_{bs}l)}{D_t}$$

$$a1=EQbs*l/Dt;$$

$$a_2 \equiv \frac{E_c A_c l^2}{D_t}$$

$$a2=EAc*1*l/Dt;$$

$$a_3 \equiv \frac{(EA)_{bs} l^2}{D_t}$$

$$a3=EAbs*1*l/Dt;$$

$$splot=0;$$

syms x

***Define length of each element***

$$h=1/nem;$$

***Define interpolation functions.***

$$v_1 = 1 - 3\left(\frac{x}{h}\right)^2 + 2\left(\frac{x}{h}\right)^3$$

$$v1=1-3*(x/h)^2+2*(x/h)^3;$$

$$v_2 = -x\left(1 - \frac{x}{h}\right)^2$$

$$v2=-x*(1-x/h)^2;$$

$$v_3 = 3\frac{x^2}{h^2} - 2\frac{x^3}{h^3}$$

$$v3=3*(x/h)^2-2*(x/h)^3;$$

$$v_4 = -x\left(\frac{x^2}{h^2} - \frac{x}{h}\right)$$

$$v4=-x*(x^2/h^2-x/h);$$

$$\theta_1 = \Phi_1 = 1 - \frac{x}{h}$$

$$th1=1-x/h;$$

$$\theta_2 = \Phi_2 = \frac{x}{h}$$

$$th2=x/h;$$

$$\text{for } sr=1:100:5000$$

$$s=sr*i*(p*l^4/Dt)^{.5*pi*2};$$

$$K_1 = 1 - \frac{a_1^2}{a_3}$$

$$k1=(1-a1^2/a3);$$

$$K_2 = \frac{a_1}{a_3} \beta \varepsilon - \varepsilon$$

$$k_2 = (a_1/a_3 * B * E - E);$$

$$K_3 = \beta^2 \varepsilon \frac{a_1}{a_3} - \beta \varepsilon$$

$$k_3 = B^2 * E * a_1/a_3 - B * E;$$

$$K_4 = \beta \varepsilon - c_2^2 s^2 \frac{a_1}{a_3} - \beta^2 \varepsilon \frac{a_1}{a_3}$$

$$k_4 = B * E - c_2 * s^2 * a_1/a_3 - B^2 * E * a_1/a_3;$$

$$K_8 = -\beta \varepsilon$$

$$k_8 = -B * E;$$

$$K_5 = c_1^2 s^2 + \beta^2 \varepsilon$$

$$k_5 = c_1 * s^2 + B^2 * E;$$

$$K_6 = -\beta^2 \varepsilon$$

$$k_6 = -B^2 * E;$$

$$K_7 = c_2^2 s^2 + \beta^2 \varepsilon$$

$$k_7 = c_2 * s^2 + B^2 * E;$$

***Define the elements of the K Matrix***

***Assembly of the K Matrix***

$$\begin{bmatrix} K_{11}^e & K_{12}^e & K_{13}^e & K_{14}^e & K_{15}^e & K_{16}^e & K_{17}^e & K_{18}^e \\ K_{21}^e & K_{22}^e & K_{23}^e & K_{24}^e & K_{25}^e & K_{26}^e & K_{27}^e & K_{28}^e \\ K_{31}^e & K_{32}^e & K_{33}^e & K_{34}^e & K_{35}^e & K_{36}^e & K_{37}^e & K_{38}^e \\ K_{41}^e & K_{42}^e & K_{43}^e & K_{44}^e & K_{45}^e & K_{46}^e & K_{47}^e & K_{48}^e \\ K_{51}^e & K_{52}^e & K_{53}^e & K_{54}^e & K_{55}^e & K_{56}^e & K_{57}^e & K_{58}^e \\ K_{61}^e & K_{62}^e & K_{63}^e & K_{64}^e & K_{65}^e & K_{66}^e & K_{67}^e & K_{68}^e \\ K_{71}^e & K_{72}^e & K_{73}^e & K_{74}^e & K_{75}^e & K_{76}^e & K_{77}^e & K_{78}^e \\ K_{81}^e & K_{82}^e & K_{83}^e & K_{84}^e & K_{85}^e & K_{86}^e & K_{87}^e & K_{88}^e \end{bmatrix} \begin{Bmatrix} u_1^e \\ u_2^e \\ u_3^e \\ u_4^e \\ u_5^e \\ u_6^e \\ u_7^e \\ u_8^e \end{Bmatrix} = \begin{Bmatrix} f_1^e \\ f_2^e \\ f_3^e \\ f_4^e \\ f_5^e \\ f_6^e \\ f_7^e \\ f_8^e \end{Bmatrix} + \begin{Bmatrix} Q_1^e \\ Q_2^e \\ Q_3^e \\ Q_4^e \\ Q_5^e \\ Q_6^e \\ Q_7^e \\ Q_8^e \end{Bmatrix}$$

KK=[ K11, K12, K15, K17, K13, K14, K16, K18;  
K21, K22, K25, K27, K23, K24, K26, K28;  
K51, K52, K55, K57, K53, K54, K56, K58;  
K71, K72, K75, K77, K73, K74, K76, K78;  
K31, K32, K35, K37, K33, K34, K36, K38;  
K41, K42, K45, K47, K43, K44, K46, K48;  
K61, K62, K65, K67, K63, K64, K66, K68;  
K81, K82, K85, K87, K83, K84, K86, K88];

### ***Integrating the K Matrix over the element***

K=int(KK,x,0,h);  
K=double(K);

### ***Assembly of the overall K Matrix***

KO=zeros((nem+1)\*4);  
  
for n=1:nem  
  
KO(n\*4-3:n\*4+4,n\*4-3:n\*4+4)=KO(n\*4-3:n\*4+4,n\*4-3:n\*4+4)+K;  
  
end

### ***Reducing the overall K Matrix by incorporating the boundary conditions***

KK=zeros(nem\*4+1);  
KK(2:nem\*4+1,2:nem\*4+1)=KO(5:4\*nem+4,5:4\*nem+4);  
KK(1,1)=KO(3,3);  
KK(1,2:5)=KO(3,5:8);  
KK(2:5,1)=KO(5:8,3);

### ***Incorporating the last boundary condition (shear force equilibrium at the free end)***

```
KK((nem-1)*4+2,(nem*4))=KK((nem-1)*4+2,(nem*4))+k3;
KK((nem-1)*4+2,(nem*4+1))=KK((nem-1)*4+2,(nem*4+1))+k4;
```

### ***Defining the F Matrix***

```
F=[-KO(1,3);-KO(1,5);-KO(1,6);-KO(1,7);-KO(1,8);zeros(nem*4-4,1)];
```

### ***Calculating the nodal variable values***

```
X=KK^-1*F;
```

### ***Plotting***

```
splot=splot+1;
w(splot)=abs(real(X(nem*4-2)));
ww(splot)=sr;
end
```

A complete listing of the MATLAB code is given in Section A.2 of the appendix.

## **5.3 Slotted Psol Finite Element Model Matlab Program**

This model consists of 11 elements with every second element slotted, i.e. with no modulus of elasticity.

The inclusion of the slots in the model can be achieved by varying the properties of the stand off layer of the elements. In fact, variation of properties of other layers is also possible. The matrices of the elements with different properties have to be computed separately and then combined in the overall matrix. If the properties of the layers are varied excessively, then a large number of matrices need to be integrated which leads to a large increase in computing time.

The following if-else statement is used for combining the matrices

K1 = Integrated matrix for full element

K2= Integrated matrix for slotted element

For Element No. = 1 : No. of Elements

if Element = Slotted

Overall Stiffness Matrix = Overall Stiffness Matrix + K2

Else

if Element = Full

Overall Stiffness Matrix = Overall Stiffness Matrix + K1

End

A complete listing of the MATLAB code is given in Section A.3 of the appendix.

## 5.4 Summary

MATLAB programs for the distributed transfer function method and finite element method have been developed. The finite element program has been further modified to incorporate the slots in stand off layer (by varying the properties) along the length of the beam. However, slots in the viscoelastic and constraining layers can also be included. The full code of the programs is given in the index of program codes in the index of computer programs.

## **CHAPTER 6**

# **ANSYS Modeling and Comparison**

### **6.1 Overview**

In this chapter, the predictions of the developed finite element model and the distributed transfer function method are compared with the predictions of the commercial software package ANSYS.

### **6.2 Damping In Ansys**

In the implementation of the ANSYS simulation, it is very critical to account for the damping of the viscoelastic and the beam materials accurately.

Damping in ANSYS Version 8.0 is classified into two broad categories: Viscous damping and Structural damping. This can be done by two different analysis methods called the full method and the mode-superposition method. Figure (19) illustrates the various damping input functions in ANSYS

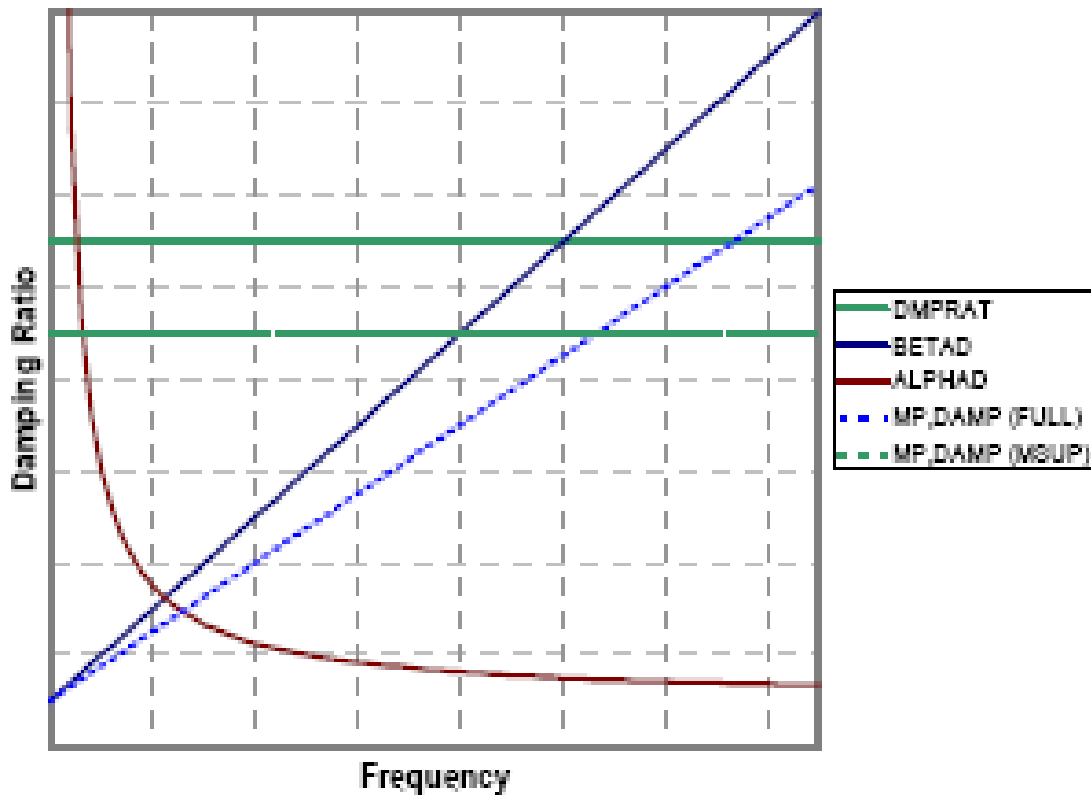


**Figure (19) - Damping in ANSYS**

The **DMPRAT** command is used to define constant damping ratios throughout the considered frequency range.

The **MDAMP** command is used however to define the modal damping ratios in which damping is specified for each mode independent of frequency.

The **ALPHAD** command defines damping ratios which are inversely proportional to frequency.

The **BETAD** command defines damping ratios which are directly proportional to frequency.

Finally, the **MP,DAMP** command represents stiffness multiplier in full analysis method



and it represents structural damping or constant damping ratio.

### 6.3 Modeling In Ansys

A Two-dimensional model is developed using ANSYS commercial software package. In that model, PLANE element 183 is used to discretize the cantilever beam which is subjected to harmonic excitation at its fixed end. Figures (20) and (21) display the ANSYS solid and meshed models respectively.

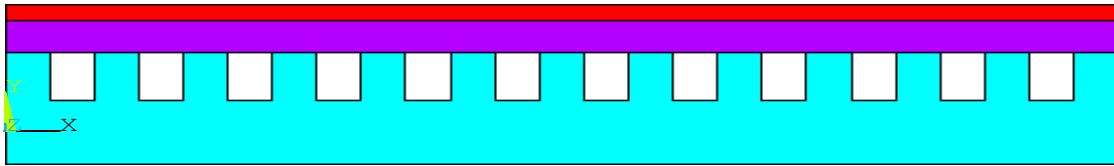


**Figure (20) - Modeling in ANSYS**

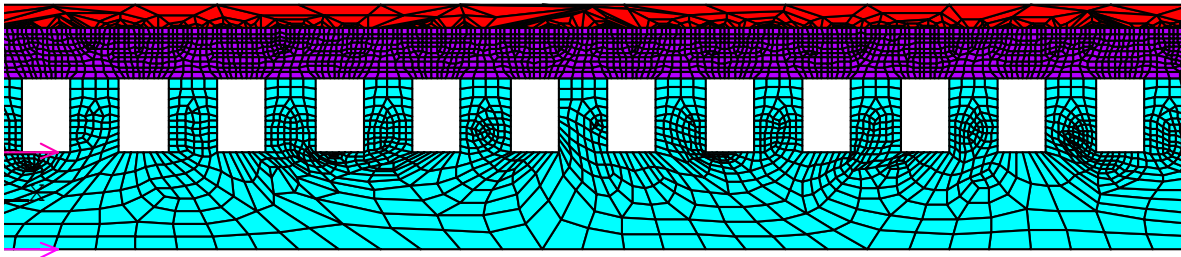


**Figure (21) - Meshed Model in ANSYS**

## 6.4 Comparison

### a. plain beam

The response of plain base beams as predicted by the developed finite element model and the distributed transfer function method are compared with the predictions of the commercial software package ANSYS. The considered base beam is made of aluminum whose length = .15 m, width = .01175m, and height = .00229m.

Figures (22), (23), and (24) display such responses and Figure (25) presents a comparison between all the three different methods. Close agreement is evident between the predictions of all the three methods.

#### Response

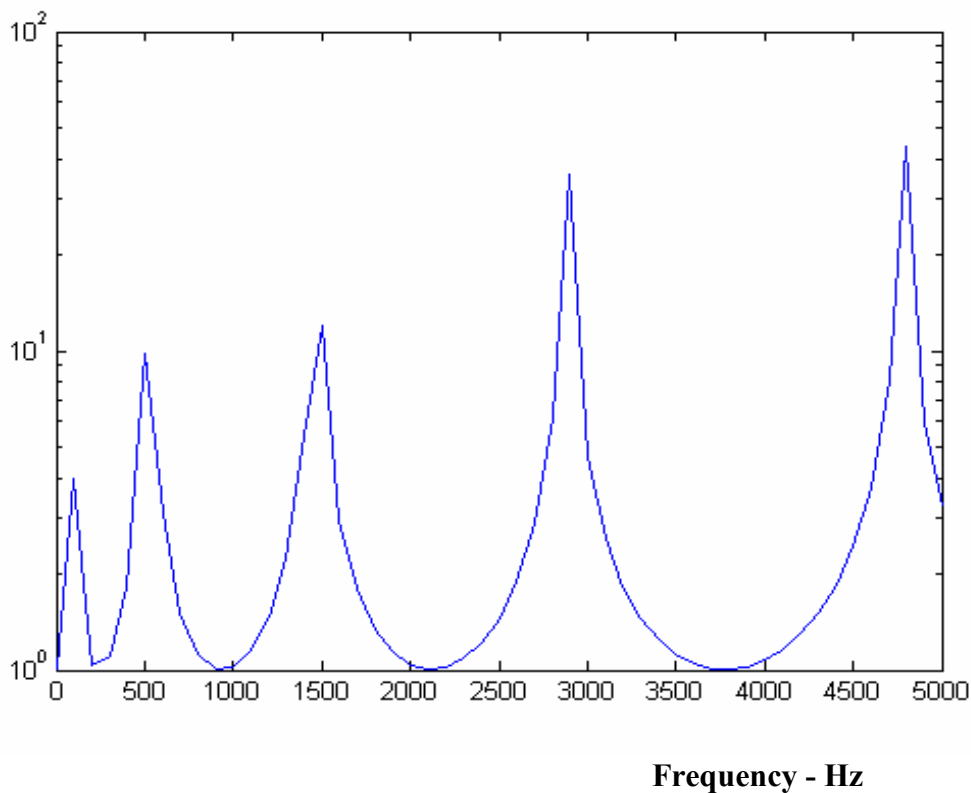


**Figure (22)** – Response of plain beam using the distributed transfer function method

## Response

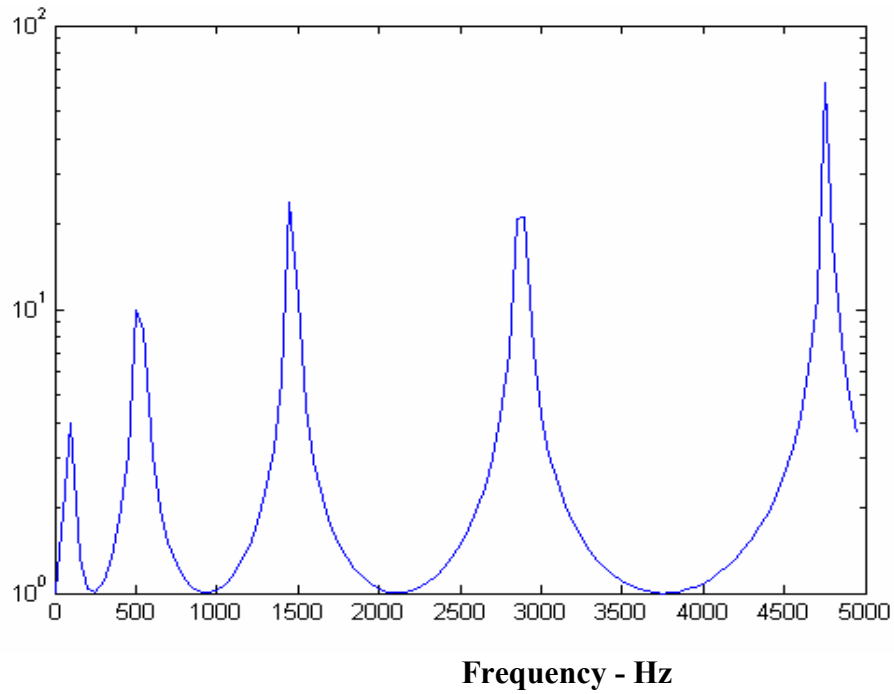


**Figure (23)** - Response of plain beam using the developed FEM

## Response

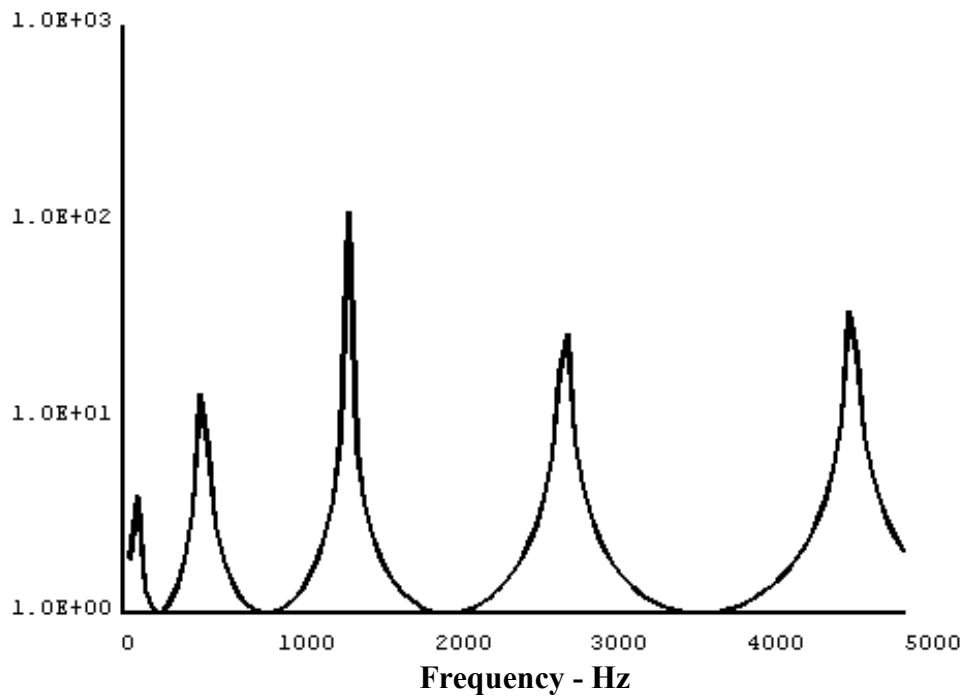


**Figure (24)** - Response of plain beam using ANSYS

## Response

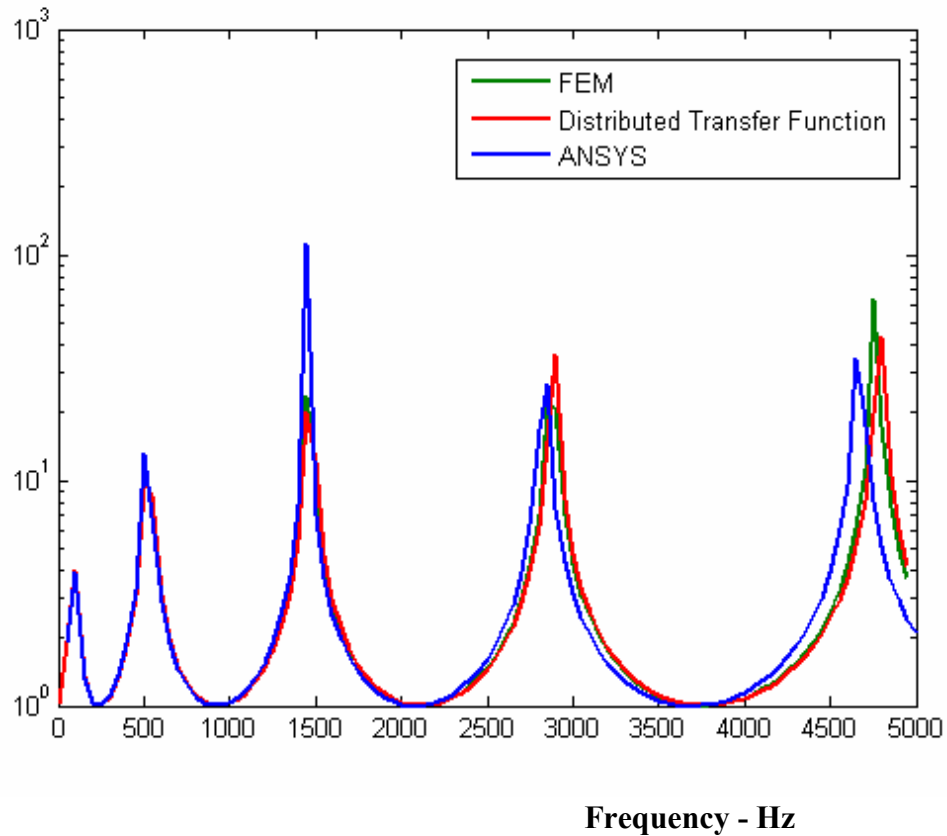


**Figure ( 25) -** Comparison between the response of a plain beam using the different methods

### **b. beam with passive SOL**

The main properties of the considered beam which is treated with passive SOL are:

**Base Material** = Aluminum , Length = .15 m, Width = .01175m, Height = .00229m

**SOL Material** = Aluminum, Height = .00264m

**VEM Material Properties**, Modulus Elasticity =  $1e5 \text{ N/m}^2$

Damping Ratio =  $1e-4 \times \pi \times \text{frequency}$  (linearly dependent on frequency), Height = .000127m,  
and Density =  $1100 \text{ Kg/m}^3$

**Constraining Layer** = Aluminum, Height = .000203 m.

Figures (26), (27), and (28) display such responses and Figure (29) presents a comparison between all the three different methods. Close agreement is evident between the predictions of all the three methods.

### Response

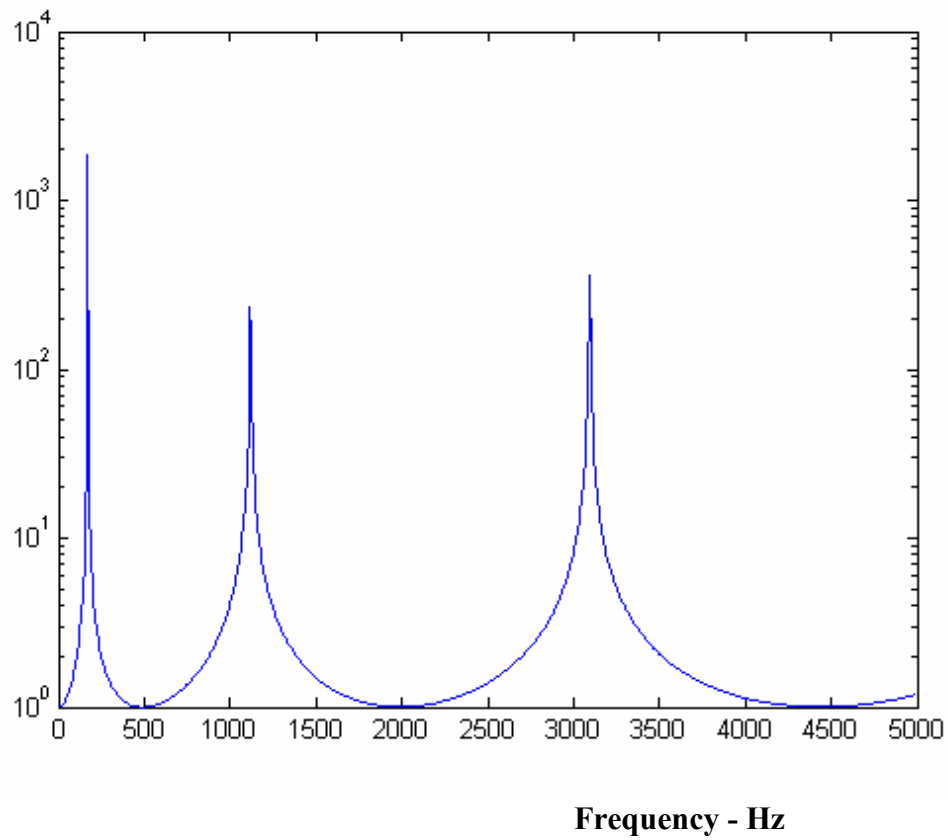


**Figure (26)** - Response of a beam with SOL using the distributed transfer function method

## Response

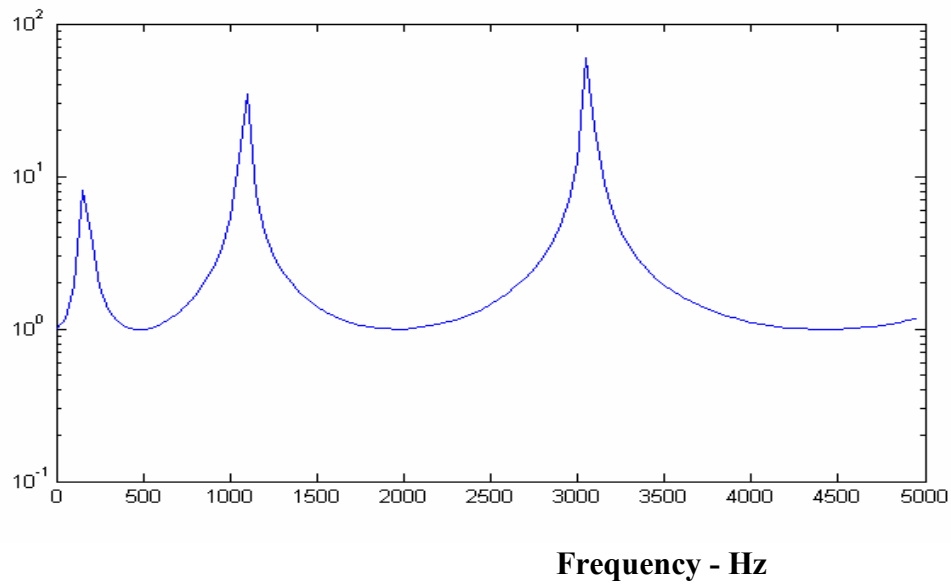


**Figure (27)** - Response of a beam with SOL using the developed FEM

## Response

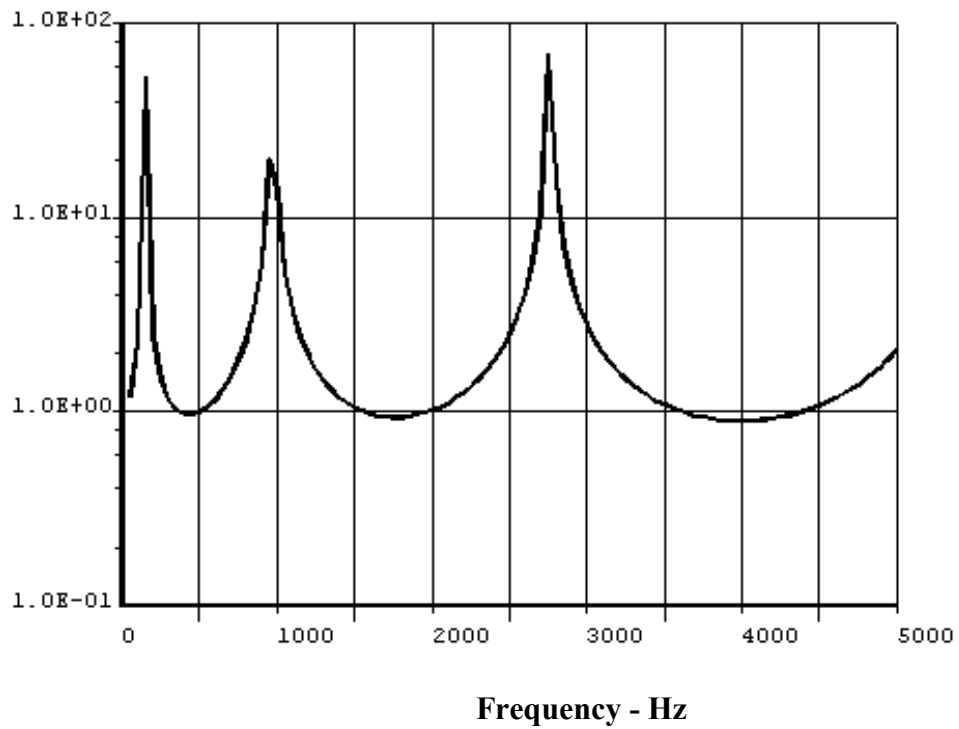


**Figure (28)** - Response of a beam with SOL using ANSYS

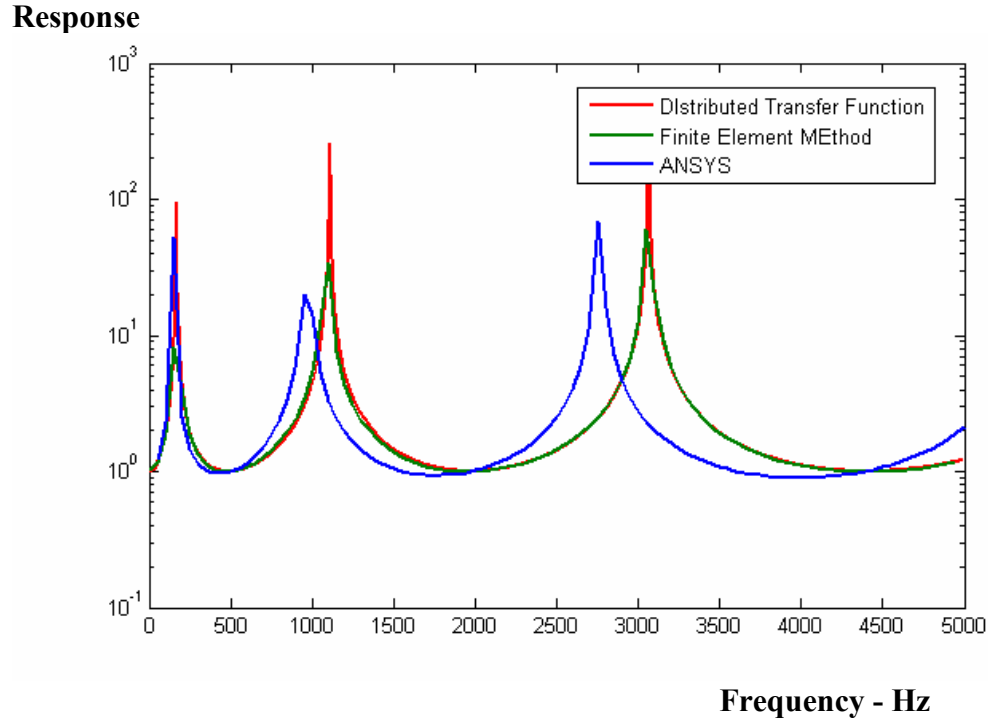


**Figure (29)** - Comparison between the response of a beam with SOL using the different methods

Note that the discrepancy between ANSYS model and the other two methods is due to the fact that ANSYS considers the VEM to have bending moment while the Distributed Transfer Function and Finite Element Methods do not take into account the bending moment in the Viscoelastic layer.

## 6.5 Summary

A comparison between the results obtained from the while Distributed Transfer Function and Finite Element Methods has been presented for different types of models. The results from ANSYS conform with those obtained by the developed methods for plain beams. However, due to the assumption that there is no bending stiffness in viscoelastic layer, the predictions are not exactly same for beams with SOL treatment.

## **CHAPTER 7**

# **Experimental Verification**

### **7.1 Experimental Setup**

Several experiments were performed to substantiate the results obtained by the analytical models. For this purpose, acrylic was chosen as the base material and as stand-off layer whereas aluminum was used as the constraining layer. Dyad 606 was used as viscoelastic material. Figures (30) and (31) display the loss factor and the storage modulus of the acrylic as obtained by the Dynamic, Mechanical, and Thermal Analyzer (DMTA) at different operating temperatures and excitation frequencies.



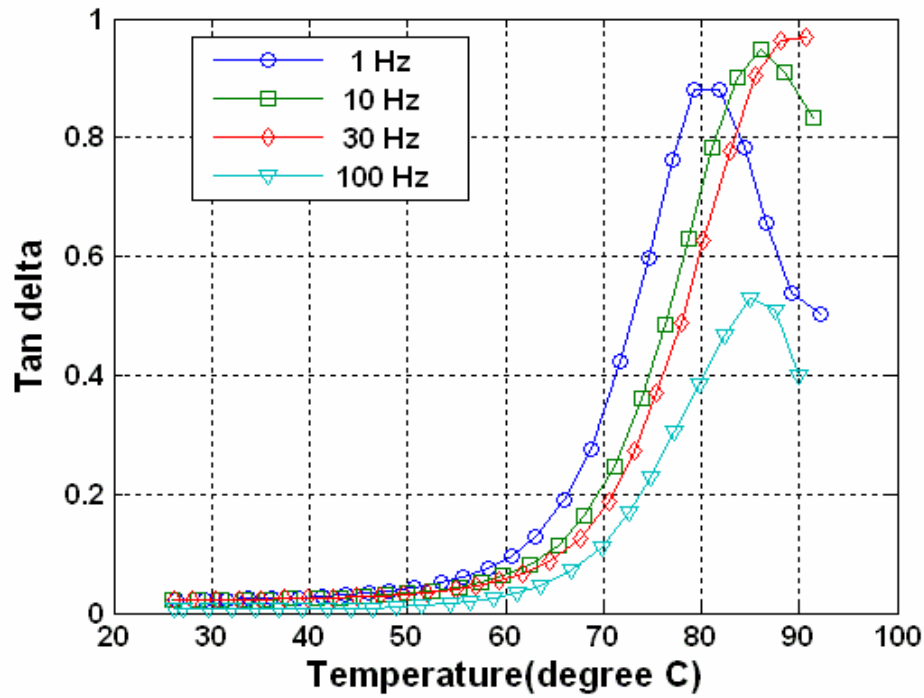


Figure (30) - Temperature-loss factor characteristics for Acrylic

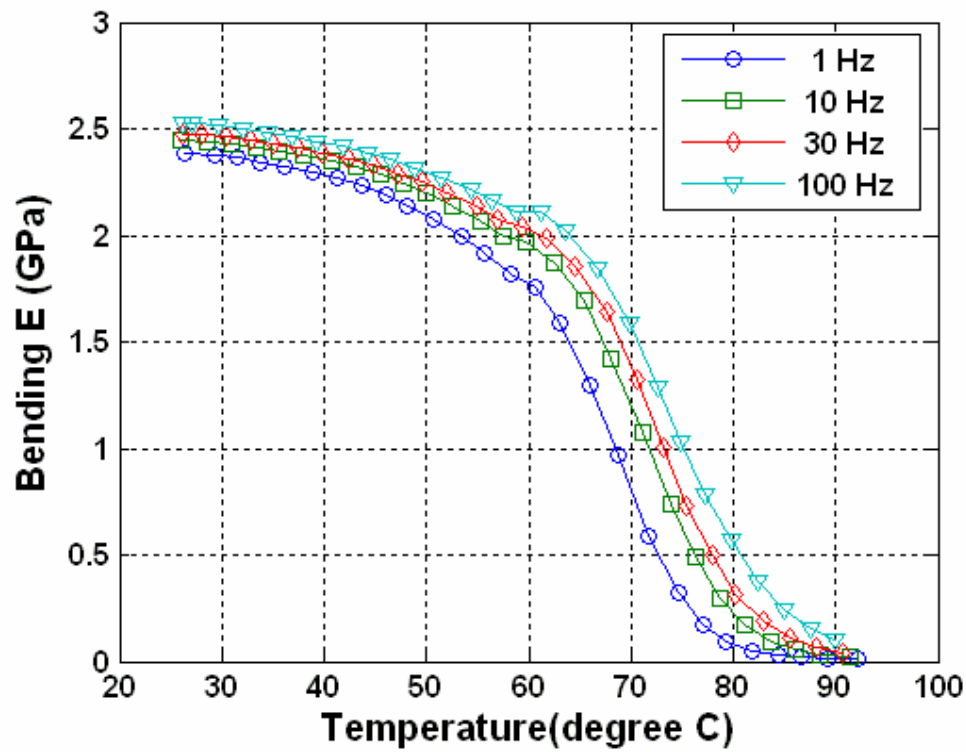
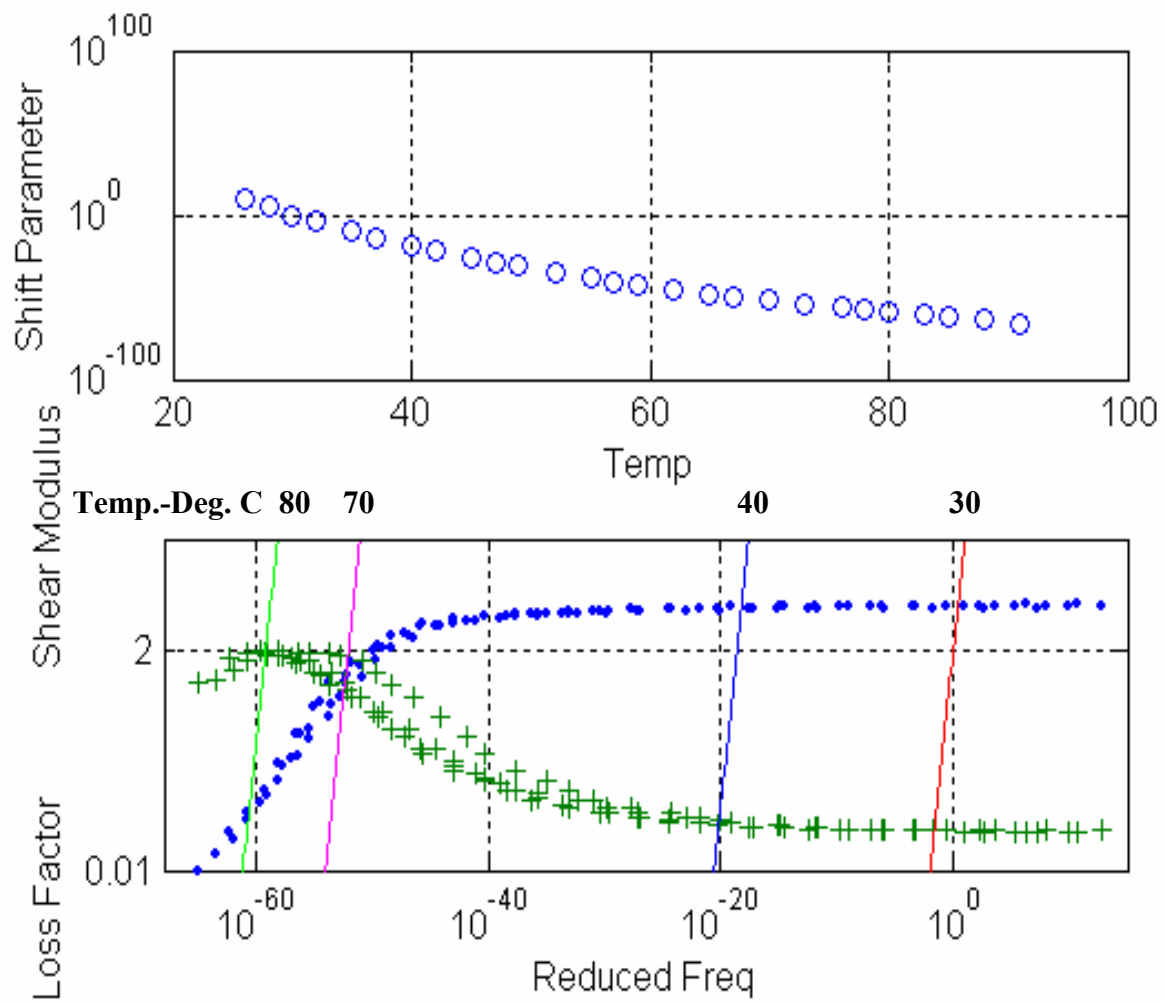


Figure (31) - Temperature-Storage Modulus characteristics for Acrylic

The following master curves were produced for acrylic.



**Figure (32) - Master Curves for Acrylic**

For the experiments, a cantilever beam model was subject to excitation at its fixed end was made and the input from the free end of the beam was fed to a signal analyzer. The resulting plots were recorded and compared.

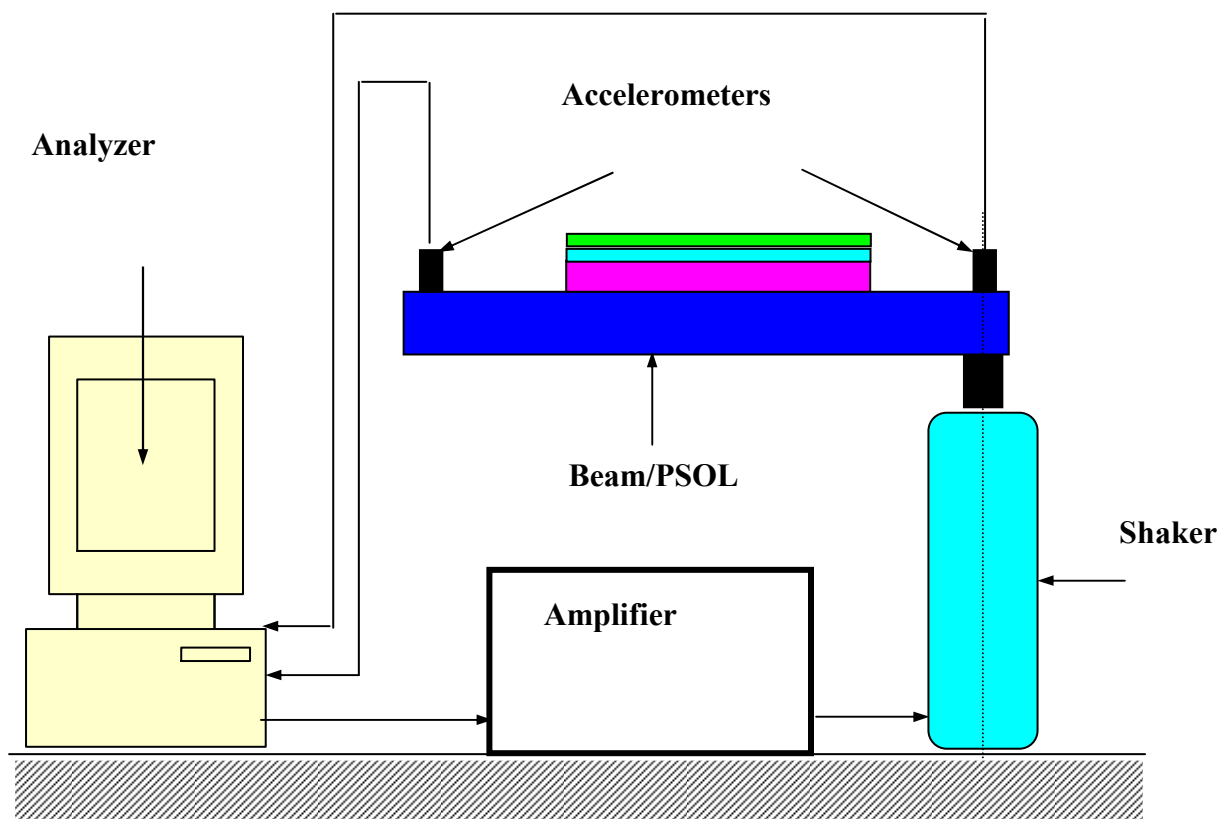


**Figure (33)** - Experimental Setup

### c. Test beams

Table (1) lists the considered test specimens along with their main geometrical and physical parameters.

**Table (1) - The main geometrical and physical parameters of the tested PSOL treatments**

| <b>MODEL</b>                             | <b>1</b> | <b>2</b> | <b>3</b>    | <b>4</b>    | <b>5</b>    | <b>6</b>    | <b>7</b>    |
|--|----------|----------|-------------|-------------|-------------|-------------|-------------|
| <b>Beam</b>                              | Acrylic  | Acrylic  | Acrylic     | Acrylic     | Acrylic     | Acrylic     | Acrylic     |
| <b>SOL Material</b>                      | -        | -        | Acrylic     | Acrylic     | Acrylic     | Acrylic     | Acrylic     |
| <b>VEM</b>                               | -        | -        | DYAD<br>606 | DYAD<br>606 | DYAD<br>606 | DYAD<br>606 | DYAD<br>606 |
| <b>Constraining Layer</b>                | -        | -        | Al.         | Al.         | Al.         | Al.         | Al.         |
| <b>Beam thickness (mm)</b>               | 5.00     | 3.00     | 3.50        | 3.50        | 3.50        | 3.125       | 3.125       |
| <b>Beam Length (mm)</b>                  | 280      | 280      | 280         | 280         | 280         | 125         | 125         |
| <b>Beam Width (mm)</b>                   | 25       | 25       | 25          | 25          | 25          | 25          | 25          |
| <b>SOL thickness (mm)</b>                | -        | -        | 2.0         | 2.0         | 2.0         | 3.125       | 3.125       |
| <b>SOL length (mm)</b>                   | -        | -        | 125         | 125         | 205.5       | 125         | 125         |
| <b>Slot width (mm)</b>                   | -        | -        | 0 (solid)   | 6.26        | 6.26        | 2.38        | 1.6         |
| <b>VEM thickness (mm)</b>                | -        | -        | 1.15        | 1.15        | 1.15        | 1.15        | 1.15        |
| <b>Constraining layer thickness (mm)</b> | -        | -        | 0.64        | 0.64        | 0.64        | 0.64        | 0.64        |

## Experimental Model 1

### Thick Plain Beam

The main geometrical and physical parameters of the considered 5 mm thick beam are given in Table 1 and shown in Figure (34).

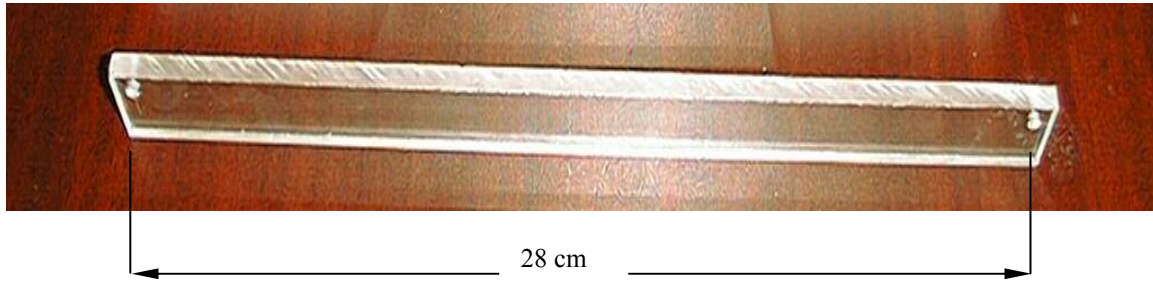


**Figure (34) – 5 mm thick plain beam (model 1)**

The complex modulus of the test beam is shown in Figures (30)-(32) and can be easily represented by:

$$\text{Elasticity Modulus} = 3e^9 [1 + 0.04 i] \quad N/m^2$$

Figure (35) displays a comparison between the theoretical and experimental frequency response characteristics of the 5 mm thick plain beam. Table (2) lists also a comparison between the theoretical and experimental modal characteristics of the plain beam. It is evident that there is a close agreement between theory and experiments.

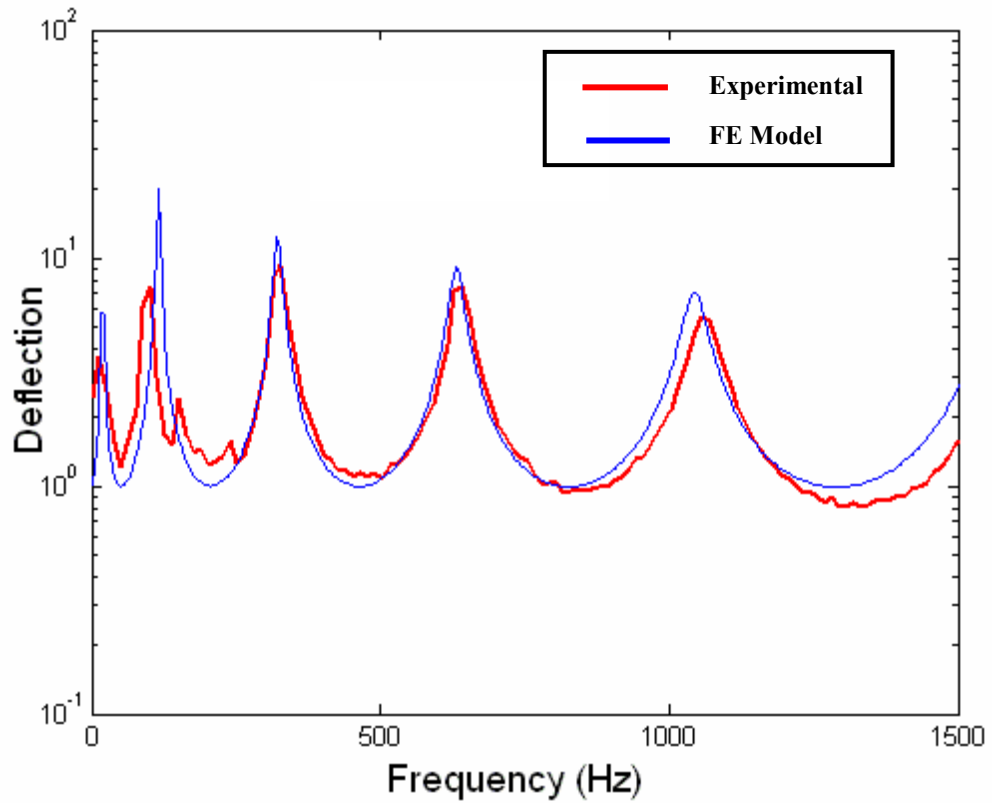


Figure (35) – Comparison between the theoretical and experimental frequency response of 5mm thick plain beam

**Table (2) - Comparison between the theoretical and experimental modal characteristics of the 5mm thick plain beam**

| Mode | Frequency (Hz) |      | Damping Ratio |      |
|------|----------------|------|---------------|------|
|      | Theory         | Exp  | Theory        | Exp  |
| 1    | 16             | 14   | .51           | na   |
| 2    | 116            | 102  | .043          | .20  |
| 3    | 321            | 328  | .041          | .07  |
| 4    | 631            | 642  | .041          | .053 |
| 5    | 1046           | 1056 | .040          | .047 |

## Experimental Model 2

### Thin Solid Beam

The main geometrical and physical parameters of the considered 3 mm thick beam are given in Table 1 and shown in Figure (36).

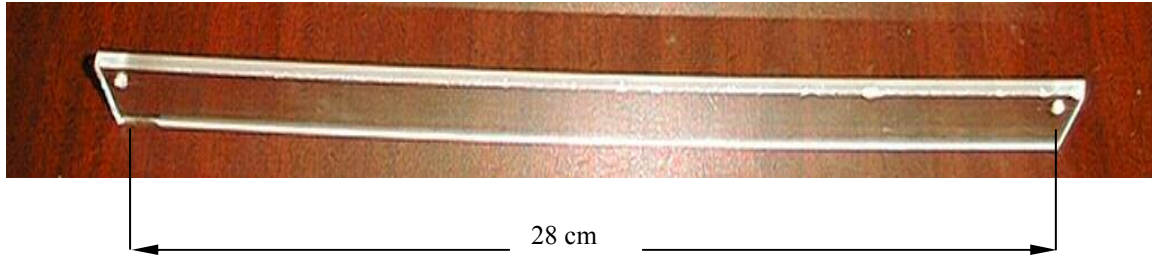


**Figure (36) – 3 mm thick plain beam (model 2)**

The complex modulus of the test beam is shown in Figures (30)-(32) and can be easily represented by:

$$\text{Elasticity Modulus} = 3e^9 [1 + 0.04 i] \quad N/m^2$$

Figure (37) displays a comparison between the theoretical and experimental frequency response characteristics of the 3 mm thick plain beam. Table (3) lists also a comparison between the theoretical and experimental modal characteristics of the plain beam. It is evident that there is a close agreement between theory and experiments.

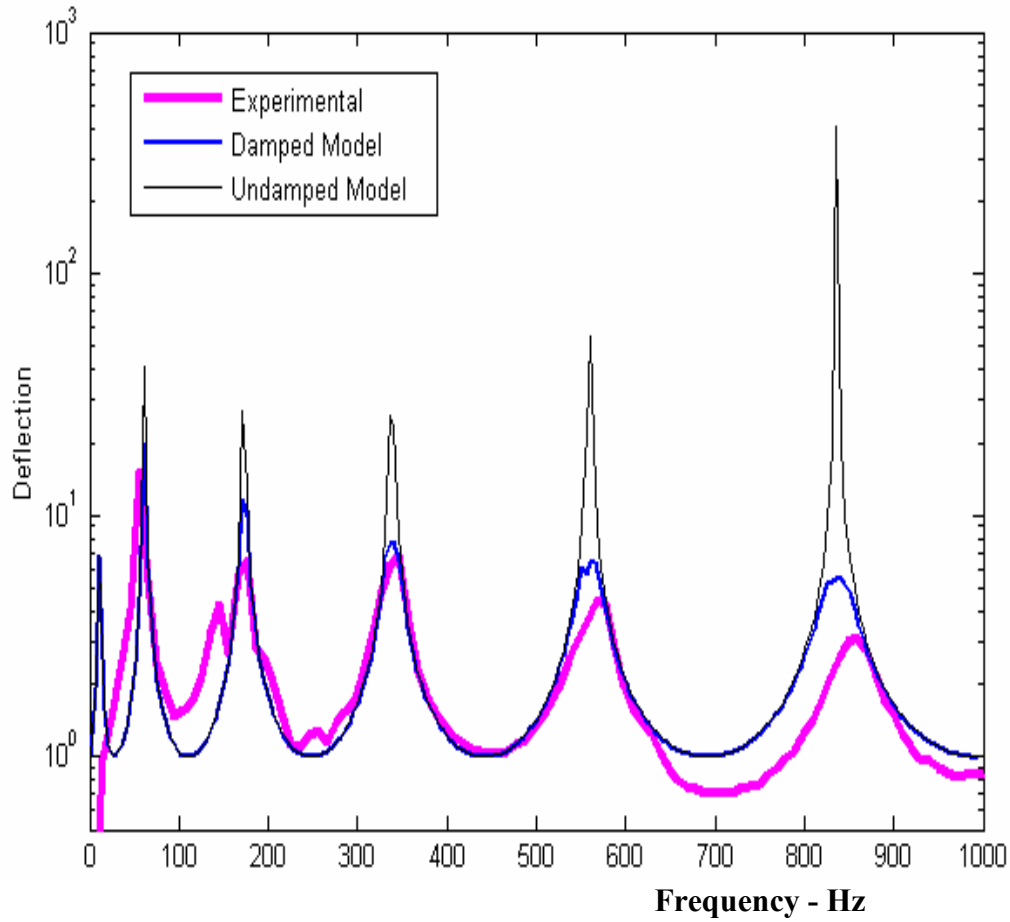


**Figure (37) - Comparison between the theoretical and experimental frequency response of 3mm thick plain beam**

In Figure (37), the effect of including the material loss factor of the acrylic beam on the accurate prediction of the frequency response of the beam is evident.

**Table (3) - Comparison between the theoretical and experimental modal characteristics of the 3mm thick plain beam**

| Mode | Frequency (Hz) |     | Damping Ratio |     |
|------|----------------|-----|---------------|-----|
|      | Theory         | Exp | Theory        | Exp |
| 1    | 11             | na  | .56           | na  |
| 2    | 61             | 56  | .10           | .13 |
| 3    | 172            | 174 | .10           | .20 |
| 4    | 339            | 342 | .08           | .09 |
| 5    | 567            | 575 | .09           | .09 |
| 6    | 835            | 857 | .09           | .09 |



## Experimental Model 3

### Beam with unslotted PSOL

The main geometrical and physical parameters of the considered 3.5 mm thick beam with 2 mm thick SOL are given in Table 1 and shown in Figure (38).

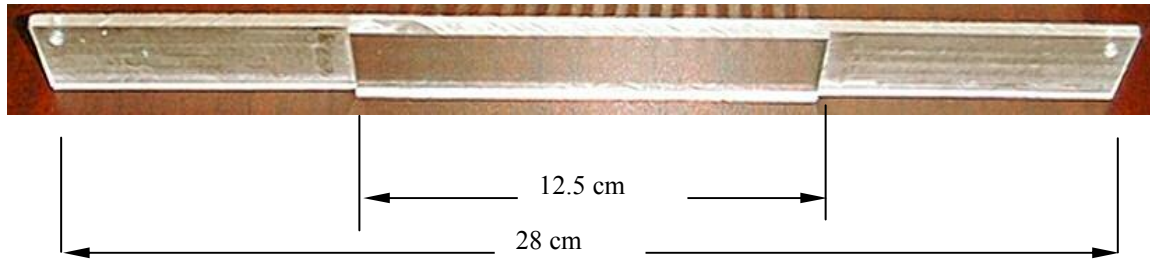


**Figure (38) – 3.5 mm thick beam with unslotted SOL (model 3)**

. The complex modulus of the test beam is shown in Figures (30)-(32) and can be easily represented by:

$$\text{Elasticity Modulus} = 3e^9 [1 + 0.04 i] \quad N/m^2$$

Figure (39) displays a comparison between the theoretical and experimental frequency response characteristics of the 3.5 mm thick beam with unslotted. Table (4) lists also a comparison between the theoretical and experimental modal characteristics of the plain beam. It is evident that there is a close agreement between theory and experiments.

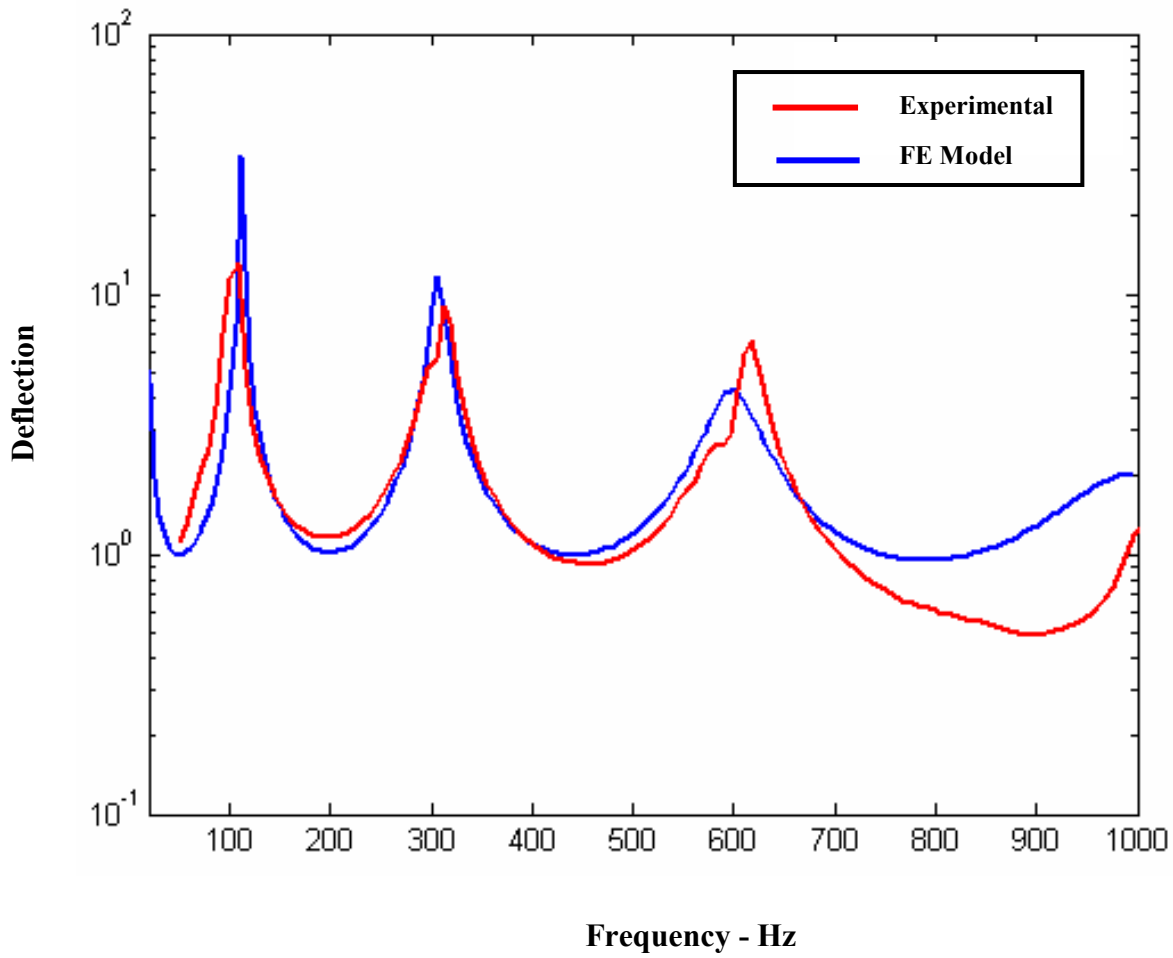


**Figure (39) - Response for beam model 3 with unslotted stand-off layer treated in middle**

**Table (4) - Comparison between the theoretical and experimental modal characteristics of the 3.5mm thick beam with unslotted SOL**

| Mode     | Frequency (Hz) |      | Damping Ratio |     |
|----------|----------------|------|---------------|-----|
|          | Theory         | Exp  | Theory        | Exp |
| <b>1</b> | 20             | n/a  | .45           | Na  |
| <b>2</b> | 105            | 120  | .19           | .09 |
| <b>3</b> | 315            | 315  | .14           | .09 |
| <b>4</b> | 620            | 605  | .13           | .08 |
| <b>5</b> | 1015           | 1005 | .14           | .11 |

## Experimental Model 4

### Beam with a slotted PSOL machined in middle

The main geometrical and physical parameters of the considered 3.5 mm thick beam with 2 mm thick SOL are given in Table 1 and shown in Figure (40).

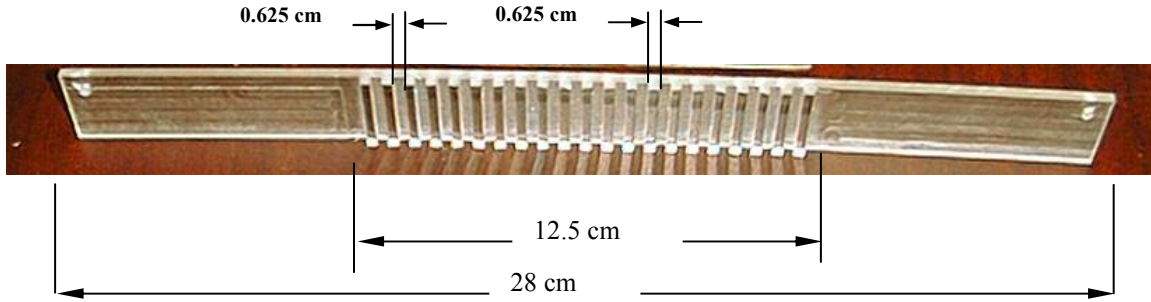


**Figure (40) – 3.5 mm thick beam with slotted PSOL (model 4)**

The complex modulus of the test beam is shown in Figures (30)-(32) and can be easily represented by:

$$\text{Elasticity Modulus} = 3e^9 [1 + 0.04 i] \quad N/m^2$$

Figure (41) displays a comparison between the theoretical and experimental frequency response characteristics of a beam with slotted PSOL machined at the beam center. Table (5) lists also a comparison between the theoretical and experimental modal characteristics of the plain beam. In this case, the theoretical predictions are qualitatively similar to the experimental results. But, there are quantitative discrepancies between theory and experiments particularly as far as the amplitude of deflections.

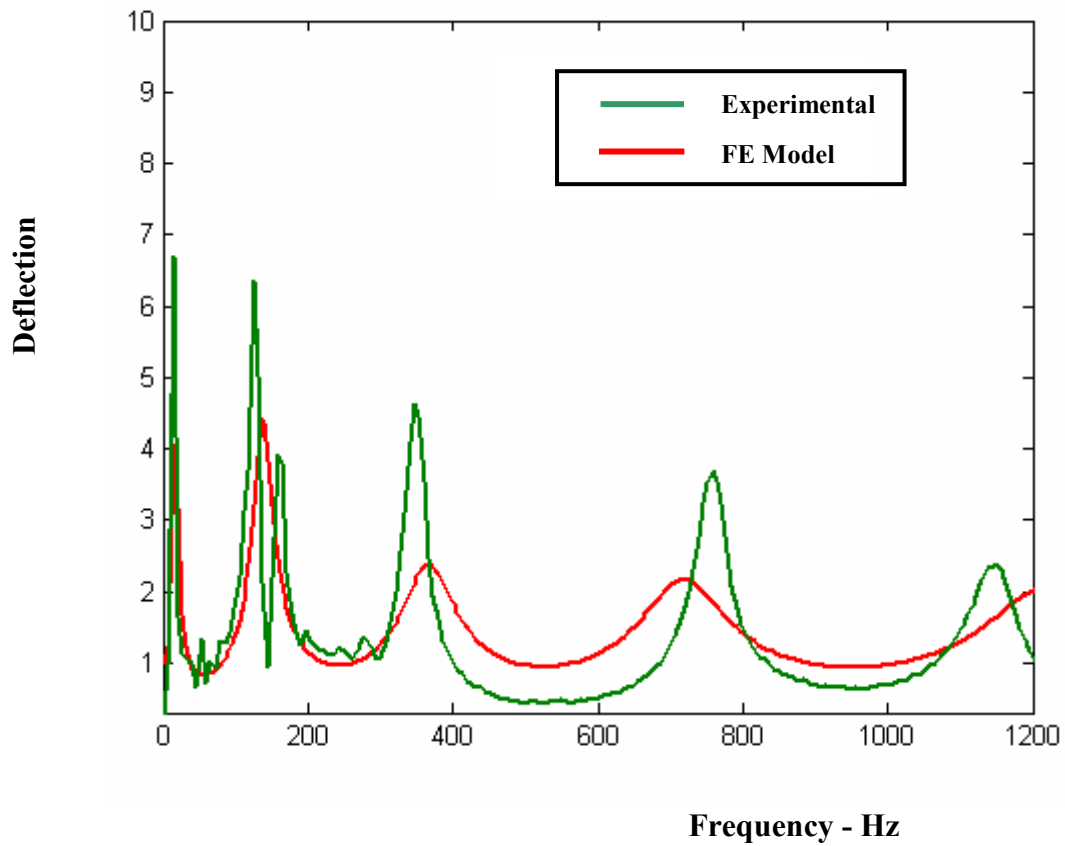


**Figure (41)** - Frequency response of a beam with slotted PSOL machined at the center

**Table (5)** - Comparison between the theoretical and experimental modal characteristics of the 3.5mm thick beam with slotted SOL near free end

| Mode | Frequency (Hz) |      | Damping Ratio |     |
|------|----------------|------|---------------|-----|
|      | Theory         | Exp  | Theory        | Exp |
| 1    | 17             | 13   | .38           | .52 |
| 2    | 136            | 125  | .15           | .08 |
| 3    | 365            | 350  | .22           | .08 |
| 4    | 720            | 755  | .18           | .06 |
| 5    | 1200           | 1150 | na            | .06 |

## Experimental Model 5

### Beam with a slotted PSOL machined at free end

The main geometrical and physical parameters of the considered 3.5 mm thick beam with 2 mm thick SOL are given in Table 1 and shown in Figure (42).

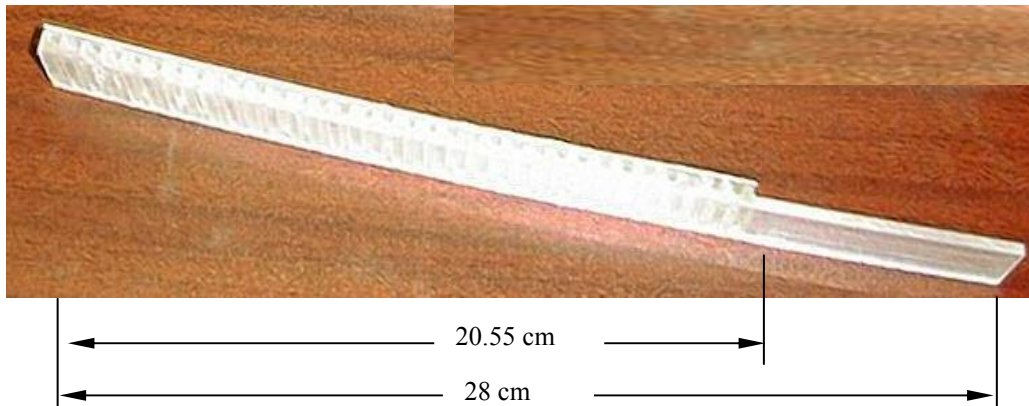


**Figure (42) – 3.5 mm thick beam with slotted PSOL machined at free end (model 5)**

Figure (43) displays a comparison between the theoretical and experimental frequency response characteristics of a beam with slotted PSOL machined at the free end. Table (6) lists also a comparison between the theoretical and experimental modal characteristics of the plain beam. In this case, the theoretical predictions are in good agreement with the experimental results.

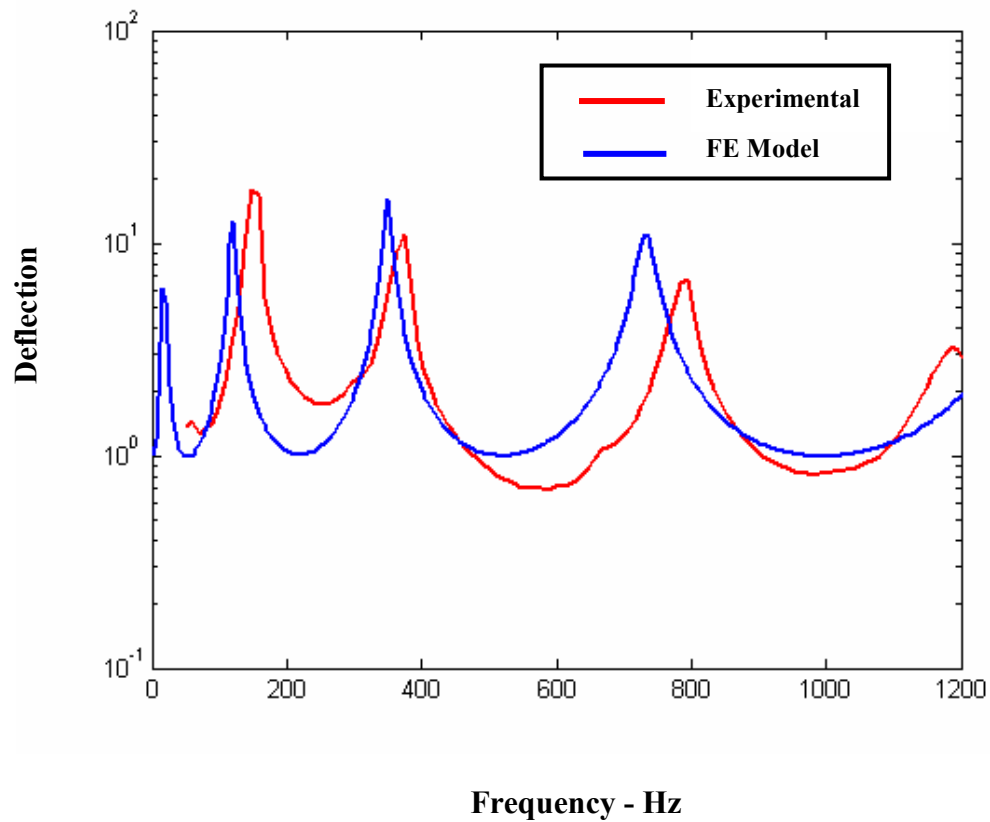


**Figure (43)** - Frequency response of a beam with slotted PSOL machined at free end

**Table (6)- Comparison between the theoretical and experimental modal characteristics of a beam with slotted PSOL machined near free end**

| Mode | Frequency (Hz) |      | Damping Ratio |      |
|------|----------------|------|---------------|------|
|      | Theory         | Exp  | Theory        | Exp  |
| 1    | 15             | 10   | .56           | .7   |
| 2    | 136            | 123  | .12           | .14  |
| 3    | 440            | 450  | .084          | .062 |
| 4    | 1015           | 1015 | .08           | .06  |

## Experimental Model 6

### Beam with a 27-slot PSOL

The main geometrical and physical parameters of the considered 3.125 mm thick beam with 3.125 mm thick SOL that has 27 slots are given in Table (1) and shown in Figure (44).

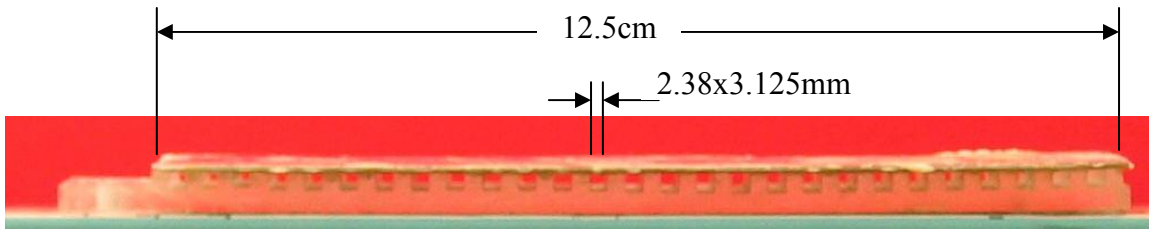


**Figure (44) – 3.125 mm thick beam with a 40-slot PSOL (model 6)**

Figure (45) displays a comparison between the theoretical and experimental frequency response characteristics of the beam with a 27-slot PSOL. Table (7) lists also a comparison between the theoretical and experimental modal characteristics of the plain beam. In this case, the theoretical predictions are in adequate agreement with the experimental results.

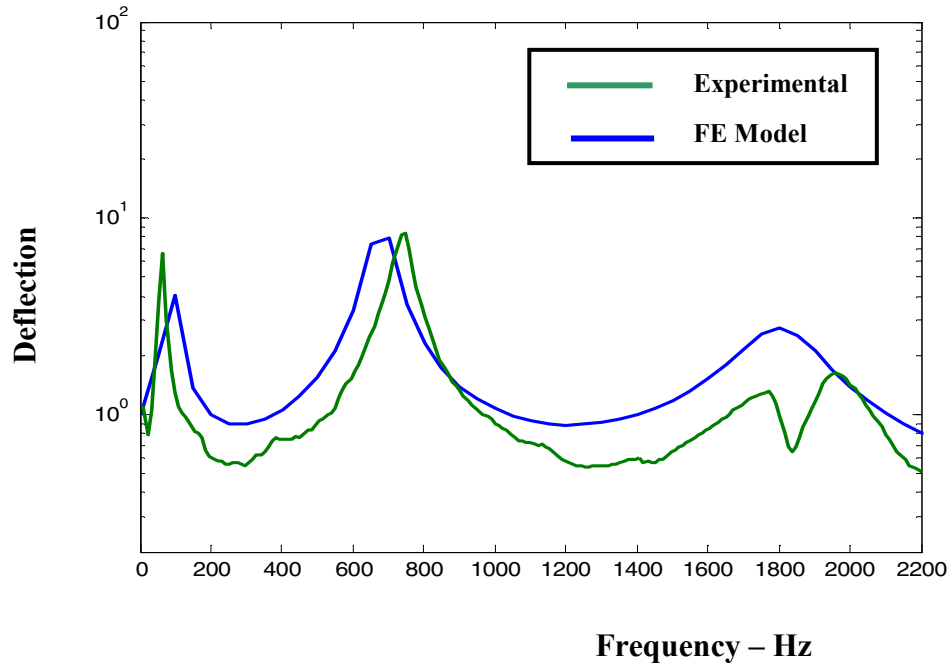


**Figure (45) – Frequency response of a beam with a 27-slot PSOL**

**Table (7) - Comparison between the theoretical and experimental modal characteristics of a beam with 27-slot PSOL**

| Mode | Frequency (Hz) |      | Damping Ratio |      |
|------|----------------|------|---------------|------|
|      | Theory         | Exp  | Theory        | Exp  |
| 1    | 100            | 50   | 0.3           | 0.3  |
| 2    | 700            | 750  | 0.08          | 0.05 |
| 3    | 1800           | 1750 | 0.21          | 0.18 |



## Experimental Model 7

### Beam with a 40-slot PSOL

The main geometrical and physical parameters of the considered 3.125 mm thick beam with 3.125 mm thick SOL that has 40 slots are given in Table 1 and shown in Figure (46).

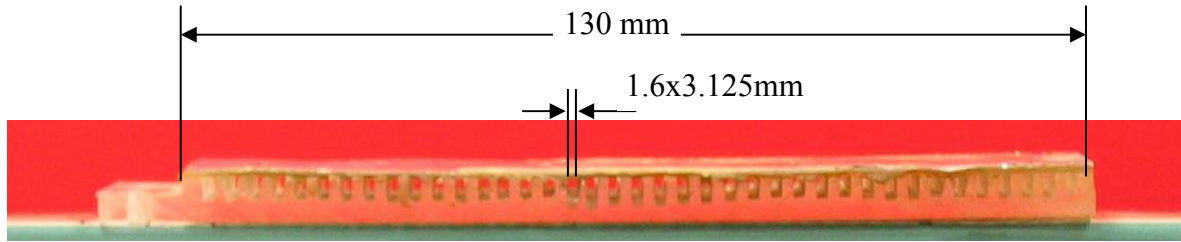


**Figure (46) – 3.125 mm thick beam with a 40-slot PSOL (model 7)**

Figure (47) displays a comparison between the theoretical and experimental frequency response characteristics of the beam with a 40-slot PSOL. Table (8) lists also a comparison between the theoretical and experimental modal characteristics of the plain beam. In this case, the theoretical predictions are in adequate agreement with the experimental results.

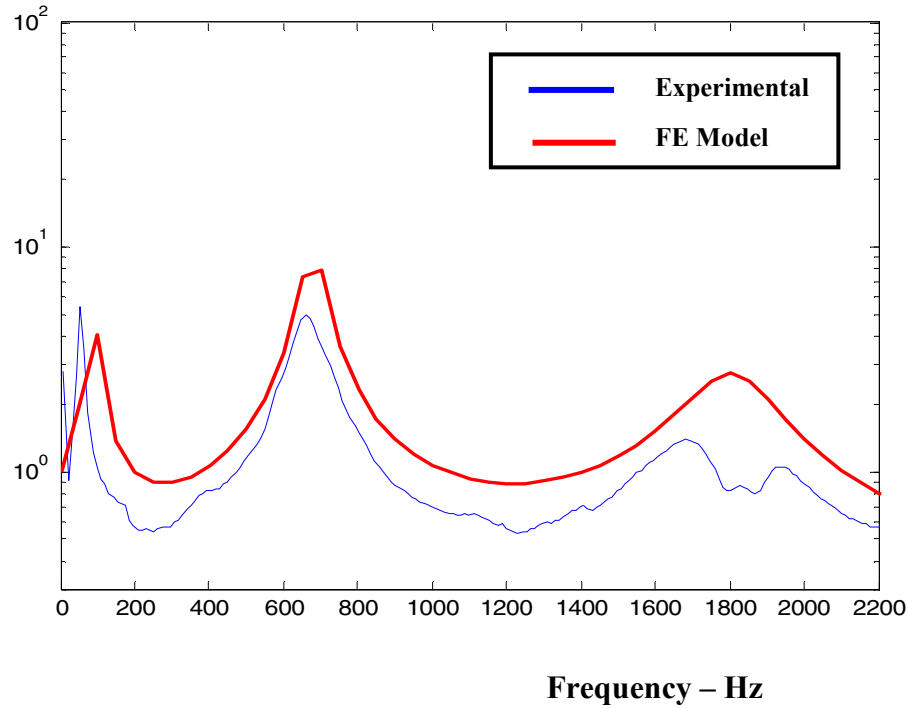


**Figure (47) – Frequency response of a beam with a 40-slot PSOL**

**Table (8)- Comparison between the theoretical and experimental modal characteristics of a beam with 40-slot PSOL**

| Mode | Frequency (Hz) |      | Damping Ratio |      |
|------|----------------|------|---------------|------|
|      | Theory         | Exp  | Theory        | Exp  |
| 1    | 100            | 50   | 0.3           | 0.3  |
| 2    | 700            | 660  | 0.08          | 0.11 |
| 3    | 1800           | 1660 | 0.21          | 0.18 |

## 7.2 Summary

The chapter has presented the experimental frequency response of beams with PSOL of different configurations along with comparisons with the theoretical predictions. It is found that the experimental results are in close agreement with the predictions of the developed finite element model.

## Chapter 8

# Effect of PSOL Parameters on its Damping Characteristics

In this chapter, the effect of changing the parameters of the different layers on the damping characteristics of beams treated with PSOL is presented. For this study, the base beam is assumed to have a total length = 0.15m, thickness = 2.29mm, and Young's modulus  $E=70e9$  N/m<sup>2</sup>.

The effect of varying the design parameters on the damping characteristics is quantified using the following performance index **AUC** denoting the area under the curve:

$$\mathbf{AUC} = \int_{\omega=0}^{\infty} w(l)d\omega \quad (71)$$

where  $w(l)$  = lateral deflection at the free end of the cantilever beam when it is subjected to sinusoidal excitation at its fixed end. Figure (48) shows a typical frequency response characteristics of a beam with PSOL and the hatched area defines the performance index AUC which will be used as a metric for optimizing the performance of the PSOL.

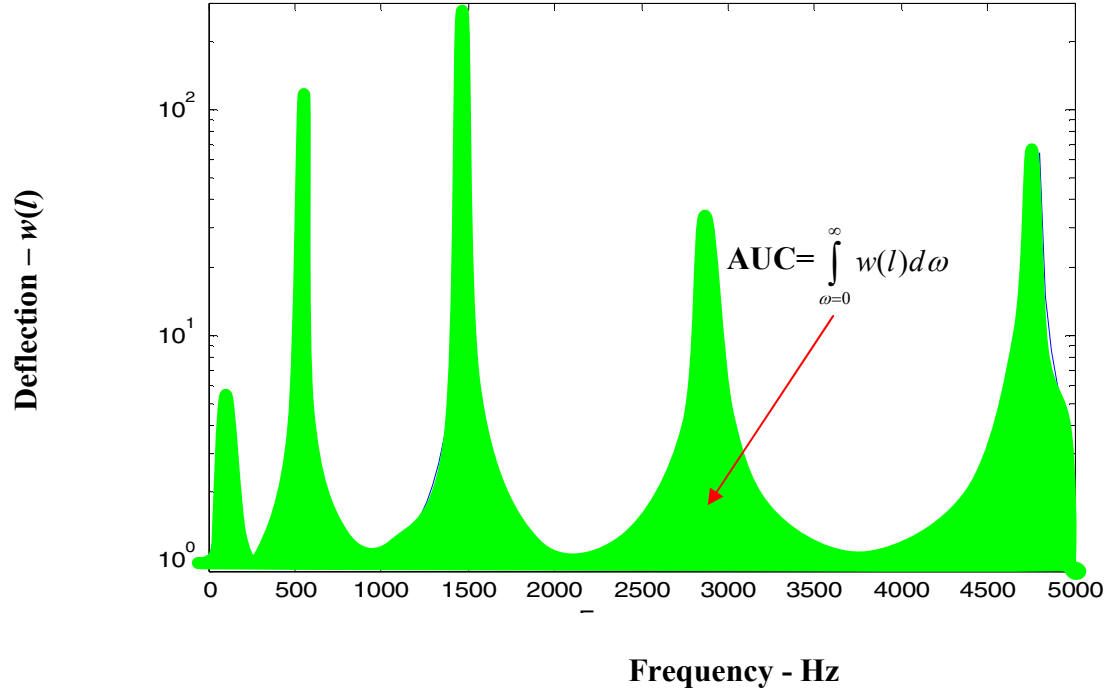


**Figure (48)** - A typical frequency response of a beam with PSOL defining the performance index AUC

In this chapter, the effect of changing the thickness and the strength of the viscoelastic material (VEM), stand-off layer (SOL), and constraining layer on the performance index AUC is investigated in an attempt to find the combination of the design parameters that minimizes the AUC. Furthermore, the effect of changing the bending and shear strength of the PSOL on the AUC is also studied for damped and undamped SOL.

## 8.1 Effect Of Thickness Of Vem And Sol Layers When Sol Layer Is Undamped

In this regard, the strength of the VEM and SOL are assumed constant and are given by:

$$\text{SOL (E)} = 1\text{e}5 \text{ N/m}^2 \text{ and VEM (E)} = 1\text{e}5(1+i) \text{ N/m}^2$$

Figure (49) shows the iso-contours of the performance index AUC as a function of the thickness of the VEM and SOL Layers. It is evident that the minimum values of the AUC occur when the VEM and SOL are of equal thicknesses and lie in the range between 0.4-0.8 mm.

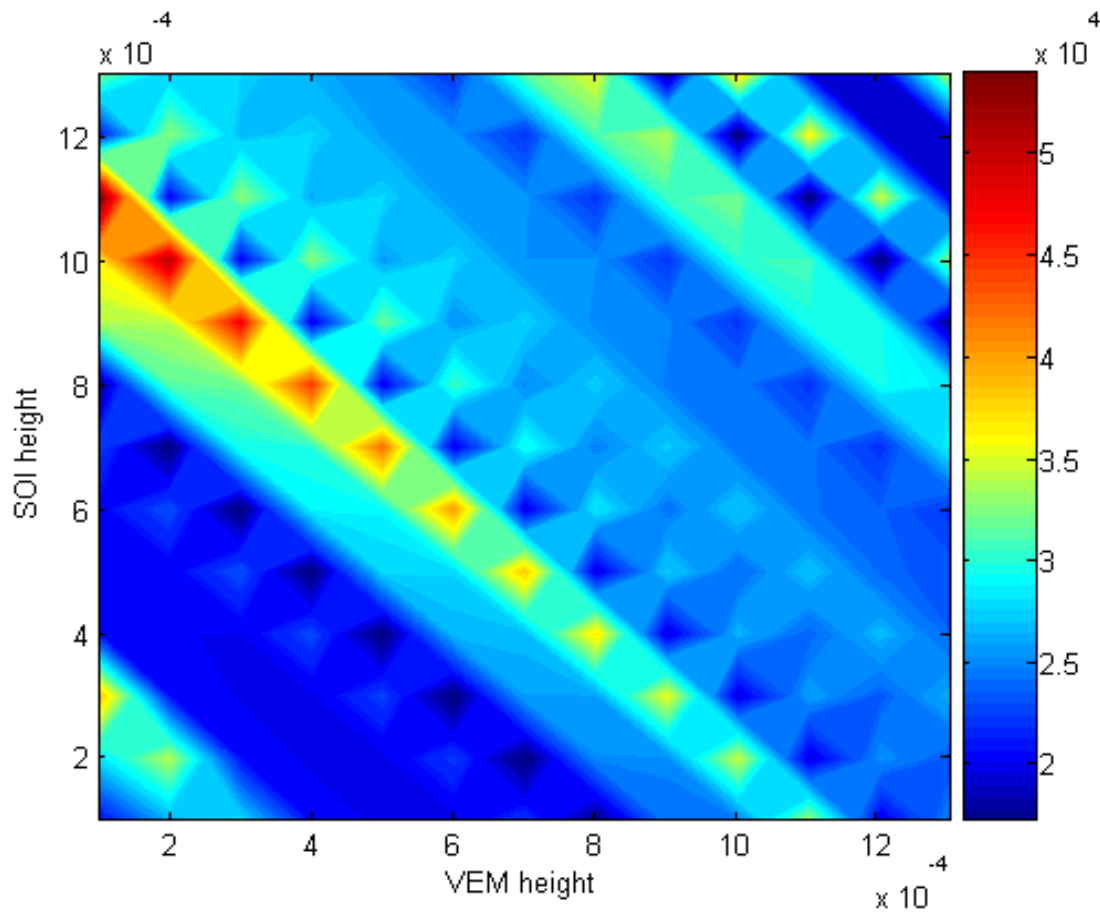
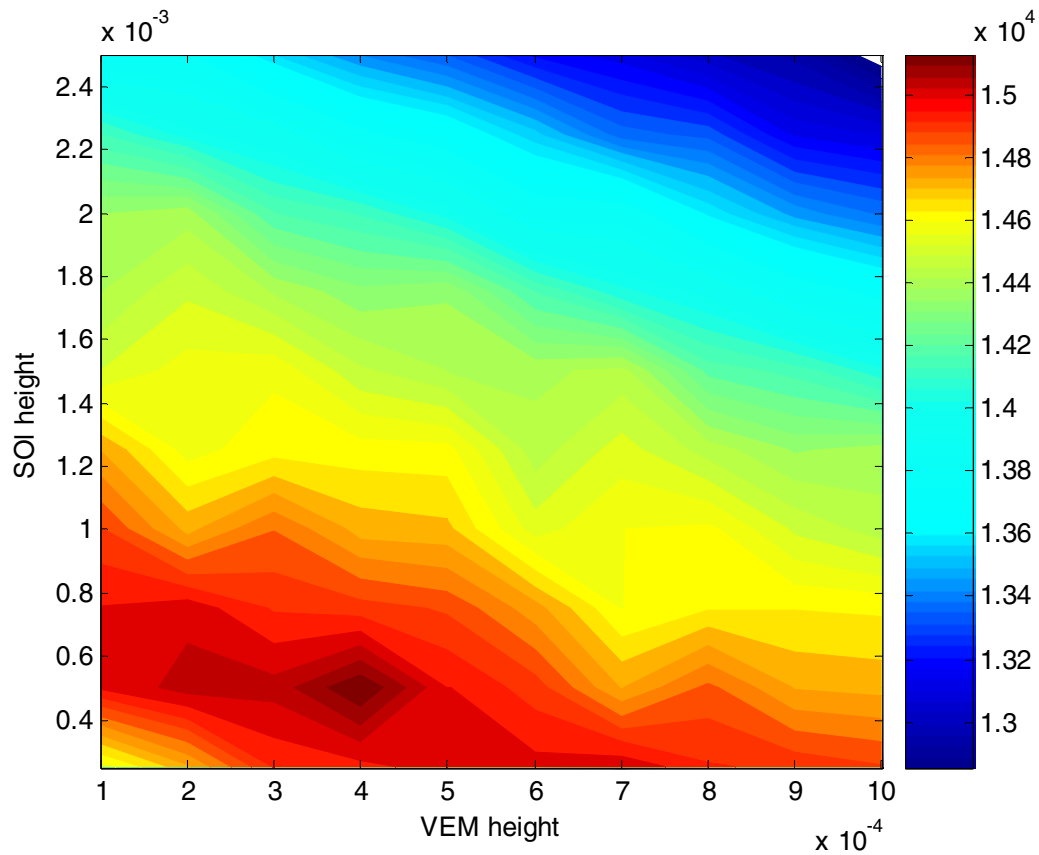


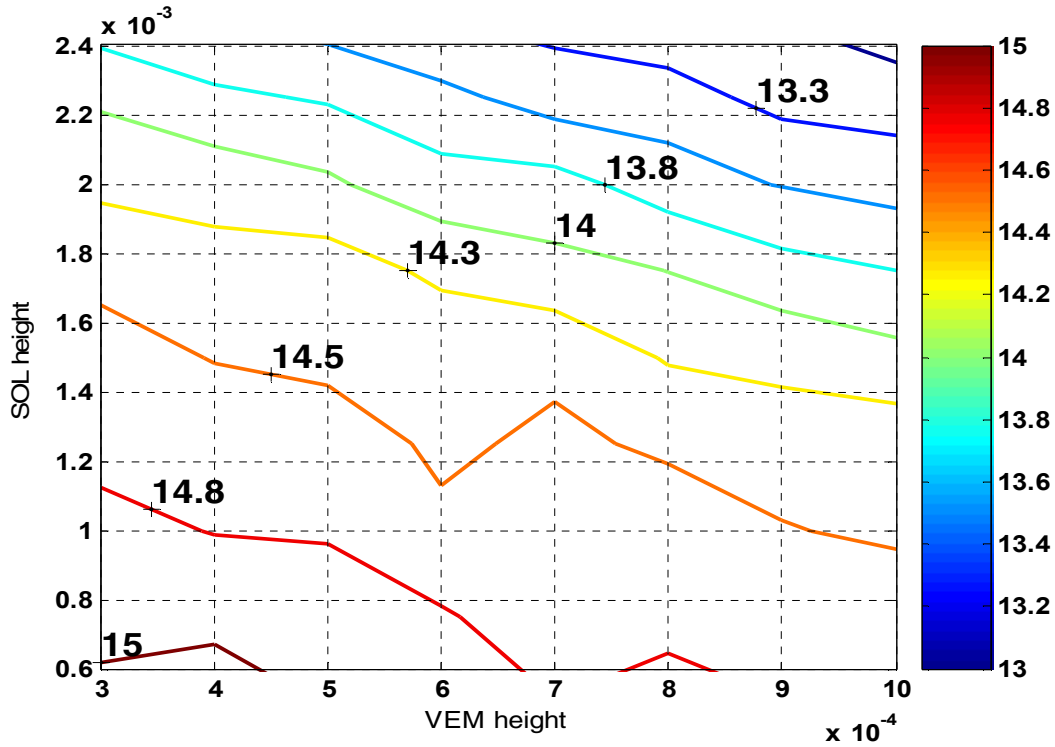
**Figure (49)** – Iso-contours of the AUC as a function of the thickness of the VEM and SOL Layers when the SOL layer is undamped

## 8.2 Effect Of Thickness Of Vem And Sol Layers When Sol Layer Is Damped

If the strengths of the SOL and VEM layers are assumed to be given by SOL strength =  $1e5(1+i)$  N/m<sup>2</sup> and VEM strength =  $1e5(1+i)$  N/m<sup>2</sup> such that the SOL layer is damped and has a loss factor =1, then the AUC iso-contours become as shown in Figures (50a) and (50b). It is evident that the minimum values of the AUC occur as the thickness of both the VEM and SOL is increased.



(a) – color contours

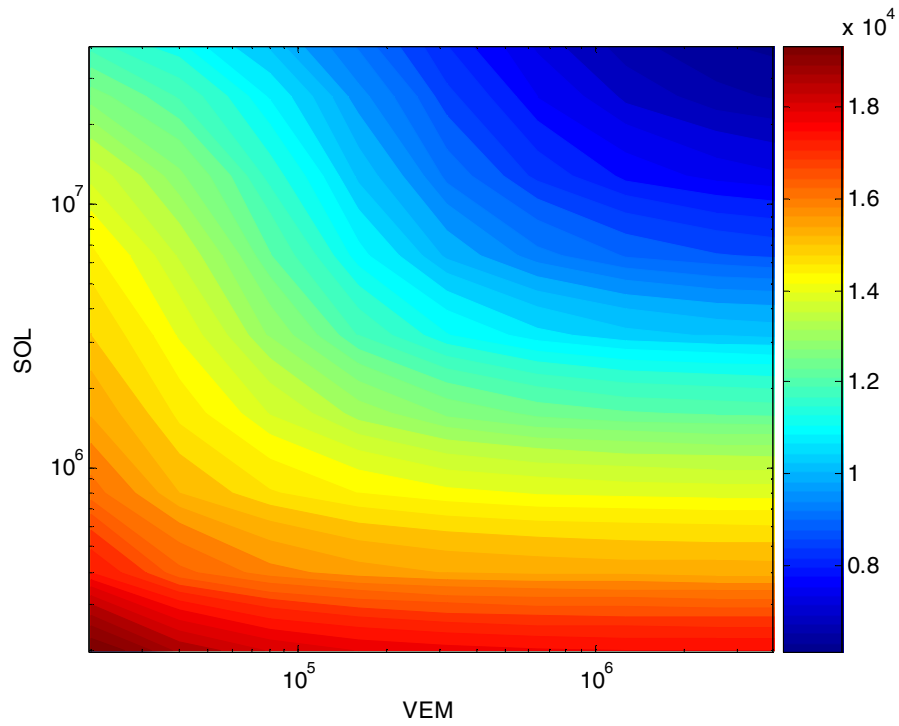


(b) – line contours

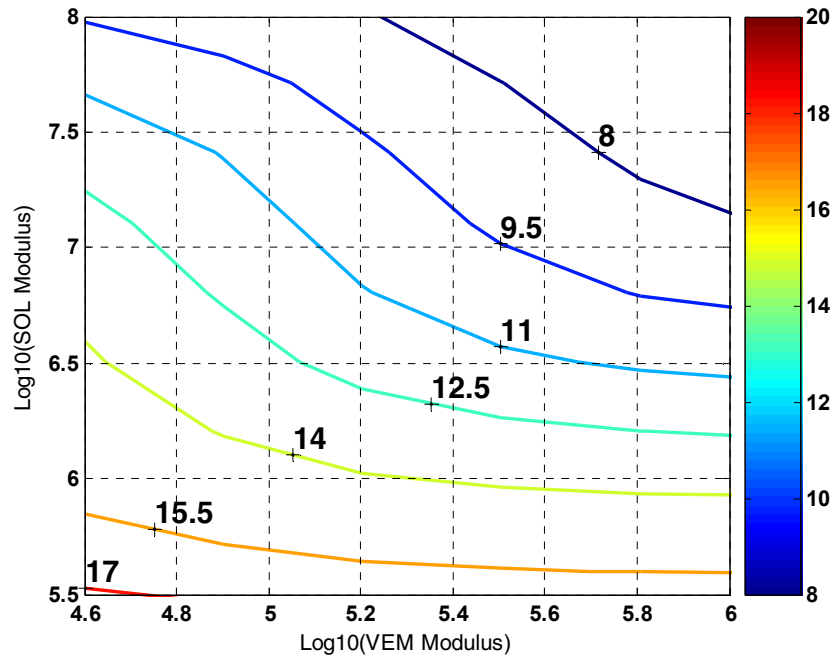
Figure (50) – Iso-contours of the AUC as a function of the thickness of the VEM and SOL Layers when the SOL layer is damped

### 8.3 Effect Of Young's Modulus Of Vem And Sol Layers When Sol Layer Is Damped

Figures (51a) and (51b) show the AUC iso-contours as affected by the Young's moduli of both the VEM and SOL layers when the SOL layer has a loss factor =1. It is evident that the minimum values of the AUC occur as the Young's modulus of both the VEM and SOL is increased.



**(a) – Color contours**



**(b) – line contours**

**Figure (51) - Iso-contours of the AUC as a function of the strength of the VEM and SOL Layers when the SOL layer is damped**



## 8.4 Effect Of Thickness And Strength Of Constraining Layer

Figure (52) shows the AUC iso-contours as affected by the thickness and strength of the constraining layer. It is evident that the minimum values of the AUC occur as the thickness of the constraining layer is increased and the strength is about  $50\text{E}9\text{N/m}^2$ .

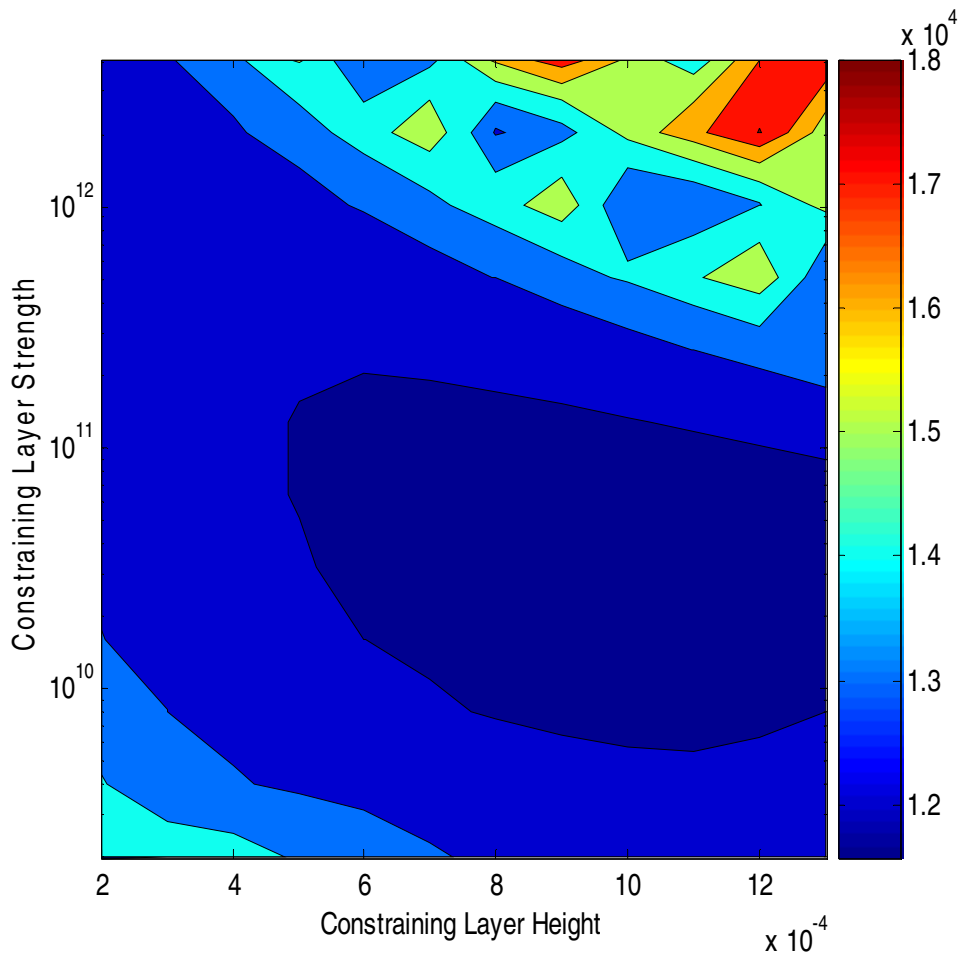
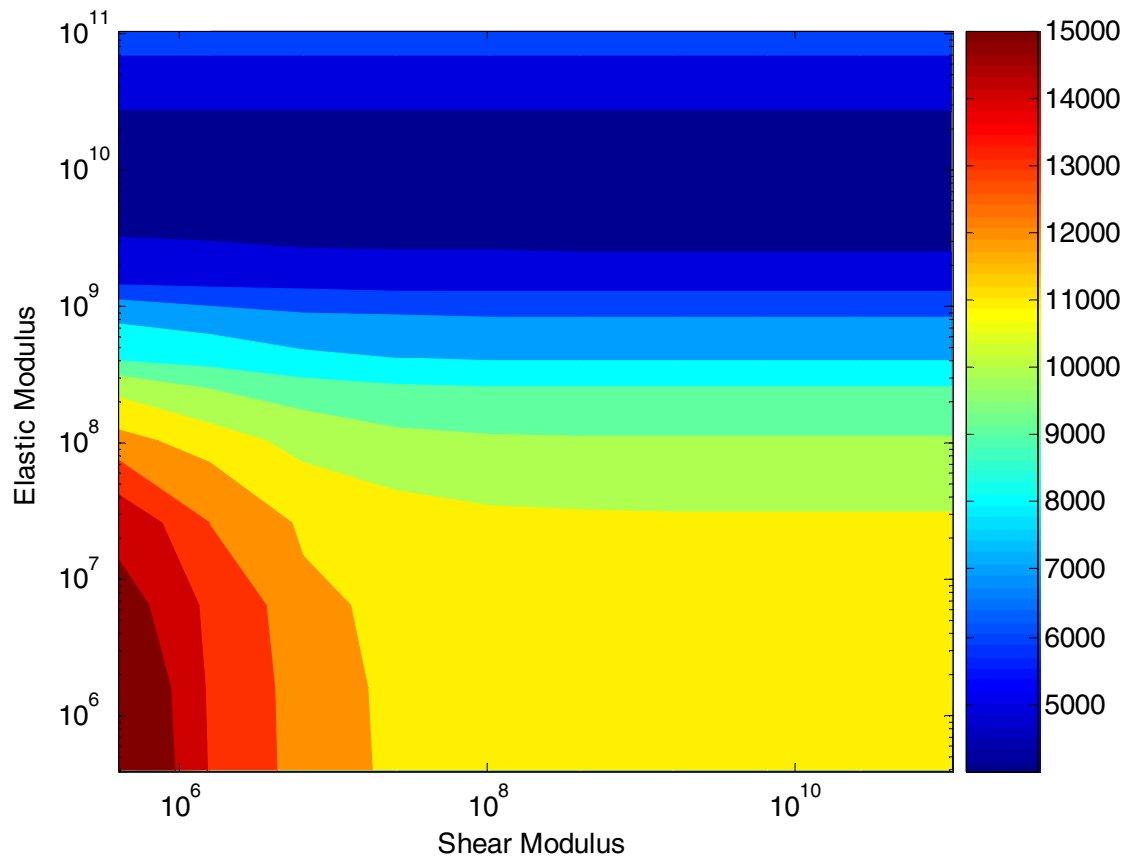


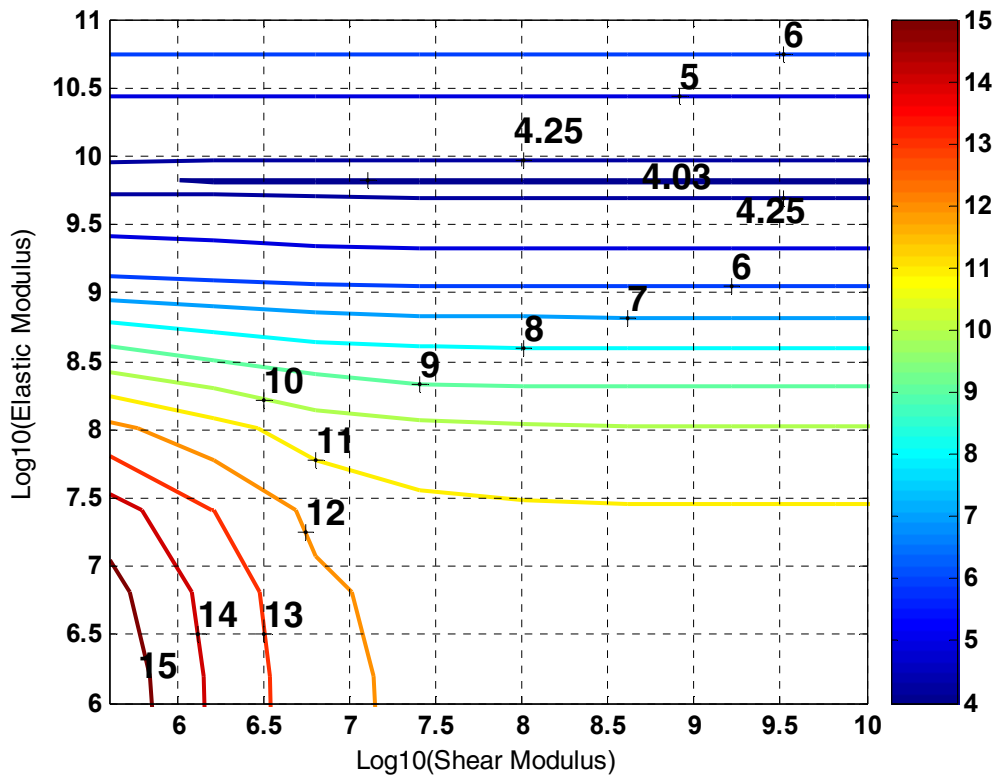
**Figure (52)** - Iso-contours of the AUC as a function of the strength and thickness of the constraining layer

## 8.5 Effect Of Elastic And Shear Modulii Of The Stand-Off Layer When Loss Factor = 1

Figures (53a) and (53b) show the AUC iso-contours as affected by the elastic and shear modulii of the SOL when it has a loss factor of 1. The figures indicate that the minimum values of the AUC occur when the elastic modulus of the SOL is much higher than its shear modulus.



(a) – color contours

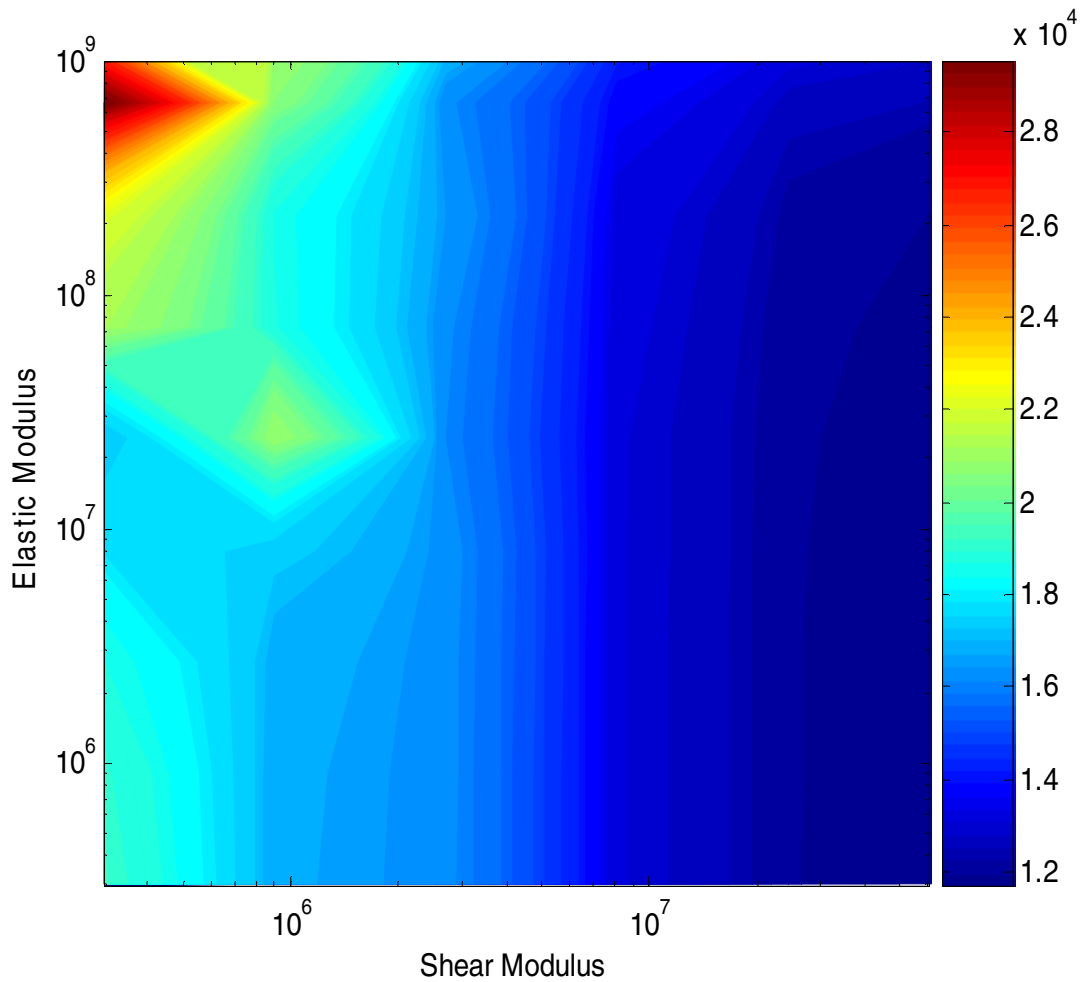


(b) – line contours

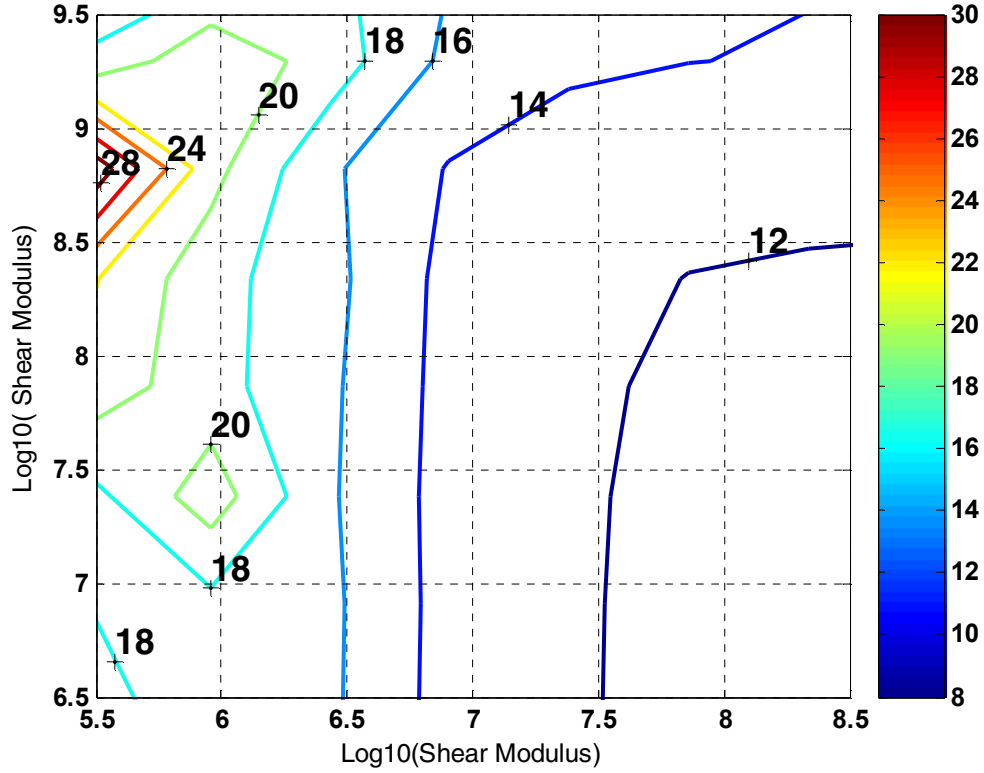
**Figure (53)** - Iso-contours of the AUC as a function of the Elastic and Shear Modulii of the SOL Layer when the loss factor =1

## 8.6 Effect Of Thickness And Strength Of The Stand-Off Layer When Loss Factor =0

Figures (54a) and (54b) show the AUC iso-contours as affected by the elastic and shear moduli of the SOL when it has a loss factor of 0. The figures indicate that the minimum values of the AUC occur when the elastic modulus of the SOL is much smaller than its shear modulus.



(a) – color contours



(b) – line contours

**Figure (54)** - Iso-contours of the AUC as a function of the Elastic and Shear Moduli of the SOL Layer when the loss factor =0

## 8.7 Summary

This chapter has presented a parametric study of the effect of changing the design parameters of the different layers of the PSOL on its damping characteristics. The results obtained suggest that a strong SOL layer with high damping gives the best results but for undamped SOL it is essential that the elastic modulus of the SOL be much smaller than its shear modulus. Furthermore, increasing the strength and thickness of the constraining layer is also effective up to a certain point but further increase would adversely affect damping performance.

## Chapter 9

# Conclusions and Recommendations

### 9.1 Conclusions

This dissertation has presented briefly the concept of passive stand-off layer (PSOL) damping treatments as a simple and effective means for enhancing the damping characteristics of constrained layer damping. In this dissertation, a review of the literature is presented in an attempt to justify the need and emphasize the importance of the present study.

A formulation of the equations of motion of the passive stand off layer treated cantilever beam subjected to dynamic loading at the fixed end is presented. The obtained equations of motion consist of  $4^{th}$  order differential equation in the lateral deflection of beam and two  $2^{nd}$  order differential equation in the axial deflections of the base beam and constraining layer.

A transfer function model of the PSOL treated beam treatment has been developed. The equations of motion have been modified to facilitate the formulation of a finite element model which constitutes the major contribution of this dissertation. Hermite interpolation functions

have been used to describe the lateral deflection and Lagrangian interpolation functions have been used to define the axial deflections of the base beam and constraining layer.

MATLAB programs for the distributed transfer function method and finite element method have been developed. The finite element program has been further modified to incorporate the slots in stand off layer (by varying the properties) along the length of the beam. However, slots in the viscoelastic and constraining layers can also be included. The full code of the programs is given in the appendix.

A comprehensive experimental evaluation of the performance of the PSOL has been conducted to investigate the effect of various configurations of the SOL on its damping characteristics. Furthermore, the obtained experimental results have been used to validate the predictions of the developed finite element model.

. The results obtained suggest that the predictions of the developed finite element model are in close agreement with the experimental results as well as with the predictions of an ANSYS model of the PSOL.

The results indicate also that a strong SOL layer with high damping gives the best results but for undamped SOL it is essential that the elastic modulus of the SOL be much smaller than its shear modulus. Furthermore, increasing the strength and thickness of the constraining layer is also effective up to a certain point but further increase would adversely affect damping performance.

## 9.2 Recommendations

Although this study has focused on the development of PSOL for one-dimensional cantilever beams, it is essential to note that the presented concepts can be equally extended to multiple dimensions for using plate and shell elements as shown in Figures (55) and (56) respectively.

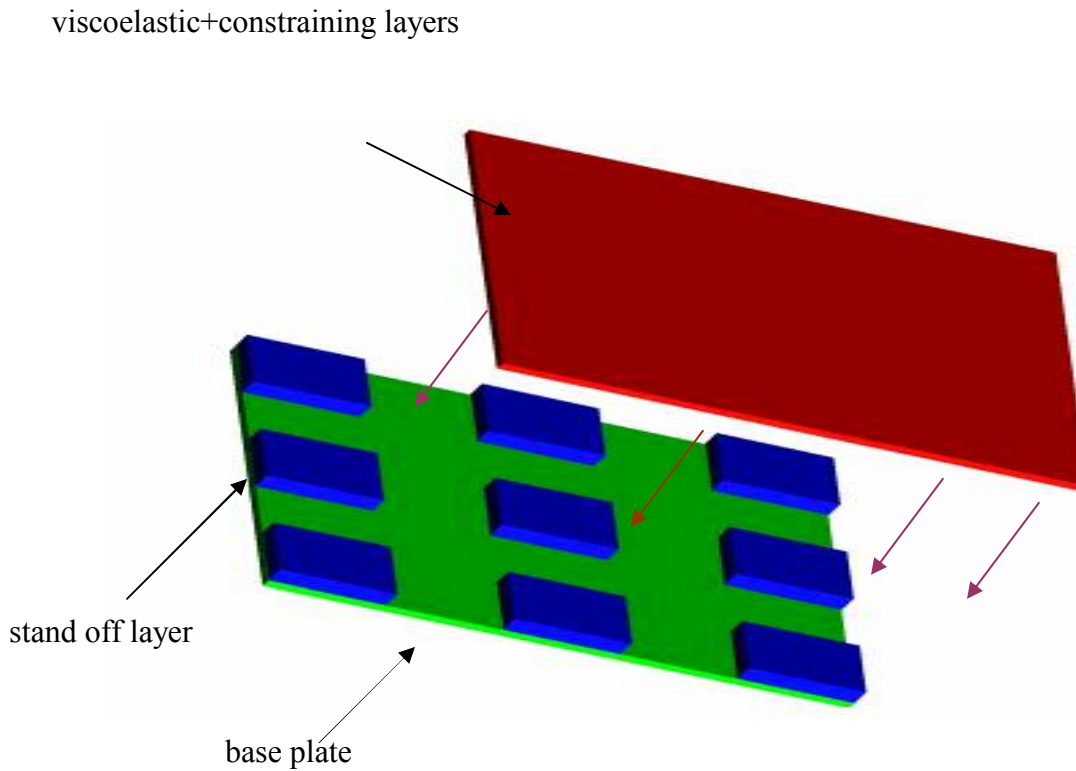


**Figure (55)** - Passive constrained layer plate with stand-off layer patches



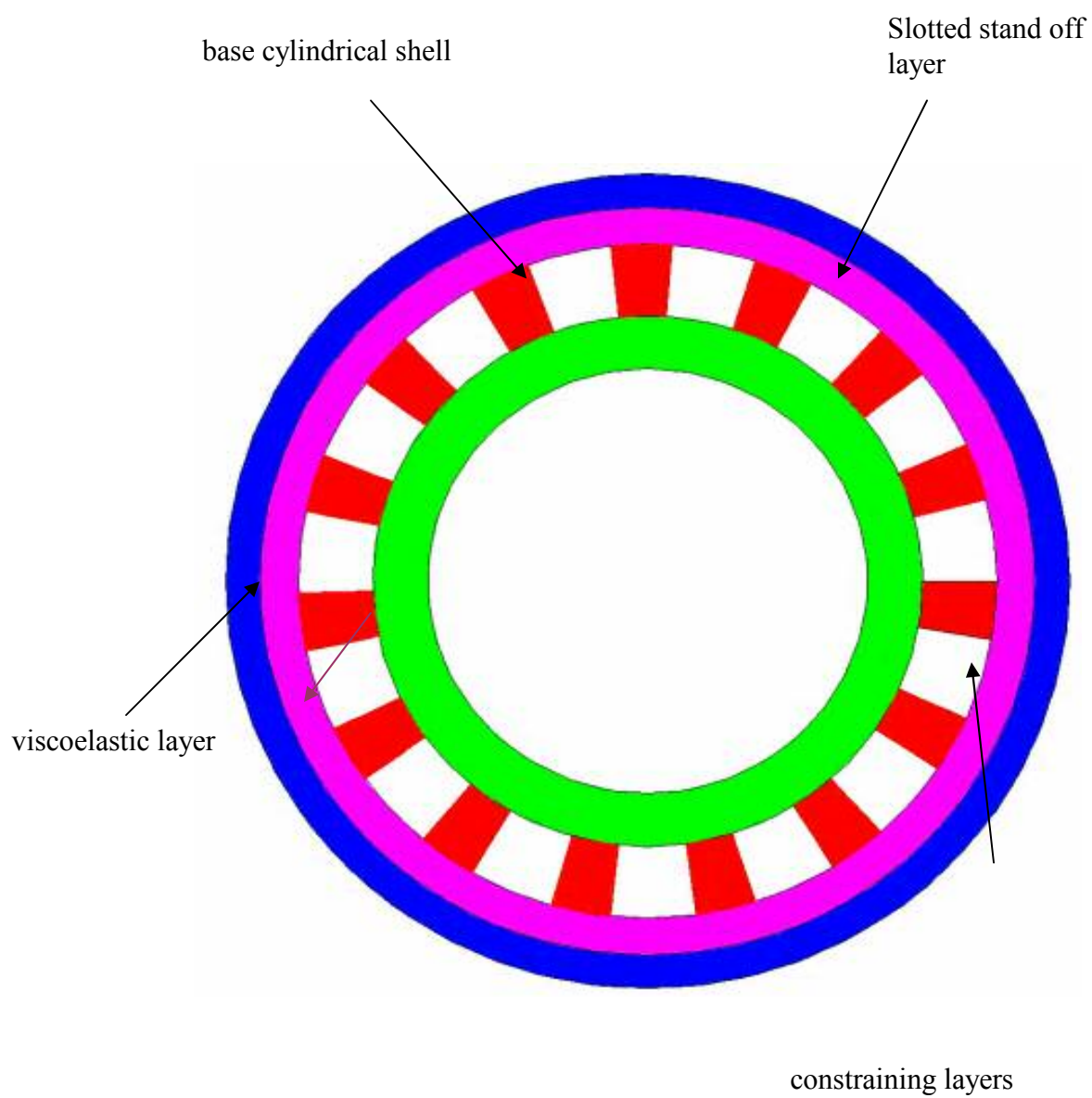


**Figure (56) - Cylindrical Shell with Slotted Stand-off layer**

Furthermore, in this dissertation it was assumed that all layers experience the same lateral deflection. Accordingly, a natural extension to this work would be to take into account variable lateral deflection across the layers PSOL as shown in Figure (57).

Furthermore, a finite element model can be developed along the same lines as outlined in this thesis to incorporate thickness variation of the layers and can also count for variations in geometry of layers in axial direction.

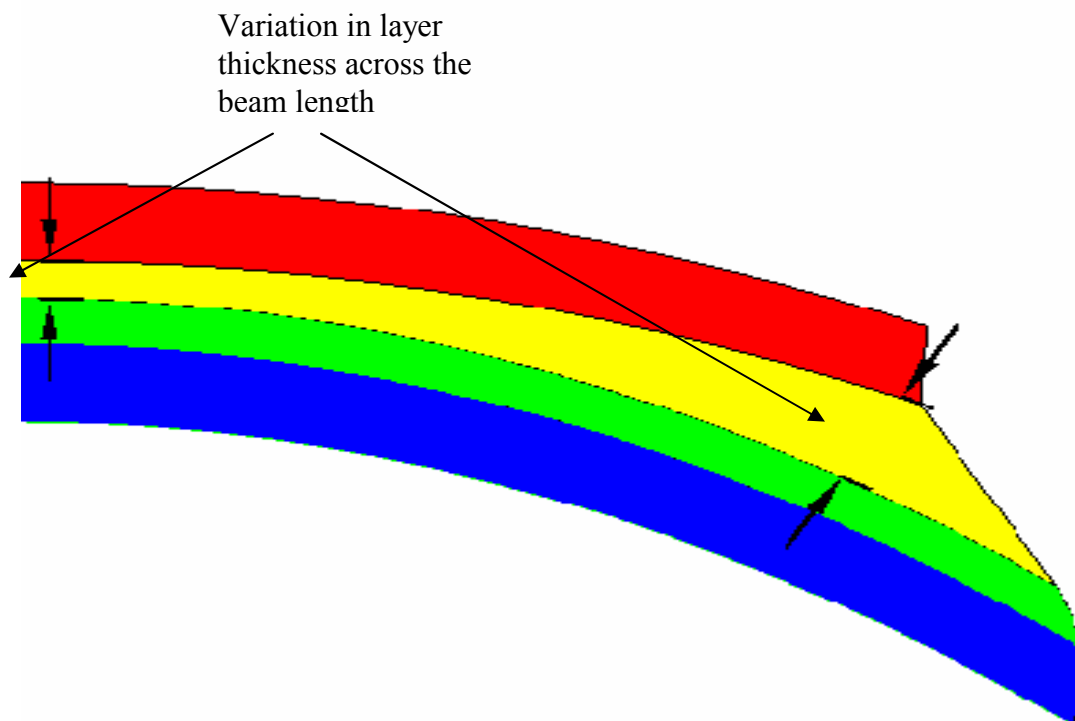


**Figure (57)** - Passive stand-off layer treated beam with lateral strain in the layers

Another natural extension of the present work would be to develop finite element models that can be easily used to incorporate slots in viscoelastic and constraining layers by simply

varying the material properties of the element as shown in Figure (58). Even the base beam can be made to vary along its length as long as singularities in the overall stiffness matrix are avoided. To avoid singularities, none of the material properties in the first and last elements should be zero, i.e., the slots should not be at the ends of the beam. This geometry of the slots in constraining, viscoelastic and stand-off layers can then be varied stepwise and the model analyzed until the optimum performance is achieved. This would provide a method of finding the optimal shape and geometry of slots for best damping performance.

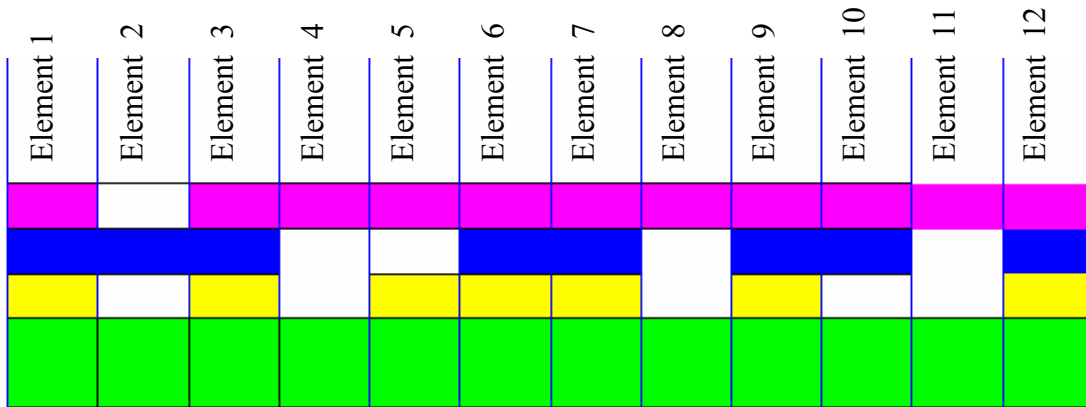


**Figure (58)** - Variation of geometry of layers along the length of the beam

# Appendix

## Computer Program Codes

### A.1. Distributed Transfer Function Method

```
P=1;
z=0 ;
l=.15;
b=.01175;
hs=.264*1e-3;
hc=.203*1e-3;
hv=.127*1e-3;
hb=2.29*1e-3;
Gv=1e5*(1+i);
Gs=1e5*(1+i);
pb=2850*b*hb;
pc=2850*b*hc;
pv=1100*b*hv;
ps=1100*b*hs;
Eb=72e9;
Ec=72e9;
Es=Gv*2.9;
Ev=Gv*2.9;
EAbs=Eb*(hb*b)+Es*(hs*b);
Elbs=Eb*(b*hb^3/12)+Es*(b*hs^3/12+b*hs*(hs/2+hb/2)^2);
EQbs=Eb*(0)*hb/4+Es*(hs*b)*(hb/2+hs/2);
EAc=Ec*b*hc;
EIc=Ec*(b*hc^3/12);
p=ps+pc+pv+pb;
Dt=Elbs+EIc;
alpha=hv+hs+(hb+hc)/2;
E=b*alpha^2*Gv*Gs*l^2/(Dt*(Gv*hs+Gs*hv));
c1=pc/p;
c2=(pb+ps)/p;
B=l/alpha;
a1=EQbs*l/Dt;
a2=EAc*l/Dt;
a3=EAbs*l/Dt;

for sr = 1:5:5000
s=sr*i*(p*l^4/Dt)^.5*pi*2;
F=[ 0,1,0,0,0,0,0,0;
```

```

0,0,1,0,0,0,0,0;
0,0,0,1,0,0,0,0;
-s^2*k,0,(E-B*E*a1/a3)*k,0,0,(E*B-E*B^2*a1/a3)*k,0,(c2*s^2*a1/a3...
+B^2*E*a1/a3-B*E)*k;
0,0,0,0,0,1,0,0;
0,E*B/a2,0,0,(c1*s^2+E*B^2)/a2,0,-E*B^2/a2,0;
0,0,0,0,0,0,0,1;
0,-B*E/a3,0,a1/a3,-E*B^2/a3,0,(c2*s^2+E*B^2)/a3,0];
M=[ 1,0,0,0,0,0,0,0;
0,1,0,0,0,0,0,0;
0,0,0,0,0,1,0,0;
0,0,0,0,0,0,0,1;
0,0,0,0,0,0,0,0;
0,0,0,0,0,0,0,0;
0,0,0,0,0,0,0,0;
0,0,0,0,0,0,0,0];

N=[ 0,0,0,0,0,0,0,0;
0,0,0,0,0,0,0,0;
0,0,0,0,0,0,0,0;
0,0,0,0,0,0,0,0;
0,0,1,0,0,0,0,0;
0,0,0,0,0,1,0,0;
0,0,0,0,0,0,0,1;
0,E*(1-B*a1/a3),0,-1/k,E*(B-B^2*a1/a3),0,-E*(B-B^2*a1/a3),0];

Gamma=[ P 0 0 0 0 0 0 0 ]';

efs=expm(F);

H=efs*(M+N*efs)^-1;
H0=eye(8)/(M+N*efs)^-1;

eta=H*Gamma;
eta0=H0*Gamma;
z=z+1;
splot(z)=sr;
w(z)=abs(real(eta(1))/real(eta0(1)));
end

Plotting
semilogy(splot,w)

```

## A.2. Finite Element Method for PSOL beam

```
nem=11;
l=.15;
b=.01175;
hs=.264*1e-3;
hc=.203*1e-3;
hv=.127*1e-3;
hb=2.29*1e-3;
Gv=1e5*(1+i);
Gs=1e5*(1+i);
pb=2850*b*hb;
pc=2850*b*hc;
pv=1100*b*hv;
ps=1100*b*hs;
Eb=72e9;
Ec=72e9;
Es=Gs*2.9;
Ev=Gv*2.9;
EAbs=Eb*(hb*b)+Es*(hs*b);
EIbs=Eb*(b*hb^3/12)+Es*(b*hs^3/12+b*hs*(hs/2+hb/2)^2);
EQbs=Eb*(0)*hb/4+Es*(hs*b)*(hb/2+hs/2);
EAc=Ec*b*hc;
EIc=Ec*(b*hc^3/12);
p=ps+pc+pv+pb;
Dt=EIbs+EIc;
alpha=hv+hs+(hb+hc)/2;
E=b*alpha^2*Gv*Gs*l^2/(Dt*(Gv*hs+Gs*hv));
c1=pc/p;
c2=(pb+ps)/p;
B=l/alpha;
a1=EQbs*l/Dt;
a2=EAc*l/Dt;
a3=EAbs*l/Dt;

splot=0;

syms x

h=1/nem;

v1=1-3*(x/h)^2+2*(x/h)^3;
v2=-x*(1-x/h)^2;
v3=3*(x/h)^2-2*(x/h)^3;
```

```

v4=-x*(x^2/h^2-x/h);
th1=1-x/h;
th2=x/h;

```

```

for sr=1:100:5000
    s=sr*i*(p*I^4/Dt)^.5*pi*2;

```

```

k1=(1-a1^2/a3);
k2=(a1/a3*B*E-E);
k3=B^2*E*a1/a3-B*E;
k4=B*E-c2*s^2*a1/a3-B^2*E*a1/a3;
k8=-B*E;
k5=c1*s^2+B^2*E;
k6=-B^2*E;
k7=c2*s^2+B^2*E;

```

```

K11=k1*diff(v1,2)*diff(v1,2)+k2*diff(v1,1)*diff(v1,1)+s^2*v1*v1;
K21=k1*diff(v1,2)*diff(v2,2)+k2*diff(v1,1)*diff(v2,1)+s^2*v1*v2;
K31=k1*diff(v1,2)*diff(v3,2)+k2*diff(v1,1)*diff(v3,1)+s^2*v1*v3;
K41=k1*diff(v1,2)*diff(v4,2)+k2*diff(v1,1)*diff(v4,1)+s^2*v1*v4;

```

```

K12=k1*diff(v2,2)*diff(v1,2)+k2*diff(v2,1)*diff(v1,1)+s^2*v2*v1;
K22=k1*diff(v2,2)*diff(v2,2)+k2*diff(v2,1)*diff(v2,1)+s^2*v2*v2;
K32=k1*diff(v2,2)*diff(v3,2)+k2*diff(v2,1)*diff(v3,1)+s^2*v2*v3;
K42=k1*diff(v2,2)*diff(v4,2)+k2*diff(v2,1)*diff(v4,1)+s^2*v2*v4;

```

```

K13=k1*diff(v3,2)*diff(v1,2)+k2*diff(v3,1)*diff(v1,1)+s^2*v3*v1;
K23=k1*diff(v3,2)*diff(v2,2)+k2*diff(v3,1)*diff(v2,1)+s^2*v3*v2;
K33=k1*diff(v3,2)*diff(v3,2)+k2*diff(v3,1)*diff(v3,1)+s^2*v3*v3;
K43=k1*diff(v3,2)*diff(v4,2)+k2*diff(v3,1)*diff(v4,1)+s^2*v3*v4;

```

```

K14=k1*diff(v4,2)*diff(v1,2)+k2*diff(v4,1)*diff(v1,1)+s^2*v4*v1;
K24=k1*diff(v4,2)*diff(v2,2)+k2*diff(v4,1)*diff(v2,1)+s^2*v4*v2;
K34=k1*diff(v4,2)*diff(v3,2)+k2*diff(v4,1)*diff(v3,1)+s^2*v4*v3;
K44=k1*diff(v4,2)*diff(v4,2)+k2*diff(v4,1)*diff(v4,1)+s^2*v4*v4;

```

```

K15=k3*diff(th1,1)*v1;
K25=k3*diff(th1,1)*v2;
K35=k3*diff(th1,1)*v3;
K45=k3*diff(th1,1)*v4;

```

```

K16=k3*diff(th2,1)*v1;
K26=k3*diff(th2,1)*v2;
K36=k3*diff(th2,1)*v3;

```

$$K46=k3*\text{diff}(th2,1)*v4;$$

$$K17=k4*\text{diff}(th1,1)*v1;$$

$$K27=k4*\text{diff}(th1,1)*v2;$$

$$K37=k4*\text{diff}(th1,1)*v3;$$

$$K47=k4*\text{diff}(th1,1)*v4;$$

$$K18=k4*\text{diff}(th2,1)*v1;$$

$$K28=k4*\text{diff}(th2,1)*v2;$$

$$K38=k4*\text{diff}(th2,1)*v3;$$

$$K48=k4*\text{diff}(th2,1)*v4;$$

$$K51=-k8*\text{diff}(v1,1)*th1;$$

$$K61=-k8*\text{diff}(v1,1)*th2;$$

$$K52=-k8*\text{diff}(v2,1)*th1;$$

$$K62=-k8*\text{diff}(v2,1)*th2;$$

$$K53=-k8*\text{diff}(v3,1)*th1;$$

$$K63=-k8*\text{diff}(v3,1)*th2;$$

$$K54=-k8*\text{diff}(v4,1)*th1;$$

$$K64=-k8*\text{diff}(v4,1)*th2;$$

$$K55=a2*\text{diff}(th1,1)*\text{diff}(th1,1)+k5*th1*th1;$$

$$K65=a2*\text{diff}(th1,1)*\text{diff}(th2,1)+k5*th1*th2;$$

$$K56=a2*\text{diff}(th2,1)*\text{diff}(th1,1)+k5*th2*th1;$$

$$K66=a2*\text{diff}(th2,1)*\text{diff}(th2,1)+k5*th2*th2;$$

$$K57=k6*th1*th1;$$

$$K67=k6*th1*th2;$$

$$K58=k6*th2*th1;$$

$$K68=k6*th2*th2;$$

$$K71=(a1*\text{diff}(v1,3)+k8*\text{diff}(v1,1))*th1;$$

$$K81=(a1*\text{diff}(v1,3)+k8*\text{diff}(v1,1))*th2;$$

$$K72=(a1*\text{diff}(v2,3)+k8*\text{diff}(v2,1))*th1;$$

$$K82=(a1*\text{diff}(v2,3)+k8*\text{diff}(v2,1))*th2;$$

$$K73=(a1*\text{diff}(v3,3)+k8*\text{diff}(v3,1))*th1;$$

$$K83=(a1*\text{diff}(v3,3)+k8*\text{diff}(v3,1))*th2;$$



```
K74=(a1*diff(v4,3)+k8*diff(v4,1))*th1;
K84=(a1*diff(v4,3)+k8*diff(v4,1))*th2;
```

```
K75=k6*th1*th1;
K85=k6*th1*th2;
```

```
K76=k6*th2*th1;
K86=k6*th2*th2;
```

```
K77=a3*diff(th1,1)*diff(th1,1)+k7*th1*th1;
K87=a3*diff(th1,1)*diff(th2,1)+k7*th1*th2;
```

```
K78=a3*diff(th2,1)*diff(th1,1)+k7*th2*th1;
K88=a3*diff(th2,1)*diff(th2,1)+k7*th2*th2;
```

```
KK=[ K11, K12, K15, K17, K13, K14, K16, K18;
K21, K22, K25, K27, K23, K24, K26, K28;
K51, K52, K55, K57, K53, K54, K56, K58;
K71, K72, K75, K77, K73, K74, K76, K78;
K31, K32, K35, K37, K33, K34, K36, K38;
K41, K42, K45, K47, K43, K44, K46, K48;
K61, K62, K65, K67, K63, K64, K66, K68;
K81, K82, K85, K87, K83, K84, K86, K88];
```

```
K=int(KK,x,0,h);
K=double(K);
```

```
KO=zeros((nem+1)*4);
for n=1:nem
KO(n*4-3:n*4+4,n*4-3:n*4+4)=KO(n*4-3:n*4+4,n*4-3:n*4+4)+K;
end
```

```
KK=zeros(nem*4+1);
KK(2:nem*4+1,2:nem*4+1)=KO(5:4*nem+4,5:4*nem+4);
KK(1,1)=KO(3,3);
KK(1,2:5)=KO(3,5:8);
KK(2:5,1)=KO(5:8,3);
```

```
KK((nem-1)*4+2,(nem*4))=KK((nem-1)*4+2,(nem*4))+k3;
KK((nem-1)*4+2,(nem*4+1))=KK((nem-1)*4+2,(nem*4+1))+k4;
```

```
F=[-KO(1,3);-KO(1,5);-KO(1,6);-KO(1,7);-KO(1,8);zeros(nem*4-4,1)];
```

```
X=KK^-1*F;
```

```

splot=splot+1;
w(splot)=abs(real(X(nem*4-2)));
ww(splot)=sr;
end
semilogy(ww,w)

```

### A.3. Finite Element Method for slotted PSOL beam

```

%nem=input('nem')
nem=11;

l=.15;
b=.01175;
hs=.264*1e-3;
hc=.203*1e-3;
hv=.127*1e-3;
hb=2.29*1e-3;
Gv=1e5*(1+i);
Gs=1e5*(1+i);
CCGs=0;
pb=2850*b*hb;
pc=2850*b*hc;
pv=1100*b*hv;
ps=1100*b*hs;
Eb=72e9;
Ec=72e9;
Es=Gv*2.9;
CCEs=0;
Ev=Gv*2.9;
EAb=Eb*(hb*b)+Es*(hs*b);
CCEAb=Eb*(hb*b);
EIb=Eb*(b*hb^3/12)+Es*(b*hs^3/12+b*hs*(hs/2+hb/2)^2);
CCEIb=Eb*(b*hb^3/12);
EQb=Eb*(0)*hb/4+Es*(hs*b)*(hb/2+hs/2);
CCEQb=0;
EAe=Ec*b*hc;
EIe=Ec*(b*hc^3/12);
p=ps+pc+pv+pb;
Dt=EIb+EIe;
CCDt=CCEIb+EIe;
alpha=hv+hs+(hb+hc)/2;
E=b*alpha^2*Gv*Gs*l^2/(Dt*(Gv*hs+Gs*hv));
CCE=b*alpha^2*Gv*CCGs*l^2/(CCDt*(Gv*hs+CCGs*hv));
cl=pc/p;

```

```

c2=(pb+ps)/p;
B=l/alpha;
a1=EQbs*l/Dt;
CCa1=0
a2=EAc*l/Dt;
CCa2=EAc*l/CCDt;
a3=EAbs*l/Dt;
CCa3=CCEAbs*l/CCDt;

splot=0
syms x
h=1/nem;
v1=1-3*(x/h)^2+2*(x/h)^3;
v2=-x*(1-x/h)^2;
v3=3*(x/h)^2-2*(x/h)^3;
v4=-x*(x^2/h^2-x/h);
th1=1-x/h;
th2=x/h;
%w=w1*v1+w2*v2+w3*v3+w4*v4;
%uc=uc1*th1+uc2*th2;
%ub=ub1*th1+ub2*th2;

%sr=1
for sr=1:10:5000
    s=sr*i*(p*l^4/Dt)^.5*pi*2;

k1=(1-a1^2/a3);
cck1=1;
k2=(a1/a3*B*E-E);
cck2=-CCE;
k3=B^2*E*a1/a3-B*E;
cck3=-B*CCE;
k4=B*E-c2*s^2*a1/a3-B^2*E*a1/a3;
cck4=B*CCE;
k8=-B*E;
cck8=-B*CCE;
k5=c1*s^2+B^2*E;
cck5=c1*s^2+B^2*CCE;
k6=-B^2*E;
cck6=-B^2*CCE;
k7=c2*s^2+B^2*E;
cck7=c2*s^2+B^2*CCE;

K11=k1*diff(v1,2)*diff(v1,2)+k2*diff(v1,1)*diff(v1,1)+s^2*v1*v1;

```

$K21=k1*diff(v1,2)*diff(v2,2)+k2*diff(v1,1)*diff(v2,1)+s^2*v1*v2;$   
 $K31=k1*diff(v1,2)*diff(v3,2)+k2*diff(v1,1)*diff(v3,1)+s^2*v1*v3;$   
 $K41=k1*diff(v1,2)*diff(v4,2)+k2*diff(v1,1)*diff(v4,1)+s^2*v1*v4;$

$K12=k1*diff(v2,2)*diff(v1,2)+k2*diff(v2,1)*diff(v1,1)+s^2*v2*v1;$   
 $K22=k1*diff(v2,2)*diff(v2,2)+k2*diff(v2,1)*diff(v2,1)+s^2*v2*v2;$   
 $K32=k1*diff(v2,2)*diff(v3,2)+k2*diff(v2,1)*diff(v3,1)+s^2*v2*v3;$   
 $K42=k1*diff(v2,2)*diff(v4,2)+k2*diff(v2,1)*diff(v4,1)+s^2*v2*v4;$

$K13=k1*diff(v3,2)*diff(v1,2)+k2*diff(v3,1)*diff(v1,1)+s^2*v3*v1;$   
 $K23=k1*diff(v3,2)*diff(v2,2)+k2*diff(v3,1)*diff(v2,1)+s^2*v3*v2;$   
 $K33=k1*diff(v3,2)*diff(v3,2)+k2*diff(v3,1)*diff(v3,1)+s^2*v3*v3;$   
 $K43=k1*diff(v3,2)*diff(v4,2)+k2*diff(v3,1)*diff(v4,1)+s^2*v3*v4;$

$K14=k1*diff(v4,2)*diff(v1,2)+k2*diff(v4,1)*diff(v1,1)+s^2*v4*v1;$   
 $K24=k1*diff(v4,2)*diff(v2,2)+k2*diff(v4,1)*diff(v2,1)+s^2*v4*v2;$   
 $K34=k1*diff(v4,2)*diff(v3,2)+k2*diff(v4,1)*diff(v3,1)+s^2*v4*v3;$   
 $K44=k1*diff(v4,2)*diff(v4,2)+k2*diff(v4,1)*diff(v4,1)+s^2*v4*v4;$

$K15=k3*diff(th1,1)*v1;$   
 $K25=k3*diff(th1,1)*v2;$   
 $K35=k3*diff(th1,1)*v3;$   
 $K45=k3*diff(th1,1)*v4;$

$K16=k3*diff(th2,1)*v1;$   
 $K26=k3*diff(th2,1)*v2;$   
 $K36=k3*diff(th2,1)*v3;$   
 $K46=k3*diff(th2,1)*v4;$

$K17=k4*diff(th1,1)*v1;$   
 $K27=k4*diff(th1,1)*v2;$   
 $K37=k4*diff(th1,1)*v3;$   
 $K47=k4*diff(th1,1)*v4;$

$K18=k4*diff(th2,1)*v1;$   
 $K28=k4*diff(th2,1)*v2;$   
 $K38=k4*diff(th2,1)*v3;$   
 $K48=k4*diff(th2,1)*v4;$

$K51=-k8*diff(v1,1)*th1;$   
 $K61=-k8*diff(v1,1)*th2;$

$K52=-k8*diff(v2,1)*th1;$   
 $K62=-k8*diff(v2,1)*th2;$

$$K53=-k8*\text{diff}(v3,1)*th1;$$

$$K63=-k8*\text{diff}(v3,1)*th2;$$

$$K54=-k8*\text{diff}(v4,1)*th1;$$

$$K64=-k8*\text{diff}(v4,1)*th2;$$

$$K55=a2*\text{diff}(th1,1)*\text{diff}(th1,1)+k5*th1*th1;$$

$$K65=a2*\text{diff}(th1,1)*\text{diff}(th2,1)+k5*th1*th2;$$

$$K56=a2*\text{diff}(th2,1)*\text{diff}(th1,1)+k5*th2*th1;$$

$$K66=a2*\text{diff}(th2,1)*\text{diff}(th2,1)+k5*th2*th2;$$

$$K57=k6*th1*th1;$$

$$K67=k6*th1*th2;$$

$$K58=k6*th2*th1;$$

$$K68=k6*th2*th2;$$

$$K71=(a1*\text{diff}(v1,3)+k8*\text{diff}(v1,1))*th1;$$

$$K81=(a1*\text{diff}(v1,3)+k8*\text{diff}(v1,1))*th2;$$

$$K72=(a1*\text{diff}(v2,3)+k8*\text{diff}(v2,1))*th1;$$

$$K82=(a1*\text{diff}(v2,3)+k8*\text{diff}(v2,1))*th2;$$

$$K73=(a1*\text{diff}(v3,3)+k8*\text{diff}(v3,1))*th1;$$

$$K83=(a1*\text{diff}(v3,3)+k8*\text{diff}(v3,1))*th2;$$

$$K74=(a1*\text{diff}(v4,3)+k8*\text{diff}(v4,1))*th1;$$

$$K84=(a1*\text{diff}(v4,3)+k8*\text{diff}(v4,1))*th2;$$

$$K75=k6*th1*th1;$$

$$K85=k6*th1*th2;$$

$$K76=k6*th2*th1;$$

$$K86=k6*th2*th2;$$

$$K77=a3*\text{diff}(th1,1)*\text{diff}(th1,1)+k7*th1*th1;$$

$$K87=a3*\text{diff}(th1,1)*\text{diff}(th2,1)+k7*th1*th2;$$

$$K78=a3*\text{diff}(th2,1)*\text{diff}(th1,1)+k7*th2*th1;$$

$$K88=a3*\text{diff}(th2,1)*\text{diff}(th2,1)+k7*th2*th2;$$

$$cK11=cck1*\text{diff}(v1,2)*\text{diff}(v1,2)+cck2*\text{diff}(v1,1)*\text{diff}(v1,1)+s^2*v1*v1;$$

$$cK21=cck1*\text{diff}(v1,2)*\text{diff}(v2,2)+cck2*\text{diff}(v1,1)*\text{diff}(v2,1)+s^2*v1*v2;$$

$$cK31=cck1*\text{diff}(v1,2)*\text{diff}(v3,2)+cck2*\text{diff}(v1,1)*\text{diff}(v3,1)+s^2*v1*v3;$$

$$cK41=cck1*diff(v1,2)*diff(v4,2)+cck2*diff(v1,1)*diff(v4,1)+s^2*v1*v4;$$

$$cK12=cck1*diff(v2,2)*diff(v1,2)+cck2*diff(v2,1)*diff(v1,1)+s^2*v2*v1;$$

$$cK22=cck1*diff(v2,2)*diff(v2,2)+cck2*diff(v2,1)*diff(v2,1)+s^2*v2*v2;$$

$$cK32=cck1*diff(v2,2)*diff(v3,2)+cck2*diff(v2,1)*diff(v3,1)+s^2*v2*v3;$$

$$cK42=cck1*diff(v2,2)*diff(v4,2)+cck2*diff(v2,1)*diff(v4,1)+s^2*v2*v4;$$

$$cK13=cck1*diff(v3,2)*diff(v1,2)+cck2*diff(v3,1)*diff(v1,1)+s^2*v3*v1;$$

$$cK23=cck1*diff(v3,2)*diff(v2,2)+cck2*diff(v3,1)*diff(v2,1)+s^2*v3*v2;$$

$$cK33=cck1*diff(v3,2)*diff(v3,2)+cck2*diff(v3,1)*diff(v3,1)+s^2*v3*v3;$$

$$cK43=cck1*diff(v3,2)*diff(v4,2)+cck2*diff(v3,1)*diff(v4,1)+s^2*v3*v4;$$

$$cK14=cck1*diff(v4,2)*diff(v1,2)+cck2*diff(v4,1)*diff(v1,1)+s^2*v4*v1;$$

$$cK24=cck1*diff(v4,2)*diff(v2,2)+cck2*diff(v4,1)*diff(v2,1)+s^2*v4*v2;$$

$$cK34=cck1*diff(v4,2)*diff(v3,2)+cck2*diff(v4,1)*diff(v3,1)+s^2*v4*v3;$$

$$cK44=cck1*diff(v4,2)*diff(v4,2)+cck2*diff(v4,1)*diff(v4,1)+s^2*v4*v4;$$

$$cK15=cck3*diff(th1,1)*v1;$$

$$cK25=cck3*diff(th1,1)*v2;$$

$$cK35=cck3*diff(th1,1)*v3;$$

$$cK45=cck3*diff(th1,1)*v4;$$

$$cK16=cck3*diff(th2,1)*v1;$$

$$cK26=cck3*diff(th2,1)*v2;$$

$$cK36=cck3*diff(th2,1)*v3;$$

$$cK46=cck3*diff(th2,1)*v4;$$

$$cK17=cck4*diff(th1,1)*v1;$$

$$cK27=cck4*diff(th1,1)*v2;$$

$$cK37=cck4*diff(th1,1)*v3;$$

$$cK47=cck4*diff(th1,1)*v4;$$

$$cK18=cck4*diff(th2,1)*v1;$$

$$cK28=cck4*diff(th2,1)*v2;$$

$$cK38=cck4*diff(th2,1)*v3;$$

$$cK48=cck4*diff(th2,1)*v4;$$

$$cK51=-cck8*diff(v1,1)*th1;$$

$$cK61=-cck8*diff(v1,1)*th2;$$

$$cK52=-cck8*diff(v2,1)*th1;$$

$$cK62=-cck8*diff(v2,1)*th2;$$

$$cK53=-cck8*diff(v3,1)*th1;$$

$$cK63=-cck8*diff(v3,1)*th2;$$

cK54=-cck8\*diff(v4,1)\*th1;  
cK64=-cck8\*diff(v4,1)\*th2;

cK55=CCa2\*diff(th1,1)\*diff(th1,1)+cck5\*th1\*th1;  
cK65=CCa2\*diff(th1,1)\*diff(th2,1)+cck5\*th1\*th2;

cK56=CCa2\*diff(th2,1)\*diff(th1,1)+cck5\*th2\*th1;  
cK66=CCa2\*diff(th2,1)\*diff(th2,1)+cck5\*th2\*th2;

cK57=cck6\*th1\*th1;  
cK67=cck6\*th1\*th2;

cK58=cck6\*th2\*th1;  
cK68=cck6\*th2\*th2;

cK71=(CCa1\*diff(v1,3)+cck8\*diff(v1,1))\*th1;  
cK81=(CCa1\*diff(v1,3)+cck8\*diff(v1,1))\*th2;

cK72=(CCa1\*diff(v2,3)+cck8\*diff(v2,1))\*th1;  
cK82=(CCa1\*diff(v2,3)+cck8\*diff(v2,1))\*th2;

cK73=(CCa1\*diff(v3,3)+cck8\*diff(v3,1))\*th1;  
cK83=(CCa1\*diff(v3,3)+cck8\*diff(v3,1))\*th2;

cK74=(CCa1\*diff(v4,3)+cck8\*diff(v4,1))\*th1;  
cK84=(CCa1\*diff(v4,3)+cck8\*diff(v4,1))\*th2;

cK75=k6\*th1\*th1;  
cK85=k6\*th1\*th2;

cK76=k6\*th2\*th1;  
cK86=k6\*th2\*th2;

cK77=CCa3\*diff(th1,1)\*diff(th1,1)+cck7\*th1\*th1;  
cK87=CCa3\*diff(th1,1)\*diff(th2,1)+cck7\*th1\*th2;

cK78=CCa3\*diff(th2,1)\*diff(th1,1)+cck7\*th2\*th1;  
cK88=CCa3\*diff(th2,1)\*diff(th2,1)+cck7\*th2\*th2;

KK=[ K11, K12, K15, K17, K13, K14, K16, K18;  
K21, K22, K25, K27, K23, K24, K26, K28;  
K51, K52, K55, K57, K53, K54, K56, K58;  
K71, K72, K75, K77, K73, K74, K76, K78;  
K31, K32, K35, K37, K33, K34, K36, K38;

```

K41, K42, K45, K47, K43, K44, K46, K48;
K61, K62, K65, K67, K63, K64, K66, K68;
K81, K82, K85, K87, K83, K84, K86, K88];
K=int(KK,x,0,h);
K=double(K);

cKK =[ cK11, cK12, cK15, cK17, cK13, cK14, cK16, cK18;
cK21, cK22, cK25, cK27, cK23, cK24, cK26, cK28;
cK51, cK52, cK55, cK57, cK53, cK54, cK56, cK58;
cK71, cK72, cK75, cK77, cK73, cK74, cK76, cK78;
cK31, cK32, cK35, cK37, cK33, cK34, cK36, cK38;
cK41, cK42, cK45, cK47, cK43, cK44, cK46, cK48;
cK61, cK62, cK65, cK67, cK63, cK64, cK66, cK68;
cK81, cK82, cK85, cK87, cK83, cK84, cK86, cK88];
cK=int(cKK,x,0,h);
cK=double(cK);

KO=zeros((nem+1)*4);

for n=1:nem
    if rem(n,2)==0
KO(n*4-3:n*4+4,n*4-3:n*4+4)=KO(n*4-3:n*4+4,n*4-3:n*4+4)+cK;
        else
KO(n*4-3:n*4+4,n*4-3:n*4+4)=KO(n*4-3:n*4+4,n*4-3:n*4+4)+K;
        end
    end
KK=zeros(nem*4+1);
KK(2:nem*4+1,2:nem*4+1)=KO(5:4*nem+4,5:4*nem+4);
KK(1,1)=KO(3,3);
KK(1,2:5)=KO(3,5:8);
KK(2:5,1)=KO(5:8,3);

KK((nem-1)*4+2,(nem*4))=KK((nem-1)*4+2,(nem*4))+k3;
KK((nem-1)*4+2,(nem*4+1))=KK((nem-1)*4+2,(nem*4+1))+k4;

F=[-KO(1,3);-KO(1,5);-KO(1,6);-KO(1,7);-KO(1,8);zeros(nem*4-4,1)];
X=KK^-1*F;
splot=splot+1;
w(splot)=abs(real(X(nem*4-2)));
ww(splot)=sr;

end
semilogy(ww,w)
A.4. ANSYS program

```





LSTR, 3, 4  
 LSTR, 4, 1  
 LSTR, 4, 5  
 LSTR, 5, 6  
 LSTR, 6, 3  
 LSTR, 5, 8  
 LSTR, 8, 7  
 LSTR, 7, 6  
 LSTR, 8, 9  
 LSTR, 9, 10  
 LSTR, 10, 7  
 FLST,2,4,4  
 FITEM,2,1  
 FITEM,2,2  
 FITEM,2,3  
 FITEM,2,4  
 AL,P51X  
 FLST,2,4,4  
 FITEM,2,3  
 FITEM,2,5  
 FITEM,2,6  
 FITEM,2,7  
 AL,P51X  
 FLST,2,4,4  
 FITEM,2,6  
 FITEM,2,8  
 FITEM,2,9  
 FITEM,2,10  
 AL,P51X  
 FLST,2,4,4  
 FITEM,2,9  
 FITEM,2,11  
 FITEM,2,12  
 FITEM,2,13  
 AL,P51X  
 TYPE, 1  
 MAT, 1  
 REAL, 1  
 ESYS, 0  
 SECNUM,  
 FLST,2,2,5,ORDE,2  
 FITEM,2,1  
 FITEM,2,4  
 AESIZE,P51X,.001,  
 MSHAPE,0,2D

```

MSHKEY,1
FLST,5,2,5,ORDE,2
FITEM,5,1
FITEM,5,4
CM,_Y,AREA
ASEL, , , ,P51X
CM,_Y1,AREA
CHKMSH,'AREA'
CMSEL,S,_Y
AMESH,_Y1
CMDELE,_Y
CMDELE,_Y1
CMDELE,_Y2
TYPE, 1
MAT, 2
REAL, 1
ESYS, 0
SECNUM,
FLST,2,1,5,ORDE,1
FITEM,2,2
AESIZE,P51X,0.001,
CM,_Y,AREA
ASEL, , , , 2
CM,_Y1,AREA
CHKMSH,'AREA'
CMSEL,S,_Y
AMESH,_Y1
CMDELE,_Y
CMDELE,_Y1
CMDELE,_Y2
TYPE, 1
MAT, 2
REAL, 1
ESYS, 0
SECNUM,
FLST,2,1,5,ORDE,1
FITEM,2,3
AESIZE,P51X,0.001,
CM,_Y,AREA
ASEL, , , , 3
CM,_Y1,AREA
CHKMSH,'AREA'
CMSEL,S,_Y
AMESH,_Y1
CMDELE,_Y

```

```

CMDELE,_Y1
CMDELE,_Y2
ACLEAR, 2
TYPE, 1
MAT, 3
REAL, 1
ESYS, 0
SECNUM,
FLST,2,1,5,ORDE,1
FITEM,2,2
AESIZE,P51X,0.001,
TYPE, 1
MAT, 3
REAL, 1
ESYS, 0
SECNUM,
/UI,MESH,OFF
/PREP7
TYPE, 1
MAT, 3
REAL, 1
ESYS, 0
SECNUM,
FLST,2,1,5,ORDE,1
FITEM,2,2
AESIZE,P51X,.001,
CM,_Y,AREA
ASEL, , , 2
CM,_Y1,AREA
CHKMSH,'AREA'
CMSEL,S,_Y
AMESH,_Y1
CMDELE,_Y
CMDELE,_Y1
CMDELE,_Y2
/UI,MESH,OFF
FINISH

```

```

/SOL
ANTYPE,3
FLST,2,2,3,ORDE,2
FITEM,2,1
FITEM,2,4
/GO

```

```
DK,P51X,,0,,0,UX,ROTZ,,,,,  
FLST,2,1,3,ORDE,1  
FITEM,2,1  
/GO  
DK,P51X,,1,,0,UY,,,,,  
HARFRQ,0,5000,  
NSUBST,50,  
KBC,1  
SOLVE  
FINISH
```

```
/POST26  
FINISH  
/POST1  
INRES,BASIC  
FILE,'file','rst','.'  
SET,LAST  
FINISH  
/POST26  
FILE,'file','rst','.'  
/UI,COLL,1  
NUMVAR,200  
SOLU,191,NCMIT  
STORE,MERGE  
FILLDATA,191,,,,1,1  
REALVAR,191,191  
NSOL,3,2,U,Y,UY_3  
STORE,MERGE  
FINISH  
/SOL
```

## References

- [1] **Mead, D. J.**, *Passive Vibration Control*, Wiley, London, 1998.
- [2] **Whittier, J. S.**, “The Effect of Configurational Additions using Viscoelastic Interfaces on the damping of a Cantilever Beam”, Wright Air Development Center, WADC Technical Report 58-568, 1959.
- [3] **Rogers, L., and Parin, M.**, “Experimental Results for Stand-off Passive Vibration Damping Treatment,” *Passive Damping and Isolation, Proceedings SPIE Smart Structures and Materials*, Vol. 2445, pp. 374–383, 1995.
- [4] **Falugi, M.**, “Analysis of Five Layer Viscoelastic Constrained Layer Beam”, *Proceedings of Damping '91, Vol. II, Paper No. CCB*, 1991.
- [5] **Falugi, M., Moon, Y., and Arnold, R.**, “Investigation of a Four Layer Viscoelastic Constrained Layer Damping System,” USAF/WL/FIBA/ASIAC, Report No. 189.1A, 1989.
- [6] **Parin, M., Rogers L., Moon Y. I., and Falugi M.**, “Practical Stand-Off Damping Treatment for Sheet Metal”, *Proceeding of Damping '89, Vol. II, Paper No. IBA.*, 1989.
- [7] **Garrison M. R., Miles R. N., Sun J., and Bao W.**, “Random response of a plate partially covered by a constrained layer damper”, *Journal of Sound and Vibration* 172, pp 231-245, 1994.
- [8] **Tao Y., Morris D. G., Spann F., Haugse E.**, “Low Frequency noise reducing structures using passive and active damping methods”, *Passive Damping and Isolation, Proceedings*

of SPIE Smart Structures and Materials, Vol. 3672, 1999.

- [9] **Yellin J. M., Shen I. Y., Reinhall P. G., and Huang P.**, “An Analytical and Experimental Analysis for a One-Dimensional Passive Stand-Off Layer Damping Treatment”, *ASME Journal of Vibration and Acoustics*, Vol. **122**, pp. 440-447, 2000.
- [10] **Yang, B. and Tan, C. A.**, “Transfer Functions of One-Dimensional Distributed Parameter Systems”, *Journal of Applied Mechanics*, Vol. **59**, pp. 1009–1014, 1992.